UCRL-16970

University of California
Ernest O. Lawrence Radiation Laboratory

I. THE QUANTUM CONVERSION PROCESS OF PHOTOSYNTHESIS
II. PARAMAGNETIC RESONANCE OF TRANSITION METAL COMPLEXES HAVING BIOLOGICAL INTEREST

TWO-WEEK LOAN COPY

This is a Library Circulating Copy which may be borrowed for two weeks. For a personal retention copy, call Tech. Info. Division, Ext. 5545

DISCLAIMER

This document was prepared as an account of work sponsored by the United States Government. While this document is believed to contain correct information, neither the United States Government nor any agency thereof, nor the Regents of the University of California, nor any of their employees, makes any warranty, express or implied, or assumes any legal responsibility for the accuracy, completeness, or usefulness of any information, apparatus, product, or process disclosed, or represents that its use would not infringe privately owned rights. Reference herein to any specific commercial product, process, or service by its trade name, trademark, manufacturer, or otherwise, does not necessarily constitute or imply its endorsement, recommendation, or favoring by the United States Government or any agency thereof, or the Regents of the University of California. The views and opinions of authors expressed herein do not necessarily state or reflect those of the United States Government or any agency thereof or the Regents of the University of California.

Research and Development

UCRL-16970

UNIVERSITY OF CALIFORNIA
Lawrence Radiation Laboratory
Berkeley, California

AEC Contract No. W-7405-eng-48

I. THE QUANTUM CONVERSION PROCESS OF PHOTOSYNTHESIS

II. PARAMAGNETIC RESONANCE OF TRANSITION METAL COMPLEXES HAVING BIOLOGICAL INTEREST

Robert T. Ross
(Ph.D. Thesis)

June 1966

I. THE QUANTUM CONVERSION PROCESS OF PHOTOSYNTHESIS

II. PARAMAGNETIC RESONANCE OF TRANSITION METAL COMPLEXES HAVING BIOLOGICAL INTEREST

Robert T. Ross

Lawrence Radiation Laboratory
University of California
Berkeley, California

ABSTRACT

PART I.

A limit on the thermodynamic potential difference between the ground and excited states of any photochemical system may be established by evaluating the potential difference at which the rate of photon absorption and emission are equal; the relationship of absorption and emission is given by a Planck law relationship between the two, provided that there is thermal equilibrium within the sublevels of the electronic bands. The maximum amount of power storage obtainable is evaluated by lowering the potential difference until the product of the potential difference and the fraction of the quanta retained is maximized. The effect of a finite rate of transfer of excitation away from the excited state on power storage and luminescence yield is found by an elementary kinetic derivation.

The Planck law relation between absorption and luminescence is used to calculate the luminescence spectra of purple bacteria from their absorption spectra; the resulting luminescence spectra compare well but not perfectly with published experimentally measured luminescence spectra. Application of the Planck law relation to published

activation spectra for Systems I and II of spinach chloroplasts permits independent calculation of the luminescence spectra of the two systems. If the luminescence yield of System I is taken to be one-third the yield of System II, then the combined luminescence spectrum closely fits a published experimental fluorescence spectrum.

Spinach chloroplasts under an illumination of 1 kilolux can produce at most a potential difference of 1.32 eV for System I, and 1.36 eV for System II. In the absence of non-radiative losses, the maximum amount of free energy stored is 1.19 eV per photon absorbed for System I and 1.23 eV per photon for System II. The bacterium Chromatium under an illumination of 10 kiloergs/cm^2sec of Na D radiation can produce at most a potential difference of 0.90 eV; the maximum amount of free energy stored is 0.79 eV per photon absorbed. The thermodynamically calculated potentials match the redox potential difference between P_{700} and Kok's -0.7 V compound in System I of plants, and the potential difference between P_{890} and ferredoxin in bacteria.

On the basis of an efficiency argument, it is hypothesized that there should be a linear relationship between the net flow through a biochemical pathway and the free energy lost per unit flow. This hypothesis is compatible with the observed light saturation behavior of photosynthesis. Preliminary extension of this model to include transient behavior correctly predicts the 1/time decay of chemiluminescence observed in plants.

Much of the theory used is presented in a preprint of an article entitled "Thermodynamic Limitations on the Conversion of Radiant Energy into Work," J. Chem. Phys. 45, No. 1 (1966).

PART II

The problems and techniques involved in the EPR spectroscopy of transition metals are reviewed, and the literature on the EPR of metal complexes which has biological significance is surveyed. Particular emphasis is placed on the conditions necessary for the observation of paramagnetic resonance, and on the EPR of manganese. A reprint of an article entitled "Dipolar Broadening of EPR Spectra Due to Solute Segregation in Frozen Aqueous Solutions," J. Chem. Phys. 42, 3919 (1965), is presented.

ACKNOWLEDGEMENTS

This thesis is, I hope, one more testimony to the interdisciplinary education which one receives under Professor Melvin Calvin. It is in his laboratory that one best learns how to carry the Berkeley tradition of "physical chemistry is anything that is interesting" into the biological sciences.

Much of a graduate student's education occurs at the hands of his fellow students, and I am particularly indebted to E. A. Dratz, D. R. Gentner, and I. D. Kuntz, Jr., in this regard. I thank Kenneth Sauer for his help in understanding the experimental literature of photosynthesis, and I thank M. P. Klein for his advice on magnetic resonance and for his instrumental genius. I am grateful to Professor Walter Knight for his tutelage in the art of teaching and for much kind advice.

Most of all, I am grateful to my wife Donna and to Tack Kuntz for the encouragement which enabled me to tackle the research problem which is reported in Part I of this thesis.

This work was supported, in part, by a National Science Foundation fellowship, and, in part, by the U.S. Atomic Energy Commission.

Table of Contents

		Page
I.	THE QUANTUM CONVERSION PROCESS OF PHOTOSYNTHESIS	1
A.	Applications of Thermodynamics to the Investigation of Photosynthesis	2
1.	Introduction	2
2.	Theory of the Photochemical Conversion of Light into Work	7
a.	Heuristic Theory for a Narrow-Band Absorber	7
b.	Formal Theory for a Broad-Band Absorber	12
c.	Losses from Slow Excitation Transfer	19
3.	Calculated Luminescence Spectra of Photosynthetic Systems	24
a.	Bacterial Luminescence	24
b.	Plant Luminescence	28
4.	Light-Driven Potential Differences and Free Energy Storage	37
a.	Calculation of Light-Driven Potentials	37
b.	Redox potentials of Light-Generated Biochemicals	44
5.	Irreversible Thermodynamics of the Biochemical Pathways	49
a.	Optimal Design for a Biochemical Pathway	49
b.	Experimental Tests of Diffusive Behavior	55
c.	Dynamic Response	56
	References	60
B.	Thermodynamic Limitations on the Conversion of Radiant Energy into Work	63

		Page
II.	PARAMAGNETIC RESONANCE OF TRANSITION METAL COMPLEXES HAVING BIOLOGICAL INTEREST	70
A.	Applications of EPR in the Investigation of Biological Metals	71
1.	Introduction	71
2.	Limits on the Observation of Metal Ion EPR	77
a.	Spin-Lattice Relaxation	77
b.	Effects of Sample Condition	79
3.	Survey of the EPR of Biological Metal Complexes	84
	References	102
B.	Dipolar Broadening of EPR Spectra Due to Solute Segregation in Frozen Aqueous Solutions	107

PART I

THE QUANTUM CONVERSION PROCESS OF PHOTOSYNTHESIS

A. Applications of Thermodynamics to the Investigation of Photosynthesis

Chapter 1

INTRODUCTION

Photosynthesis* by green plants converts radiant energy in the wavelength region from 4000 Å to 7000 Å into chemical free energy. A photon having a wavelength of 7000 Å has an energy of 1.8 electron volts, but manometric measurements of oxygen evolution indicate that only about 0.6 eV per quantum absorbed is stored as free energy in the form of stable chemical products. The original motivation for the work in Part I of this thesis was a desire to account for the "missing" 2/3 of the photon's energy.

The energy conversion process of plant photosynthesis is summarized in Figure 1-1. Light energy is captured by several types of pigment molecules, the most important of which is chlorophyll. The absorption of a photon causes the excitation of a chlorophyll molecule from its ground electronic state to the first excited singlet state. This excitation is then transferred in some manner to a site of chemical conversion; this transfer process is not well understood.

Relatively immediate consequences of this chemical conversion are the phosphorylation of ADP, giving packets of biological energy in the form of molecules of ATP; and the oxidation of water to molecular oxygen, with the production of packets of biological reducing power in

*References 1-5 are the books and review articles most pertinent to the material discussed in this thesis. References 6 and 7 are encyclopediac surveys of photosynthesis.

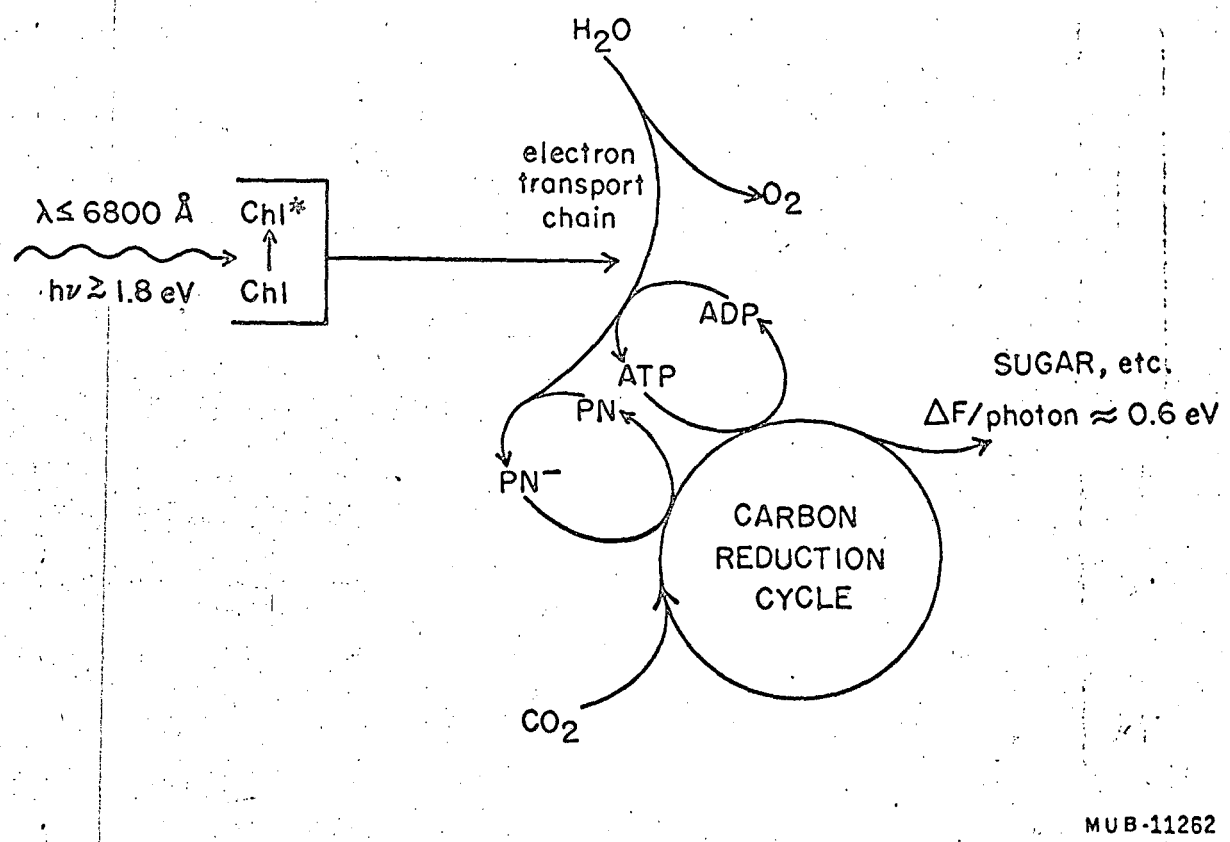

Figure 1-1. Schematic diagram of the energy conversion process of plant photosynthesis.

the form of pyridine nucleotides. These soluble, diffusible packets of energy and reducing power are then used to drive the carbon reduction cycle, which takes carbon dioxide and converts it into sugars, amino acids, and the like.

In addition to this photosynthesis by plants, with which we are more familiar, light is also used for chemical synthesis by several kinds of bacteria. These bacteria may be divided into two classes: red bacteria and green bacteria. The red bacteria use wavelengths out to 9000 Å or so for photosynthesis, and the green bacteria use light out to about 8000 Å. While plants can oxidize water to obtain the electrons necessary for biological reductions, the bacteria cannot; they must rely on an external source of reducing power such as hydrogen sulfide, other sulfur compounds, or externally obtained organic compounds such as acids or alcohols.

What can cause the difference between the 1.8 eV of energy contained in a 7000 Å photon, and the 0.6 eV of free energy stored by a plant per photon? Much of the difference between these two figures is lost in the complex biochemical pathways between the absorption of light and the output of carbohydrate; we will consider these losses in Chapter 5, but in the meanwhile we shall be concerned with two "losses" which are incurred immediately upon absorption of the light.

The first of these is simply a consideration of the entropy associated with the absorbed radiation; in other words, ΔE is not equal to ΔF. The first worker to consider this limitation on the energy conversion process of photosynthesis was the Dutch biologist L. N. M. Duysens,[3,8] who did so by a general and somewhat intuitive thermodynamic approach which is strictly applicable only for systems

which absorb only in a narrow frequency range. Since then, Mortimer and Mazo[9] and Bell[10] have considered the thermodynamics of monochromatic radiant energy conversion in a more general context; their work has expressed Duysen's insight in more formal terms, but it has not altered the basic argument. Application of the narrow band theory to photosynthesis requires some extensions in order to make it applicable to photochemical systems absorbing over broad bands; this will be considered in Chapter 2.

The second immediate loss is due to a degree of irreversibility which is necessary to cause a net flow of energy into any radiation absorber. If an absorber were in equilibrium with a radiation field, then it would reradiate at the same rate at which it received photons, meaning that the quantum yield for energy storage processes would be zero. In order to get a net retention of photons, the entropy of the absorber must be greater than the entropy of the radiation field. This loss was considered in an electrical engineering context by Shockley and Queisser.[11] In a paper[12] which is presented as Part I.B. of this thesis, I recently considered this and other losses for the general problem of radiant energy conversion; that work was undertaken with the photosynthesis problem in mind, and this Part of this thesis represents an extension on that paper.

During the extension of the theory to broad band systems in Chapter 2, we will consider some relationships between absorption spectra and luminescence spectra, and the effect which these spectra have on the chemical potential which is developed in a photochemical system. In Chapter 3 we will consider some of the available information on the absorption and fluorescence spectra of photosynthetic systems, and relate them to the theory developed.

In Chapter 4 we will use the theory of Chapter 2 and the spectra of Chapter 3, together with a little data on the intensities of the light fields in which photosynthesis operates, in order to calculate chemical potentials developed in different photosynthetic systems. These are then related to observed potentials, and the agreement is found to be rather good.

In Chapter 5 we sketchily consider the problem of the design of biochemical pathways, and the losses which are incurred between the absorption of light and the storage of carbohydrate. Some simple, thermodynamically motivated models for the behavior of this system help to account for the light saturation behavior of photosynthetic systems, and for the decay kinetics observed for chemiluminescence.

Chapter 2

THEORY OF THE PHOTOCHEMICAL CONVERSION OF LIGHT INTO WORK

a. Heuristic Theory for a Narrow-Band Absorber

Before starting a formal treatment of the thermodynamics of free energy storage in a general, broad-band-absorbing photochemical system, it may be useful to review the theory for narrow-band absorption, particularly as it applies to photochemical systems. A formal treatment of the narrow-band theory may be found in Part I.B., but for the next few pages we will make a somewhat informal and hopefully heuristic development of the theory. The formulas and arguments of the next few pages are selected for their familiarity to most chemists; they contain within them the assumptions that Boltzmann statistics apply, and that the different rate processes involved are first order. Actually the results are more general than one would infer from these assumptions.

For a concrete example of a narrow-band photochemical system, the reader is invited to consider a vapor of sodium atoms, dilute and in a very large box so that collisions are infrequent. Light at 589 nm* shining on this gas will excite atoms from the ground to an excited electronic state, and resonance fluorescence will return excited atoms to the ground state.

As light absorption greatly increases the population of the excited state over the population present thermally, there will be a free energy change associated with the transfer of an atom from one electronic state to the other. In analogy with the Nernst equation

---

*1 nm (nanometer) = 1 mμ = 10 Å

of freshman chemistry, the free energy change associated with the transfer of an atom from the excited state to the ground state is equal to

$$\mu = h\nu + kT \ln(P^*/P), \qquad (2\text{-}1)$$

where P and P* are, respectively, the population of atoms in the ground and excited electronic states. The thermodynamic potential, μ, is defined as dA/dN, where A is the Helmholtz free energy, E - TS, and N is the number of transfers from the excited to the ground state. (Since there are no substantial net volume changes in photosynthesis, we can neglect the distinction between energy and enthalpy, and refer to the more familiar ΔF rather than ΔA.)

As we can see, this chemical potential is determined by the frequency of absorption, ν, and by P*/P. This latter is in turn determined by a steady-state relationship between the rate of absorption and the rate of emission. The rate of absorption is determined by the light intensity and by the absorption cross-section, while the rate of emission is controlled by the radiative lifetime. At any given ν, however, the relative sizes of the absorption cross-section and the radiative lifetime are fixed by the Einstein coefficients. A more fundamental way of saying this is to note that the effective areas for absorption and emission must be identical. As a result, the chemical potential developed is independent of either, and depends only on the light intensity at the frequency of absorption.

What is the dependence of the potential on light intensity? Formally the relationship is very direct, as we shall see in the next section, but in order to stay with familiar formulas we use a more

indirect approach now: If our box of sodium atoms were placed in a blackbody with temperature T_R, then we know that

$$P^*/P = \exp(-h\nu/kT_R) \ . \tag{2-2}$$

Since the sodium atoms are sensitive to radiation only over a very narrow frequency range, the population of the excited state will also be given by (2-2) whenever the vapor is in a radiation field which has the same radiation intensity at 589 nm as does a blackbody at T_R. One can then describe this radiation field as having a temperature of T_R at 589 nm. It need not have the same temperature at, say, 700 nm.

By plugging (2-2) into (2-1), we see that

$$\mu = h\nu(1-T/T_R) \ , \tag{2-3}$$

where the potential is defined relative to temperature T.

The relationship between the radiation intensity and T_R is given by the Planck radiation law , which is that

$$I = (8\pi\nu^2/c^2)[\exp(h\nu/kT_R) - 1]^{-1} \tag{2-4}$$

where I is the light intensity in units such as photons per cm^2sec per unit bandwidth per 4π solid angle. (Refer to Part I.B. for a more complete discussion.)

So far we have only considered the absorption and the resonant fluorescent emission of radiation, with no provision for the storage of free energy. Now let's add another gas to our box of sodium atoms. By interacting with this "quenching" gas, sodium atoms in the excited state are returned to the ground state non-radiatively. This process

of non-radiative decay is coupled to, and can drive, an endothermic chemical reaction for which the ΔF is equal to the potential difference between the excited and ground states, μ.

The amount of chemical work done per quantum absorbed by the sodium gas will be equal to the product of the quantum yield for the energy storage process, and the light-driven chemical potential. In designing a system for the conversion of light into work, one would seek to maximize this product. Because of the competitive advantage which a plant with a more efficient energy conversion system would have, we anticipate that photosynthetic systems will have this product nearly maximized also.

In the presence of the quencher, the quantum yield for luminescence will be

$$\phi_{lum} = P^*/P^*_{max} , \qquad (2\text{-}5)$$

where P^* is the population of the excited state in the presence of the quencher, and P^*_{max} is the population in the absence of the quencher. The quantum yield for the energy storage pathway is then

$$\phi_{st} = 1 - P^*/P^*_{max} . \qquad (2\text{-}6)$$

The decrease in P^* due to the non-radiative pathway causes a decrease in the potential difference between the excited and ground states. From (2-1) we can write

$$\mu = \mu_{max} + kT \ln(P^*/P^*_{max}) , \qquad (2\text{-}7)$$

where μ_{max} is the light-driven potential in the absence of quenching.

Note that if the population of the excited state is not decreased substantially by the introduction of quenching, then the quantum yield for energy storage is relatively low, resulting in little energy storage. Note also that if the population of the excited state is decreased drastically, then the potential difference will drop significantly, also reducing the amount of power stored. There exists an optimal P* for maximum free energy storage, and this may be easily found by taking the product of (2-6) and (2-7), and setting the differential with respect to p* equal to zero.

Doing this, we find that for maximal power storage,

$$\frac{P^*_{max}}{p^*} = \frac{\mu_{max}}{kT} - \ln \frac{P^*_{max}}{P^*} - 1 . \qquad (2\text{-}8)$$

The leading term in this expression is the most significant, and for illustrative purposes we need consider only it. In the visible region, the potentials developed are about one electron volt, which is about 40 kT. Plugging this back into (2-5), we see that in our ideal system the luminescence yield should be about 2% for maximal power storage.

By substituting the leading term of (2-8) into (2-7), we find that the optimum potential is given by

$$\mu_{opt} \approx \mu_{max} - kT \ln(\mu_{max}/kT) . \qquad (2\text{-}9)$$

Now kT ln40 is about 1/10 eV, and this represents most of the loss due to this basic irreversibility.

So far we have neglected the possibility that there might be nonradiative decay which is not coupled to energy storage, and in any

real system there will be some of this. The effect of this decay is easily included in the theory: If the total rate of non-useful decay from the excited state is α times the rate of radiative decay alone, then the population of the excited state in the absence of energy storage will be reduced by a factor of α, so that μ_{max} will be decreased by $kT \ln\alpha$. When this kind of decay is present, equation (2-5) represents the quantum yield for all non-energy storing processes, rather than the quantum yield for luminescence.

With this much as background, we can consider the general broad-band theory with better understanding.

b. Formal Theory for a Broad-Band Absorber

The theoretical limits on power storage resulting from narrow-band absorption, which were sketched in the previous section and are discussed more fully in Part B, may be applied to a broad-band absorber by appropriately averaging the monochromatic limit over the frequency interval of absorption: The resulting limit has great generality, but some consideration of the structure of the radiant energy converter may permit a significantly lower limit to be set on the fraction of light energy which may appear as stored free energy. In addition, one may obtain a considerable amount of additional physical information.

First one must analyse the manner in which the absorbed quanta will be used. Fundamentally there are two types which we might consider: One would be where the absorbed energy is used as heat; in this thesis we are more interested in another kind of conversion, where excitations produced by the discrete quanta of light are utilized.

The most fundamental feature of these quantum, or photochemical, radiation conversion systems is the equality of quanta of different wavelengths. If one has a broad absorption extending from 400 nm to 700 nm, a quantum absorbed at 400 nm has the same net effect as a quantum absorbed at 700 nm. It is this equality of quanta which is the starting point for a consideration of the thermodynamics of these systems.

The purpose of this section is to discuss the limits on the amount of work appearing as a result of the broad-band absorption of light by any photochemical system. Shockley and Queisser[11] have considered such a limit on radiant energy conversion in non-degenerate semi-conductors, and the present work represents a generalization of this. The discussion in this section is independent of the structure of the photochemical system, and does not contain the limitations of the previous section.

Imagine that the ground and excited states of the sodium atoms of the previous section are generalized so that each of the two electronic states contains any arbitrary number of sub-states, at arbitrary energies, due to the presence of vibrational or other degrees of freedom.

If the sub-states within each band are in thermal equilibrium, meaning that there are no variations in thermodynamic potential within each band, then the potential difference between sub-state i of the ground electronic state and sub-state j of the excited electronic state will be independent of either i or j. In other words, there will be a single, well-defined free energy change for any possible transition between the bands.

We shall examine the validity of the assumption of thermal equilibrium within the bands later.

Evaluation of maximum potential

Our first task is to evaluate the potential difference which is developed between the excited and ground bands in the absence of non-radiative transfer between the two.

The potential of the photochemical system can be most easily evaluated when it is in equilibrium with a radiation field. Thus one needs to inquire what radiation field is in equilibrium with an absorber which has a potential difference independent of frequency.

For the interaction to be reversible at all frequencies, it must be reversible at each frequency, so we can reduce the problem to an examination of equilibrium between a radiation field and an absorber in a small frequency increment at each ν.

Reversible reaction implies that there is no change in entropy for the emission or absorption of radiation by the chemical system:

$$(\partial S/\partial N)_{absorber} + (\partial S/\partial N)_{radiation} = 0 . \qquad (2\text{-}9)$$

The potential difference of the photochemical system is

$$\mu = \partial E/\partial N - T\, \partial S/\partial N . \qquad (2\text{-}10)$$

We know that

$$\partial E/\partial N = h\nu \qquad (2\text{-}11)$$

so that

$$\partial S/\partial N = (h\nu - \mu)/T \qquad (2\text{-}12)$$

For the radiation field, the partial entropy is

$$\partial S/\partial N = -(\partial E/\partial N)/T_R \qquad (2\text{-}13)$$

where $T_R(\nu)$ is the radiation temperature which we discussed earlier.

By substituting (2-4) into (2-13), we find that

$$-\partial S/\partial N = k \ln(1+8\pi\nu^2/c^2 I) \qquad (2\text{-}14)$$

where I is the light intensity absorbed and emitted due to band-to-band transitions (as before, in units of photons per 4π solid angle, per unit bandwidth, per unit area, per unit time).

If we assume that the photochemical absorber is isotropic in its interaction with a radiation field, then by integrating over solid angle, and equating (2-12) and (2-14), we find that the rate of photon absorption and emission per unit bandwidth and unit cross-section is

$$I(\nu,\mu,T) = 8\pi\nu^2/c^2 \{\exp[(h\nu-\mu)/kT]-1\} . \qquad (2\text{-}15)$$

The figure one in (2-15) may be neglected in the visible region, simplifying (2-15) to

$$I(\nu,\mu,T) = (8\pi\nu^2/c^2) \exp[(\mu-h\nu)/kT] . \qquad (2\text{-}15')$$

If one knows the absorption cross-section for band-to-band excitation, $A(\nu,\mu,T)$, then the total rate of excitation and emission per unit bandwidth is equal to

$$A(\nu,\mu,T)\ I(\nu,\mu,T) \qquad (2\text{-}16)$$

for a photochemical system which has thermal equilibrium at temperature T within its electronic bands, and a potential difference μ between the bands, and which is in equilibrium with an isotropic radiation field at all frequencies.

Now consider that the same potential difference μ is established between the bands of the same chemical system by any manner whatsoever. This may be done by causing the same rate of excitations with an arbitrary radiation field, or even by pumping the system electrically or chemically. Regardless of how the potential is established, the emission spectrum must still be given by (2-16).

This means that, given thermal equilibrium within each band, knowledge of the absorption spectrum of any chemical system permits direct calculation of the luminescence spectrum. This relation has a fairly long and interesting history, none of which I had heard until after having derived the relation myself. It was first derived by Kennard[13] at Cornell in 1918, and he confirmed it experimentally with several dye molecules in solution. The relationship was then rediscovered independently by two Russian physical chemists, the first of which to publish was Stepanov.[14] It has been used fairly extensively by Russian physical chemists for calculating the luminescence spectra of organic molecules, and comparing these with the observed luminescence spectra.[15,16] This history of the relation has been reviewed by Mazurenko and Reporent.[16] In spite of the usefulness of the relation, it does not seem to have been used recently be molecular spectroscopists outside of the U.S.S.R.[17]

The relation was also derived, again independently, for a more restricted situation by van Roosbroeck and Shockley.[18] This has been used for calculating the spectral distribution of the radiation from the recombination of electrons and holes in semiconductors.[19]

The experimental work by the Russian workers has shown that the assumption of thermal equilibrium within the electronic bands of a

large organic molecule is fairly accurate.[20] The slight discrepancies which are observed are not sufficient to affect our calculations of potential, but they may affect the accuracy of calculated luminescence spectra.

We will now use this Planck law relationship to calculate the potential developed in a photochemical system when the absorption spectrum and incident light flux are known. For simplicity we shall assume that the absorption spectrum is independent of μ, although this may not be true. We can ignore changes with temperature since our T remains fixed.

The rate of band-to-band excitations resulting from an arbitrary radiative field is equal to

$$R_{in} = \int A(\nu) I_S(\nu) d\nu \ . \qquad (2\text{-}17)$$

where $I_S(\nu)$ is the flux distribution provided by the light source.

From (2-16), with (2-15') substituted in, the rate of radiative decay from a photochemical system having potential difference μ is

$$R_{lum} = [\exp(\mu/kT)] \int (8\pi\nu^2/c^2) A(\nu) \exp(-h\nu/kT) d\nu \ . \qquad (2\text{-}18)$$

We shall abbreviate the integral with L, so that

$$R_{lum} = e^{\mu/kT} L \ . \qquad (2\text{-}18')$$

By equating (2-17) and (2-18'), we can find the maximum possible potential of a photochemical system having an absorption spectrum $A(\nu)$, and illuminated by a radiation field of intensity and distribution $I_S(\nu)$:

$$\mu_{max} = kT \ln(R_{in}/L) \ . \qquad (2\text{-}19)$$

Maximum power storage

The potential μ_{max} was derived for the condition that the rate of luminescence equals the rate of absorption. As we saw earlier there is no net storage of energy in this situation. Net storage must be obtained by lowering the potential so that the rate of luminescence will be less than the rate of absorption.

The amount of power stored is

$$P = (R_{in} - R_{lum})\mu , \tag{2-20}$$

where μ is the potential of the photochemical system.

By combining (2-18') and (2-19), we find that

$$R_{lum}/R_{in} = \exp[(\mu-\mu_{max})/kT] , \tag{2-21}$$

so that

$$\mu = \mu_{max} + kT \ln \phi_{lum} , \tag{2-22}$$

where ϕ_{lum} is the quantum yield for luminescence, R_{lum}/R_{in} .

The amount of power stored, which may be rewritten as

$$P = R_{in}\, \mu\, (1-\phi_{lum}) , \tag{2-23}$$

may be maximized by appropriate choice of μ. By setting $dP/d\mu$ equal to zero, we find that for maximum power storage

$$1/\phi_{lum} = \mu_{max}/kT + \ln \phi_{lum} - 1 . \tag{2-24}$$

The potential for maximum power storage may be obtained by substituting ϕ_{lum} from (2-24) into (2-22).

As you can see, this more general derivation is very analogous to the less formal treatment which appeared earlier in the chapter.

I haven't figured out a neat way of expressing non-useful non-radiative decay in terms of potentials instead of populations. We can note that the potential μ_{max} of this section may be corrected downward by $kT \ln\alpha$, where the total rate of non-useful decay of the excited state is equal to α times the rate of radiative decay. In general, α may depend on μ.

c. Losses from Slow Excitation Transfer

At this point we can consider one kinetic limitation on the amount of power stored. This relates to the finite rate of transfer of the excitation from the absorbing pigment molecules into species which do not interact significantly with a radiation field. Strictly speaking, perhaps this discussion should be in Chapter 5, where we will consider other kinetic limitations on power storage, but this particular problem is easily treated in the present context.

Consider that we have the situation diagrammed in Figure 2-1(a). Here the excited state of the pigment molecules Chl* is in thermal equilibrium with a trap state. As diagrammed, the trap might be a triplet state of the pigment molecule, or some isomerization of it, but actually the arguments which we will make apply equally to chemical reactions where the trap is a distinct chemical species.

Excitations are transferred from the excited state to the trap with what we assume to be a first-order rate constant, K_{tran} ; since Figure 2-1(a) describes an equilibrium situation, the return rate must be the same. The chemical potential of the trap will be the same as the excited state, μ_{max}. The population of the excited state is P^*_{max}, and the rate of excitations is equal to the rate of radiative and non-radiative decay, $\alpha K_{rad} P^*_{max}$.

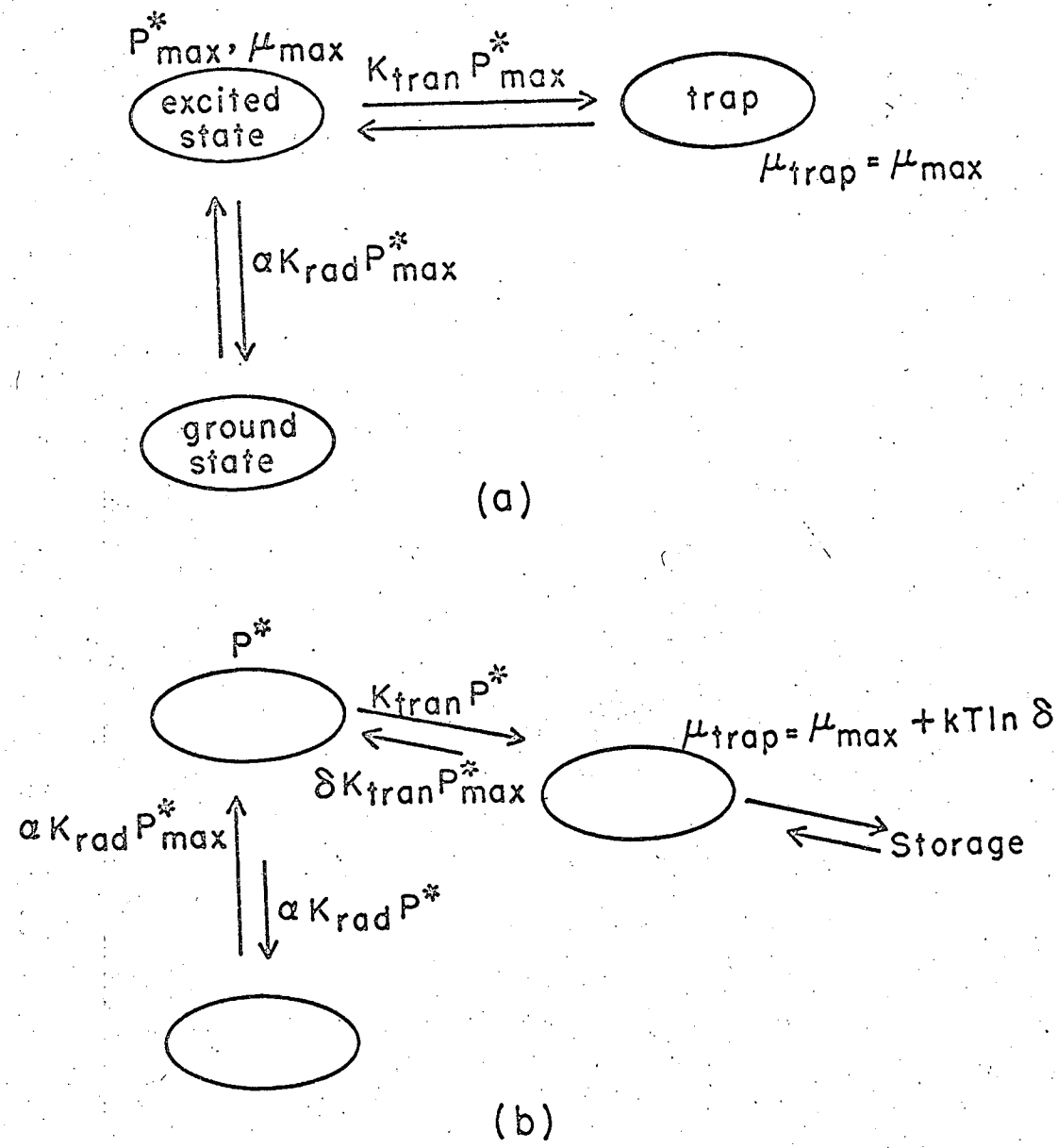

MUB-11266

Figure 2-1. Kinetics and thermodynamics of a photochemical system (a) in the absence of energy storage, and (b) in the presence of energy storage when the thermodynamic activity of the trap is a fraction δ of that in (a).

Now consider that excitations are tapped from the trap for storage, so that the thermodynamic activity (e.g., the concentration) of the trap species drops to some fraction, δ, of the activity which would be in equilibrium with an excited state population of P^*_{max}. The resulting situation is diagrammed in Figure 2-1(b).

The rate of the reverse reaction Trap → Chl* is dropped to $\delta K_{tran} P^*_{max}$, causing the population of the excited state to drop to P^*. The quantum yield for storage is, as before,

$$\emptyset_{st} = 1 - P^*/P^*_{max} , \qquad (2\text{-}6)$$

but our object in the current situation is to maximize the power stored as measured at the trap: in other words, to maximize the product $\emptyset_{st}\mu_{trap}$.

By equating the fluxes into and out of the excited state, we find the relationship

$$\alpha K_{rad}(P^* - P^*_{max}) + K_{tran}(\delta P^*_{max} - P^*) = 0 , \qquad (2\text{-}25)$$

which can be rearranged to give

$$P^*/P^*_{max} = (\alpha K_{rad} + \delta K_{tran})/(\alpha K_{rad} + K_{tran}) . \qquad (2\text{-}26)$$

Substituting (2-26) into (2-6), we find that the quantum yield for power storage is

$$\emptyset_{st} = [K_{tran}/(\alpha K_{rad} + K_{tran})](1 - \delta) . \qquad (2\text{-}27)$$

The expression within the brackets is the usual kinetically determined quantum yield in the absence of any reversibility in the Chl*, Trap reaction (i.e., $\delta = 0$).

On the other hand, the expression $(1 - \delta)$ is thermodynamically equivalent to the $(1 - P^*/P^*_{max})$ of (2-6). In other words, the quantum yield for energy storage factors into two independent fractions, one of which is determined kinetically and the other of which is determined thermodynamically. Derivation of the optimal μ_{trap} and maximal power storage is equivalent to the earlier treatments where the excited state itself was considered. The only difference is that the quantum yield is lowered by the kinetic factor shown in (2-27).

When the kinetic and thermodynamic factors of (2-27) are both close to one, then the loss quantum yield is approximately

$$\phi_{loss} \approx \alpha K_{rad}/(\alpha K_{rad} + K_{tran}) + \delta \ . \qquad (2\text{-}28)$$

The luminescence yield is $1/\alpha$ of this, or

$$\phi_{lum} \approx K_{rad}/(\alpha K_{rad} + K_{tran}) + \exp[(\mu-\mu_{max})/kT] \ , \qquad (2\text{-}29)$$

where μ_{max} is the maximum potential corrected for the presence of non-radiative losses.

The first term in (2-29) is due to the finite rate of transfer out of the excited state, and the second is due to the reversibility of the system. As the kinetic term represents spin-allowed light emission which is independent of any chemistry, this portion of the light emitted under steady-state illumination may quite properly be called fluorescence. However, the thermodynamic luminescence <u>is</u> dependent on chemistry and, furthermore, cannot be expected to decay rapidly and exponentially when the illumination is turned off; thus it is hard to call this fluorescence.

To the extent that our assumption of thermal equilibrium within the electronic bands is valid, the spectra of the two types of luminescence should be the same, and no distinction can be made at that level. As we shall discuss more fully in later chapters, experimental discrimination between the two would be very useful.

Chapter 3

CALCULATED LUMINESCENCE SPECTRA OF PHOTOSYNTHETIC SYSTEMS

The first use which we can make of the theory in Chapter 2 for photosynthesis is to use the Planck law relationship between absorption and luminescence in order to calculate the luminescence spectra of photosynthetic systems from the absorption spectra. Where the fluorescence spectrum* is known, this provides one check on our assumption of thermal equilibrium among the vibrational levels within the electronic bands of the pigments. Where the fluorescence spectrum is not known, the theory can predict it and, hopefully, make its experimental detection easier.

The theoretical predictions have particular interest in plant systems, because plants are comprized of two somewhat different photochemical systems. Because of the relative complexity of plant photosynthesis, we first consider another class of photosynthetic organisms, the bacteria, so that we may compare absorption spectra and fluorescence spectra directly.

a. Bacterial Luminescence

For the purpose of comparing predicted fluorescence with measured fluorescence spectra, we are fortunate that Olson and Stanton[20] have recently published absorption and fluorescence spectra for several species of bacteria. By using their absorption spectra

---

*operationally, the emission spectrum observed under steady illumination

together with the Planck factor, one may compute the fluorescence for these several species. The results of this calculation are compared with experiment in Figure 3-1.

The calculated and observed spectra have been normalized so that their peak heights match. We see that the agreement between experiment and theory is good but not outstanding. There are four sources for the discrepancy between the calculated and experimental spectra: (1) The absorption spectra are not accurate; (2) the experimental fluorescence spectra are not accurate; (3) the experimental absorption and fluorescence spectra are not of the same material; and (4) the assumptions of the theory are not met.

(1) and (2): The data used were obtained from published curves, and a slight distortion of the curves with respect to frequency would account for much of the discrepancy.

(1): As one moves out to long wavelengths from the last absorption peak, a sizable fraction of the attenuation of a light beam passing through a biological sample is due to light scattering and not to electronic excitations. Unless this is taken into account, there can be serious errors in the calculated fluorescence spectrum at long wavelengths. The absorption spectra used were not taken with this computation in mind, and thus cannot be expected to be accurate in this region.

(2): The fluorescence spectra must be taken of intact bacteria. This makes accurate observations difficult at wavelengths where the absorption is very strong, as the fluorescence may be strongly attenuated by reabsorption. Corrections may be applied to minimize this error, but this is difficult to do precisely.

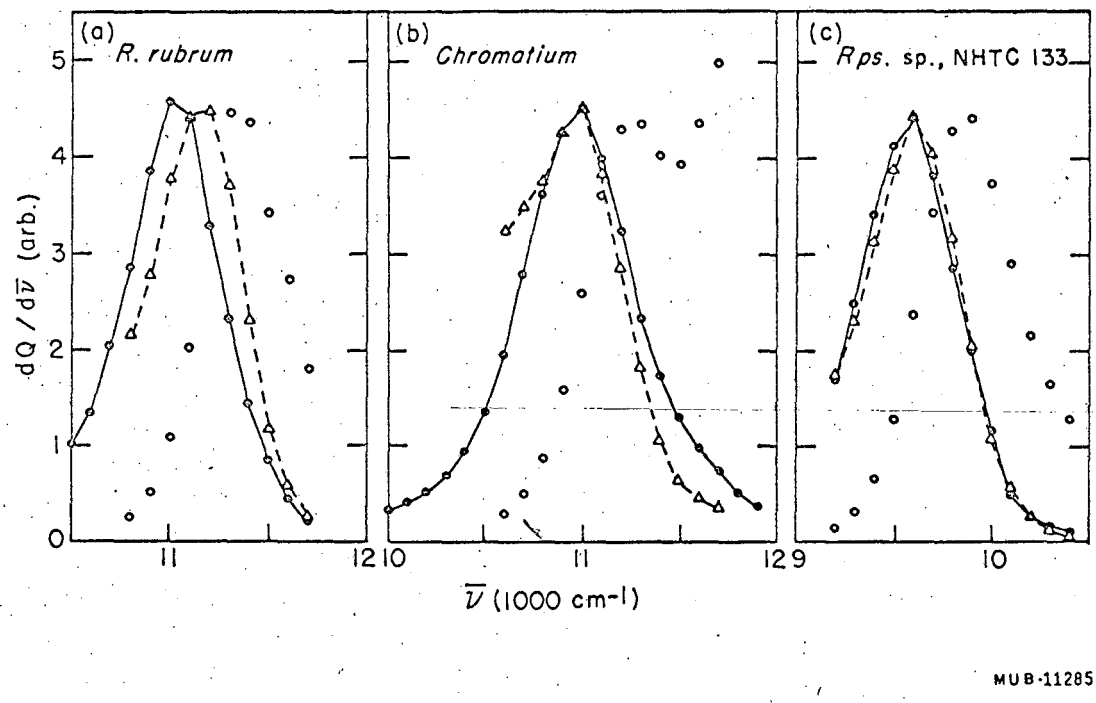

Figure 3-1. Comparison of calculated and experimental luminescence spectra of purple bacteria. Experimental absorption o and luminescence ⊙ data were taken at 100 cm^{-1} intervals from the curves of Olson and Stanton.[20] (Luminescence data in (c) from Clayton.) Solid line: experimental luminescence spectrum; dashed line: luminescence spectrum calculated from the absorption spectrum with the Planck factor for 295°K.

(3): While the fluorescence spectra are taken of intact bacteria, the absorption spectra are taken of smaller particles; this probably does not introduce any serious error. It must be kept in mind that different growth conditions for the samples used for the two measurements may cause a discrepancy.

(4): Last but not least, the assumption of thermal equilibrium within the electronic bands is not precisely true. If thermal equilibrium held exactly within the vibrational bands, then the electronic absorption spectrum, the action spectrum for the excitation of fluorescence, and the activation spectrum for chemical synthesis would correspond precisely.

Of these, the absorption spectrum and the fluorescence excitation spectrum are the most easily obtained. The two do not correspond exactly at all wavelengths for purple bacteria, although most variations are within 10% or so.

Perhaps the most dramatic demonstration of the lack of complete thermal equilibrium in a photosynthetic system is the recent work by Clayton[21] on the fluorescence and chemiluminescence spectra of green bacteria. Both the fluorescence and chemiluminescence spectra contain two bands, peaking at 750 and 840 nm. For fluorescence, the short wavelength peak is the higher, while for the chemiluminescence spectrum it is the lower. This is understandable if an excitation absorbed at shorter wavelengths relaxes through the excited electronic band at a rate which is not much faster than the rate of fluorescence. Conversely, and probably in addition to this effect, the production of pigment excitations by reversal of the energy storage process may cause a relatively greater luminescence at lower energies.

Conclusions

The agreement between the experimental and calculated fluorescence spectra of purple bacteria seems to be adequate to demonstrate that our assumption of thermal equilibrium is at least approximately true for photosynthetic systems. The variation which Clayton obtained between the fluorescence and chemiluminescence spectra of green bacteria indicates that the thermal equilibration is not complete, but variation between the two spectra is small enough to assure us that potentials calculated on the assumption of thermal equilibrium will not be seriously in error. The variations are great enough that computed luminescence spectra may deviate noticeably from the real thing, but where the luminescence spectrum is not known at all the calculation may be quite useful.

b. Plant Luminescence

We are very fortunate that Kenneth Sauer and several collaborators in this laboratory have recently made a number of detailed spectroscopic investigations of the photosynthetic unit in spinach. The availability of these data makes theoretical treatment of the luminescence spectra of this plant very rewarding.

For the purpose of making quantum yield measurements, Sauer and Biggins[22] made careful measurements of the absorption spectrum of the photosynthetic apparatus of spinach. Using a tabulation of their absorption data kindly provided by Professor Sauer,[23] I applied the Planck factor to calculate the luminescence spectrum which is displayed in Figure 3-2. This is the luminescence spectrum which one would expect if there were one single photochemical system in plant photosynthesis, and if the vibrational levels of this system were in

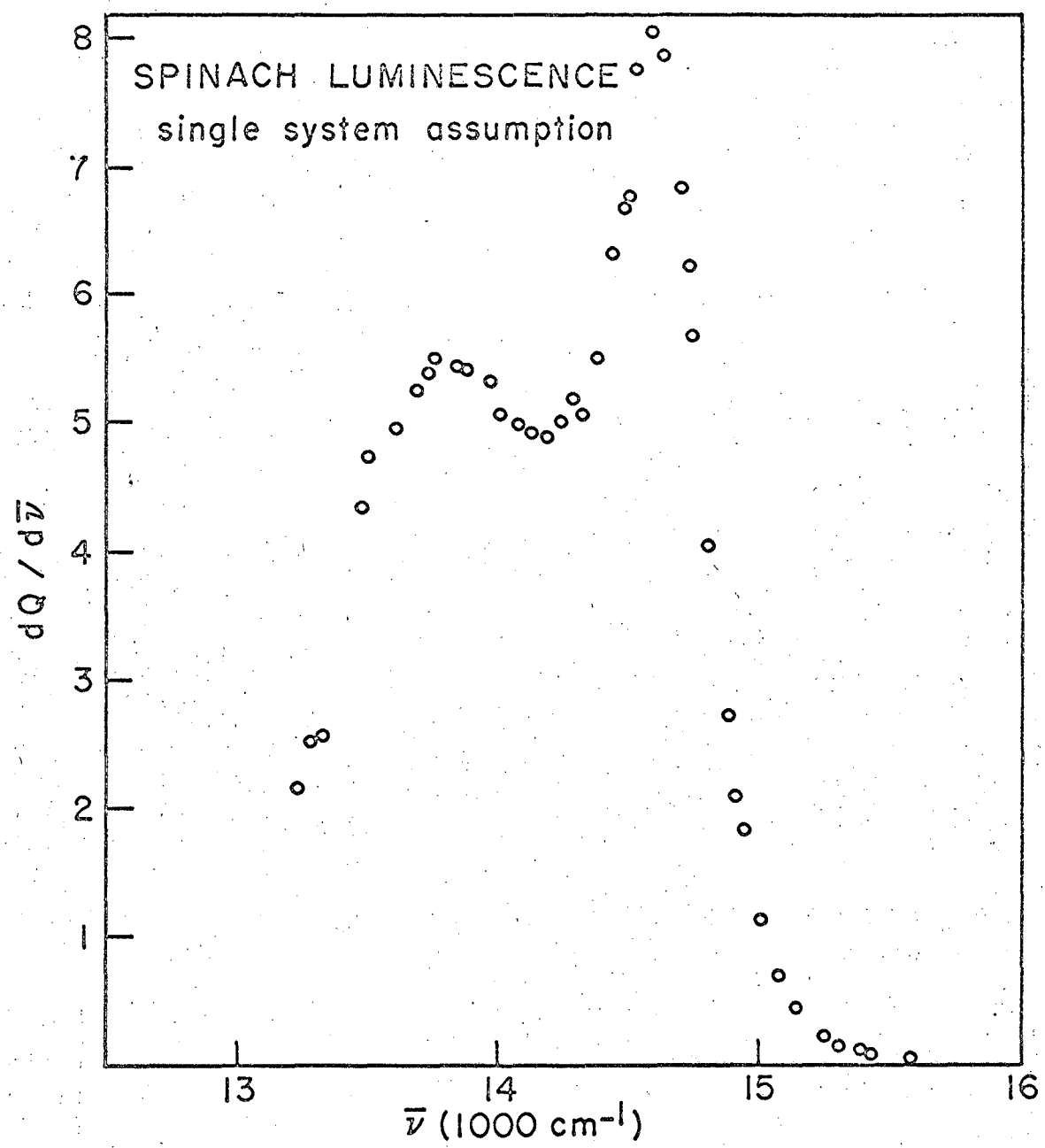

MUB-11261

Figure 3-2. The luminescence spectrum of spinach calculated with the assumption that plants contain a single photochemical system. The plotted points were obtained by multiplying the tabulated absorption spectrum of Sauer and Biggins[22,23] by the Planck law factor for 295°K.

thermal equilibrium.

However, plant photosynthesis does not appear to be comprized of one photochemical system, but rather two.[1] One of these, called System II, can be driven only with light having a wavelength less than about 680 nm; the other, called System I, can utilize radiation of longer wavelengths.

Recently Weiss[24] has reviewed the ways in which the two systems could interact at the level of electronic excitations. One possibility is that the two systems are completely distinct: the "separate box" hypothesis. One extreme of this hypothesis is the thought that the two systems may be organized in different particles. A second class of hypotheses are those in which quanta of wavelength shorter than 680 nm are alternately directed to Systems I and II by a "flip-flop" mechanism. The third class of hypotheses are those in which light of wavelength shorter than 680 nm first goes to System II; excitations in excess of the number required by this system are allowed to "spill-over" into System I.

The "separate box" hypothesis is currently the most popular, and it is the only one which I have considered in detail. At least on cursory consideration, it would seem that the "flip-flop" mechanism might be virtually equivalent for our purposes.

One of the most useful ways of separating the two chemical systems is to take a preparation of the photosynthetic apparatus of a plant, chloroplasts, and add to it metabolic poisons and spectroscopically observable redox agents with appropriate potentials. By use of the appropriate chemicals, one may observe the light driven progress of only one of the two photochemical systems.[1]

By using this technique, Sauer and Park[25] and Kelley and Sauer[26] have determined quantum yields for each of the two systems in spinach over a wide range of wavelengths. Their original data were distorted slightly because of the band pass of their instrument, but correction for this indicates that the quantum yield for System I plus the quantum yield for System II is within experimental error of 1.0 at all wavelengths.[26]

Using the assumption of separate boxes, I have smoothed their data somewhat to obtain the quantum yield partitioning diagrammed in Figure 3-3. These quantum yields may be used to calculate an activation spectrum for each of the two systems; this has been done by Kelley and Sauer, and Figure 3-4 shows this on a logarithmic plot.

Separate absorption spectra for the two systems permits a decomposition of the luminescence spectrum shown in Figure 3-2 into a component due to System I and a component due to System II. The result is displayed in Figure 3-5. The curve for System II has been magnified by a factor of 5 in order to make the area under the two curves approximately equal. If the luminescence yields for Systems I and II were about the same, then the emission spectrum of spinach should look something like the sum indicated in the figure.

The fluorescence spectrum of spinach chloroplasts has recently been measured by Murata, Nishimura, and Takamiya.[27] Comparison of their experimental spectrum with Figure 3-5 suggests that the fluorescence yield for System I is somewhat less than the fluorescence yield for System II. By adjusting the relative magnitudes of System I luminescence and System II luminescence to obtain the best fit with the experimental curve of Murata et al., it appears that the fluores-

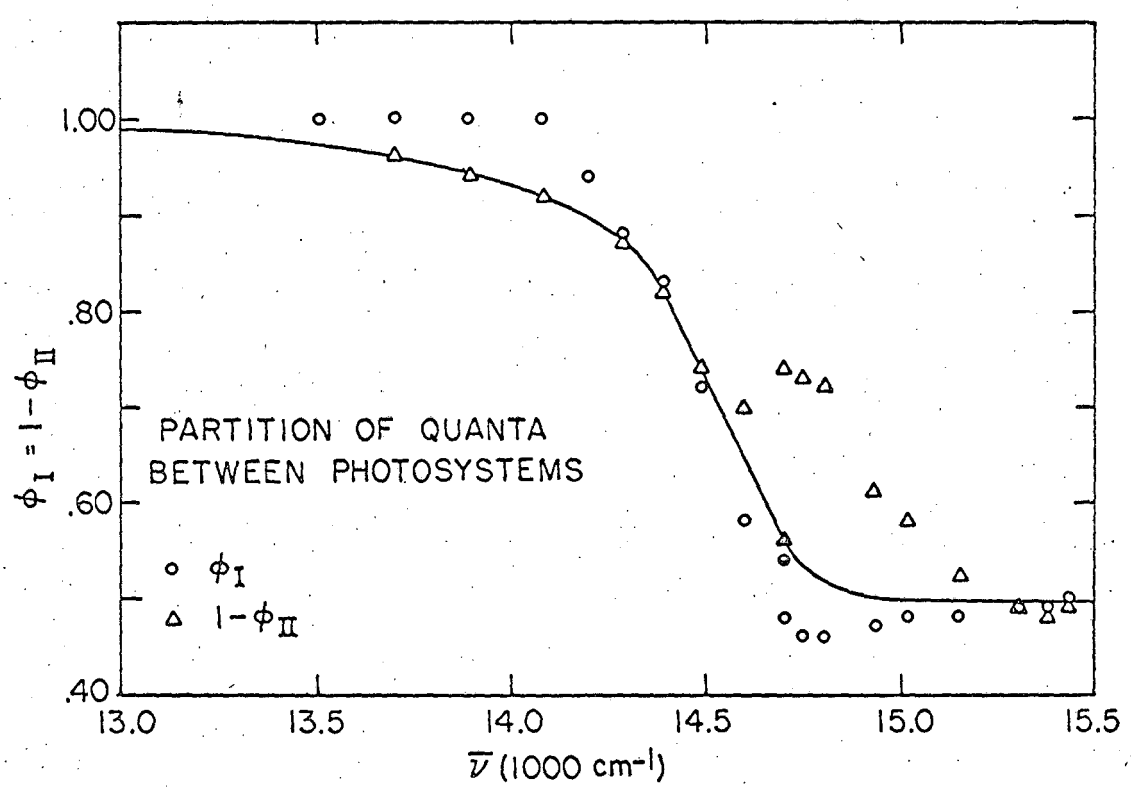

MUB-11265

Figure 3-3. Partition of quanta between photosystems I and II in spinach as a function of photon energy. Quantum yield of System I as measured by Kelley and Sauer,[26] o; difference from 1 of the quantum yield for System II as measured by Sauer and Park,[25] Δ. Filled symbols indicate corrected quantum yields obtained by extrapolating instrument band width to zero.[26] The solid line indicates the partition assumed in subsequent calculations.

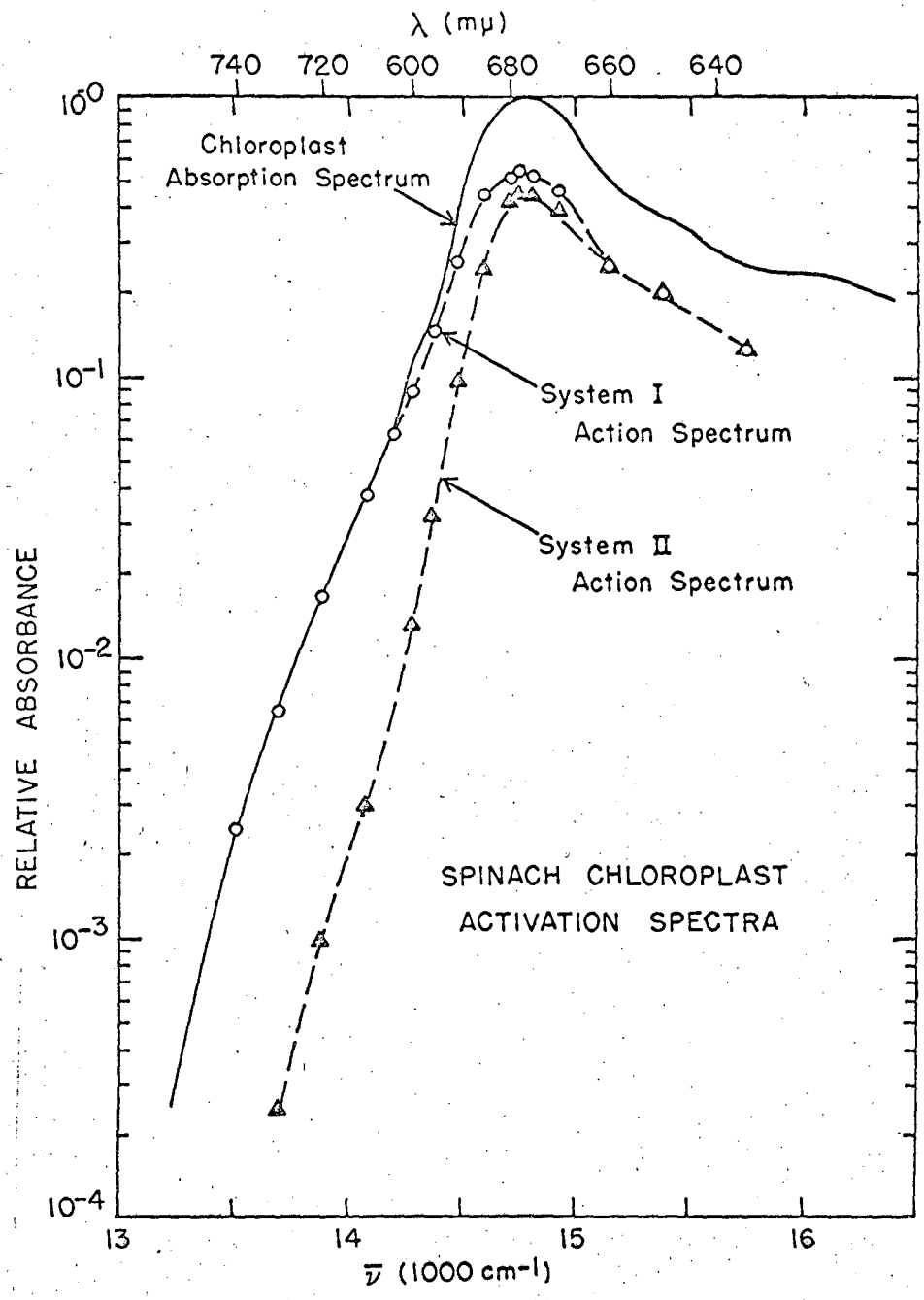

MUB-9514

Figure 3-4. Activation spectra for the two photosystems of spinach.

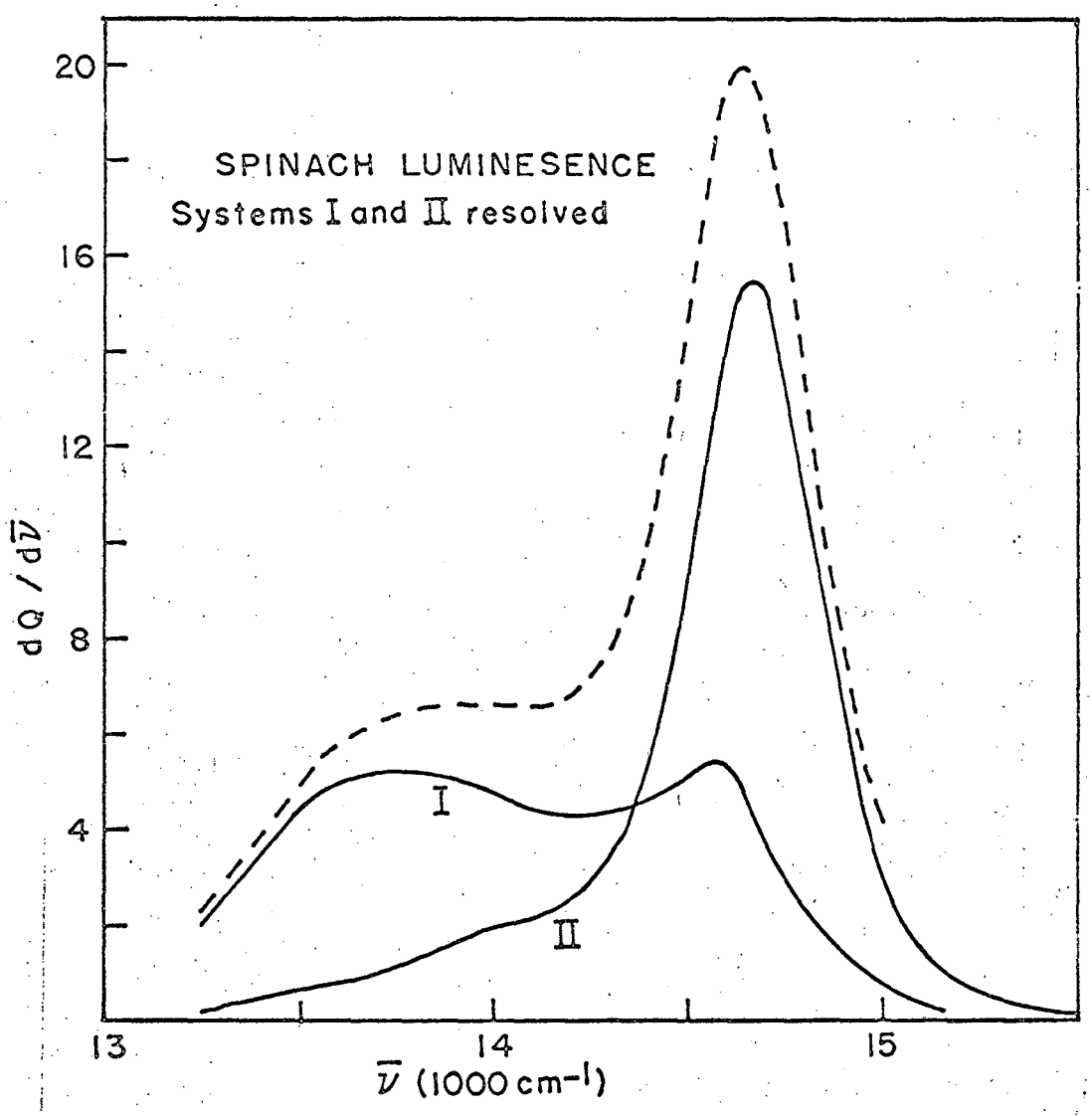

MUB-11260

Figure 3-5. Calculated luminescence spectra of Systems I and II of spinach. Vertical scale is the same as in Figure 3-3, but the curve for System II has been magnified by 5 X in order to make the area under the two curves approximately equal.

cence yield for System I is about 1/3 that of System II. The resulting fit between the theoretically calculated luminescence spectrum and the experimental spectrum is shown in Figure 3-6. Considering all the sources of error, I feel that the agreement between the two is quite good.

These calculations reinforce the notion that the fluorescence yield for System I is less than that for System II, and that the luminescence at 740 nm has a relatively greater contribution from System I than does the luminescence around 685 nm.

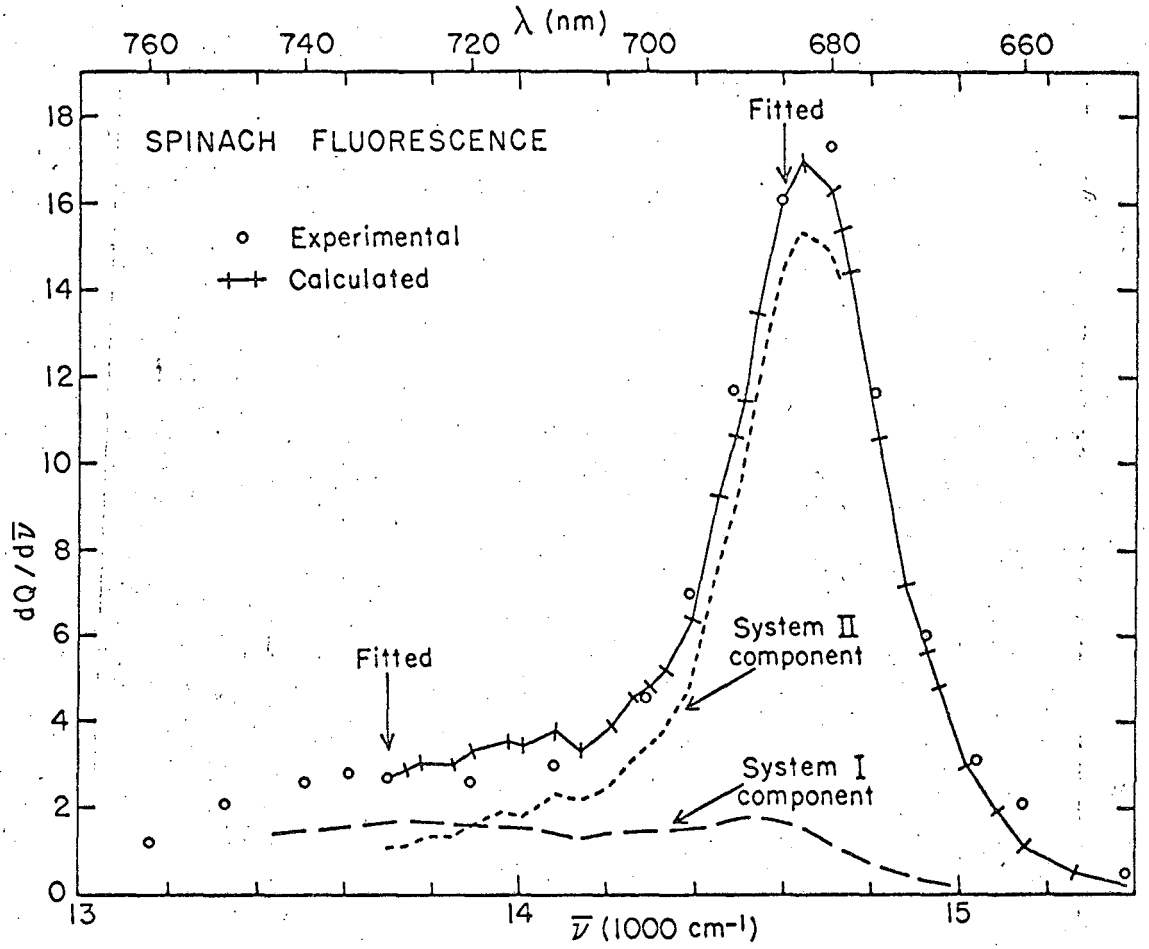

MUB-11267

Figure 3-6. Comparison of the calculated and experimental luminescence spectra of spinach chloroplasts. Experimental points from Murata, Nishimura, and Takamiya.[27] Calculated curve obtained by adjusting the amounts of System I and System II luminescence so as to match the experimental luminescence intensities at 685 nm and at 730 nm. Hatch marks indicate points at which the spectrum was calculated.

Chapter 4

LIGHT-DRIVEN POTENTIAL DIFFERENCES AND FREE ENERGY STORAGE

a. Calculation of Light-Driven Potentials

As we saw in Chapter 2, the first step in evaluating the energetics of a photochemical system is to determine the light-driven potential which is developed when the rate of luminescent emission is equal to the rate of absorption. Writing out equation (2-11) in more complete form, we have that this potential is

$$\mu_{max} = kT \ln \frac{\int A(\bar{\nu})\ I_s(\bar{\nu})d\bar{\nu}}{\int 8\pi\bar{\nu}^2 c\ A(\bar{\nu})\exp(-hc\bar{\nu}/kT)d\bar{\nu}} \qquad (4\text{-}1)$$

where I_s is the spectral distribution of photon flux incident on the system, and A is the absorption cross-section (i.e., the absorption spectrum) of the system. Since A appears in both the numerator and denominator of this expression, its absolute value is unimportant. Providing that the dimensions of the quantities involved are properly defined, these integrals may be taken over either energy (wavenumbers) or wavelength.

We see that only two quantities are necessary to evaluate the maximum potential: an incident light flux and an absorption spectrum. In order to be certain that μ_{max} is correctly evaluated, the absorption spectrum A should be taken on an organism which has been grown at light intensity I_s. Otherwise there is the possibility that an organism may vary its absorption spectrum depending on the light intensity. This has actually been observed in several species of bacteria, and the change in absorption spectra is in a direction which

would tend to keep the potential developed independent of light intensity. In the following discussion we will not be too careful about this point, partly because the data are not available, but chiefly because an error of a millivolt or so in the computed potential is insignificant when compared to other sources of error.

Once the maximum potential has been calculated, then the potential for maximum power storage can be obtained in the manner outlined in Chapter 2.

Spinach

The range of light intensities for effective plant growth is limited at the lower end by the compensation point, at which the rate of photosynthesis is just adequate to balance respiration. The upper limit is set by the saturation of the various chemical reactions which make up the energy storing process. Plants growing in dim light are usually adapted, genetically and/or environmentally, to a lower range of intensities than that found for similar organisms used to growing in bright light.[28]

The componsation point generally occurs at a light intensity of between 20 and 500 lux* of white light. Photosynthesis becomes half-saturated somewhere between 1 and 10 kilolux.[28] The spinach whose absorption we used in Chapter 3 was grown at a light intensity of about 15 kilolux.[29] However, because of the high optical density of spinach leaves, a typical photosynthetic unit might see a light intensity of more like 1 kilolux. We shall use this figure in our calculations.

---

*100 lux = 9.3 foot-candles.

By taking the product of the spectral distribution of the quantum flux from a tungsten bulb (Figure 4-1), with the absorption spectrum for spinach photosynthesis, we find that 1 kilolux of white light produces pigment excitation at the same rate as would 0.86 nanoeinsteins/cm^2sec incident at the red absorption maximum at about 680 nm. This gives us the numerator for equation (4-1), and we assume that this is split equally between Systems I and II.

The integral in the denominator of (4-1) is evaluated by finding the area under the curves in Figure 3-5, with appropriate consideration of how the vertical scale is defined. Performing the necessary arithmetic, we find that μ_{max} for System I is 1.32 eV and that μ_{max} for System II is 1.36 eV.

These potentials μ_{max} have been evaluated with the assumption that non-radiative decay is negligible. This is probably not true, and the potential must be corrected downwards accordingly. The internal conversion coefficient α which was discussed in Chapter 2 has a value _in vitro_ of 3 for the chlorophyll _a_ of plants.[30] As the fluorescing species in System II of plant photosynthesis appears to be mostly monomeric chlorophyll, we can guess that perhaps the internal conversion coefficient for this system _in vivo_ has approximately the solution value.

The fluorescence from System I occurs mostly at longer wavelengths and there is a fair amount of evidence to indicate that the species giving rise to this fluorescence are aggregated forms of chlorophyll. Pigment-pigment interactions in solution generally give rise to an increased rate of non-radiative decay, and this has been observed for chlorophyll-chlorophyll interactions. The mechanism for this increased

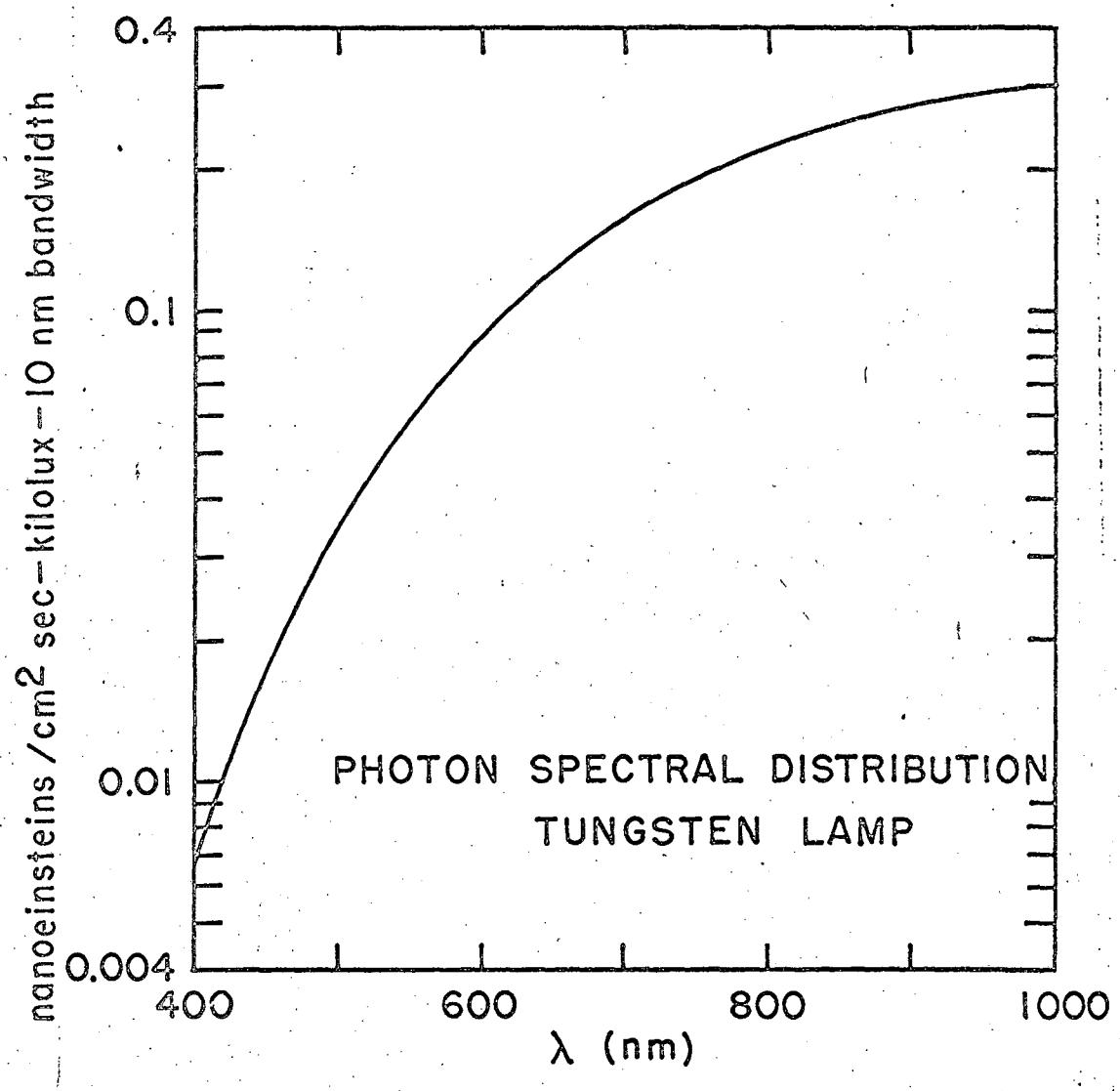

MUB-11257

Figure 4-1. Spectral distribution of photons from a high-wattage tungsten lamp. Sources: L.E. Barrow, J. Opt. Soc. Am. 49, 1122 (1959); R.B. Withrow and A.P. Withrow, in Radiation Biology, A. Hollaender, Ed. (McGraw-Hill Book Company, New York, 1956), Vol. 3, p. 249.

rate of non-radiative decay is uncertain, and it is possible that the only effect of the intermolecular interactions is to facilitate migration of the excitation to an impurity molecule which is an effective quencher. As a result, one cannot be at all certain that aggregation in a living system is indicative of a greater rate of non-radiative decay.

Recall, however, from Chapter 3 that the observed fluorescence yield of System I of spinach appears to be only 1/3 that of System II. One cause for this could be a greater rate of non-radiative decay in System I. This is fairly speculative, but for the time being we shall assume that it is true. If we assume that $\alpha = 2$ for System II and that $\alpha = 6$ for System I, then the maximum potentials for Systems I and II are 1.27 eV and 1.34 eV, respectively. Applying (2-22) and (2-24) to find the conditions for maximum power storage, we find that the optimal fraction of quanta lost for thermodynamic reasons is slightly more than 2% for each system. The optimum potentials at the trap are 1.17 eV for System I and 1.24 eV for System II.

At this point we should ask how critically dependent the amount of free energy stored is on the potential at the trap. The dependence of power stored on the potential is shown in Figure 4-2 for a μ_{max} of 1.30 eV. The potential for maximum power storage is 1.20 eV, but the potential can range between 1.12 eV and 1.24 eV with the amount of power stored remaining greater than 95% of this maximum.

Over this range in potential, the quantum yield for loss processes caused by thermodynamic reversibility ranges from 0.1% to 10%. Because power storage is so insensitive to this parameter (in the current theory at least), and because the kinetically determined

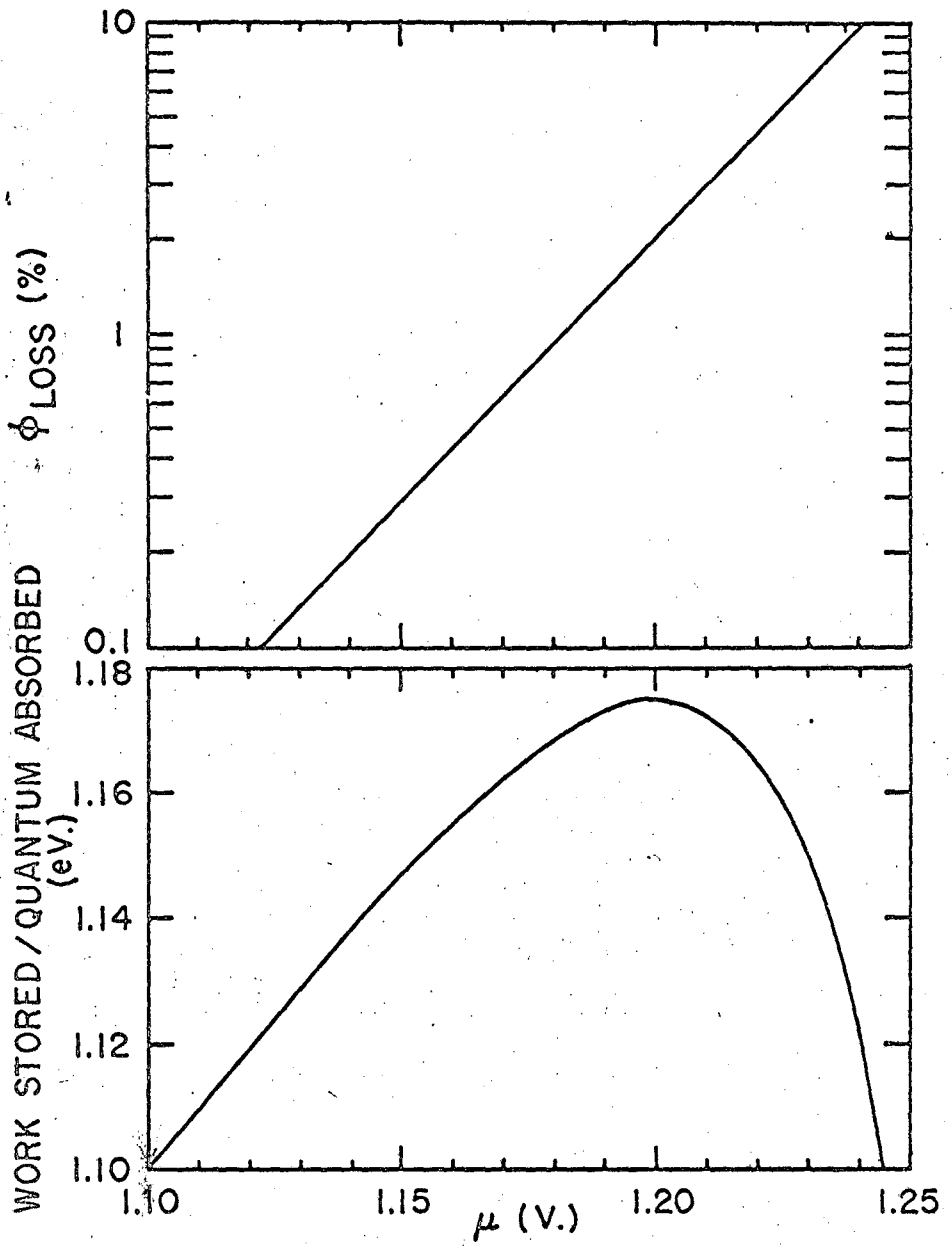

MUB-11263

Figure 4-2. Work stored and quantum yield for loss processes as a function of excited state potential when μ_{max} = 1.30 eV. Losses due to a finite transfer rate are not considered.

losses may differ between Systems I and II, we have no assurance that $\emptyset_{loss}$ should be the same for Systems I and II. For this reason, although it seems quite plausible, the assignment of a larger proportion of non-radiative decay to System I remains quite speculative with the information accumulated so far.

Purple bacteria

Unfortunately we do not know the light intensities used for growing the bacteria whose absorption and fluorescence spectra were discussed in Chapter 3. Even if we did, it is unlikely that the figure would be meaningful, as typical bacterial cultures have a high optical density, so that the mean intensity incident on a bacterium is much lower than the intensity incident on the culture as a whole.

More than 20 years ago, Katz, Wassink, and Dorrestein[31] found that the rate of photosynthesis of the purple bacterium Chromatium, as they cultured it, became half-saturated at 6 to 10 kiloergs/cm^2sec of incident sodium lamp radiation when the optical density of the bacterial suspension was low. One kiloerg from such a lamp represents 0.49 nanoeinsteins of 589 nm light.

Bacterial photosynthesis has a somewhat S-shaped dependence on light intensity, so that the efficiency of photosynthesis drops at light intensities much below the half-saturation point. For this reason we shall calculate the potential developed for 10 kiloergs/cm^2sec of sodium radiation.

For the purposes of the present calculation, we shall use the absorption and fluorescence spectra of Chromatium obtained by Olson and Stanton which were discussed in Chapter 3. The spectra of the

culture used by Katz et al. may have been different because of different growth conditions, but this should not introduce a serious error in the potential calculated.

The information necessary to evaluate the denominator of (4-1) is contained in the calculations for Figure 3-1(b). Combining all of the appropriate factors, we find that μ_{max} is 0.90 eV. The potential for maximum free energy storage is 0.81 eV and the maximum free energy storage per photon is 0.79 eV.

b. Redox Potentials of Light-Generated Biochemicals

In the previous section we found that the thermodynamic potential generated by the two systems of plant photosynthesis is about 1.2 eV, with the potential of System II being only slightly higher than System I; the thermodynamic potential developed in purple bacteria is about 0.8 eV.

When the electronic excitations carrying these potentials are converted into chemical energy, it is thought--at present at least--that the most probable immediate chemical consequence is an oxidation-reduction reaction. It is possible that one might have a conformational change using at least part of the energy relatively early in the process, but an ionization seems to be the most rapid possible, and hence preferable, first step.

If the primary oxidation and reduction steps are one electron processes, then the difference between the redox potentials of these two half-reactions should be equal to, or slightly less than, the thermodynamic potentials just calculated. One can represent the electron transport chains of bacterial and plant photosynthesis by the potential diagrams shown in Figures 4-3 and 4-4. Here the vertical

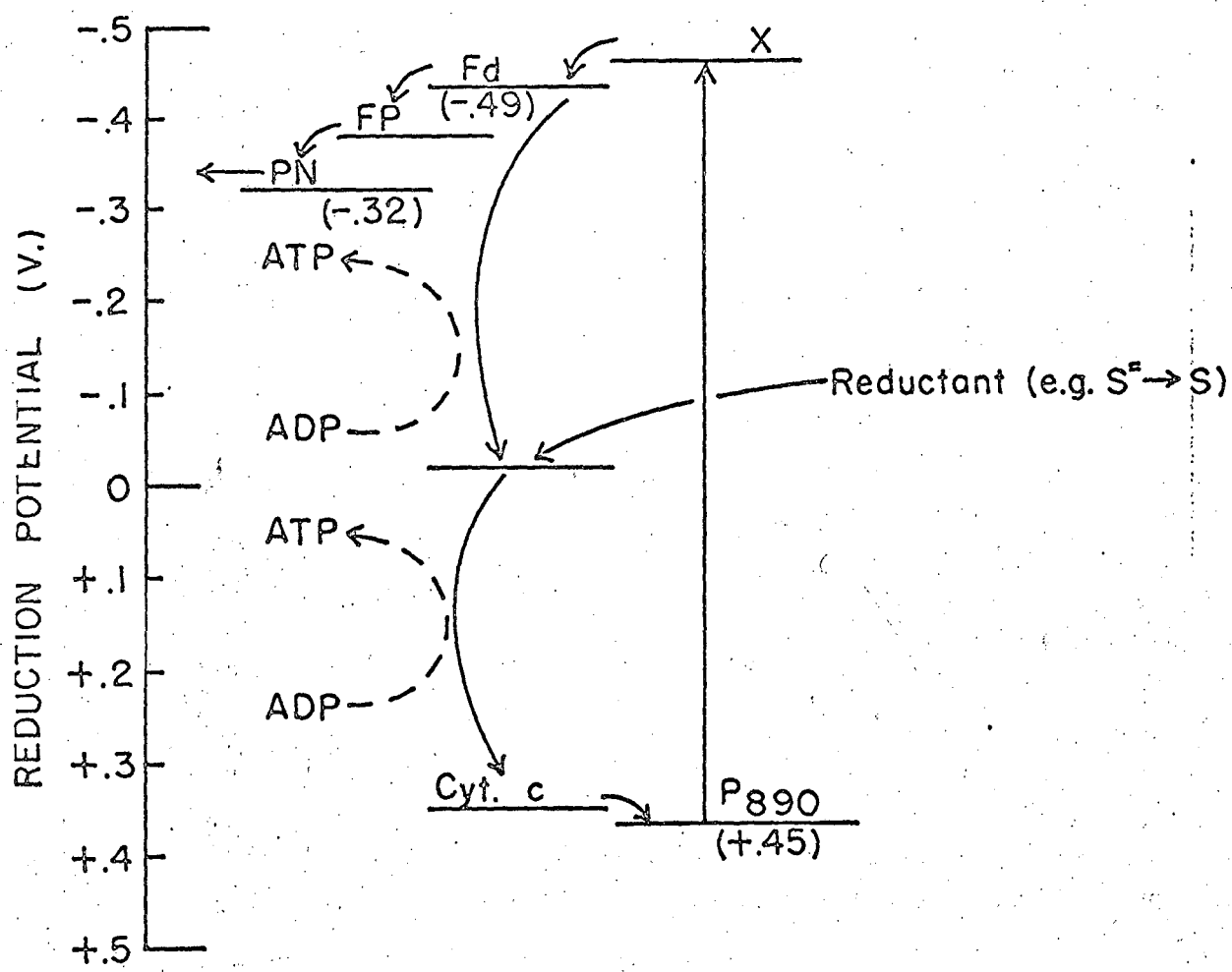

MUB-9519

Figure 4-3. Suggested electron flow diagram for bacterial photosynthesis. The potential change indicated for the light-driven step P_{890} to X was determined thermodynamically.

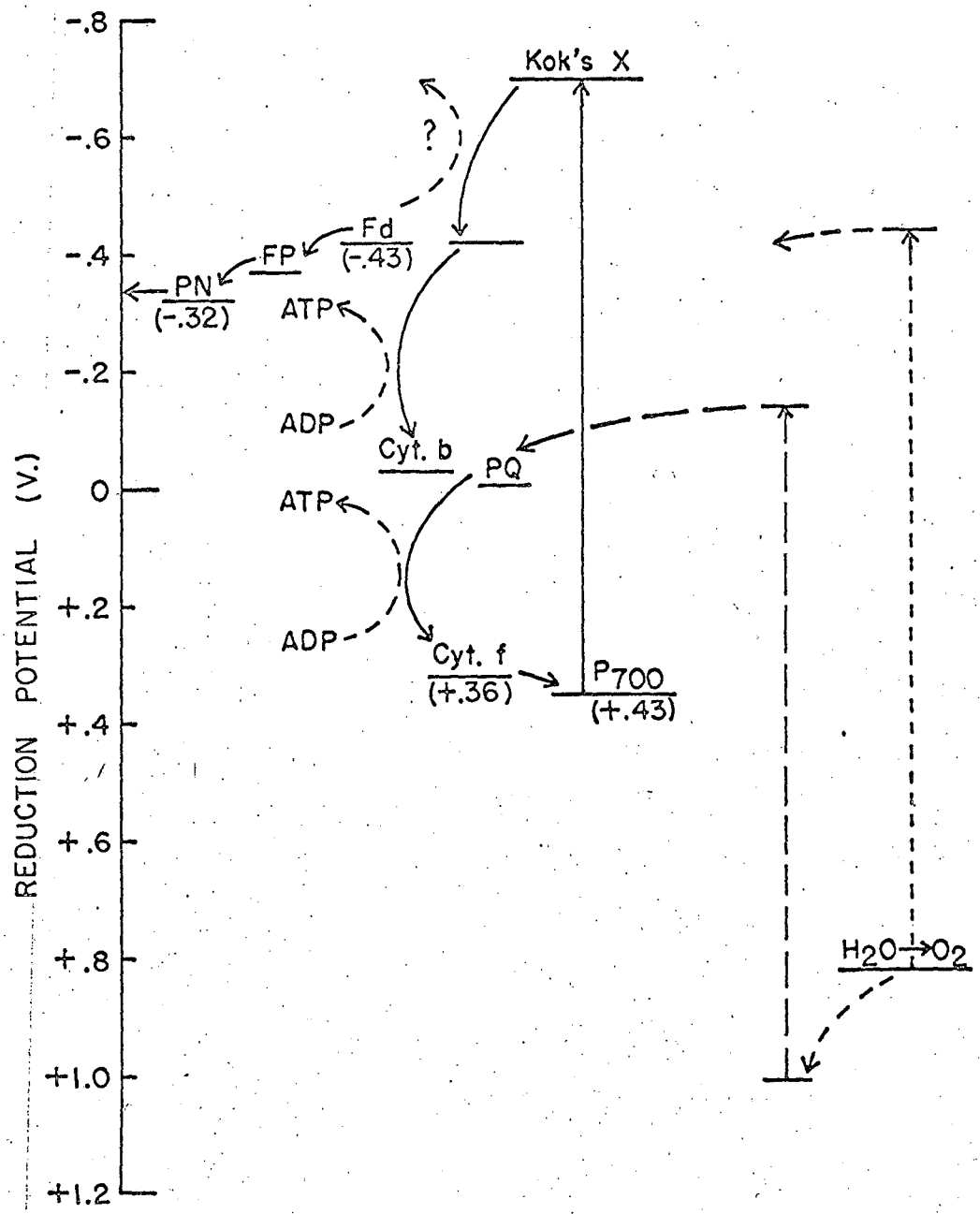

MUB-9520

Figure 4-4. Suggested electron flow diagram for plant photosynthesis. The potential changes for the light-driven steps were determined thermodynamically. The solid line indicates the light act of System I and the vertical dashed lines indicate two possible positions for System II.

arrows represent the input of free energy in the light-driven reactions, while downward arrows indicate spontaneous, or "dark" reactions. Points at which this electron transport process is thought to be coupled to energy storing phosphorylation is indicated with the curved dotted lines.

Chemicals which have been identified as participating in the electron transport pathway are indicated by their initials, and placed according to their estimated redox potential when the organism is illuminated: Fd stands for ferredoxin; FP for flavoprotein; PN for pyridine nucleotide; Cyt. for cytochrome; PQ for plastoquinone; and P_{890} and P_{700} for as yet chemically uncharacterized compounds having absorption peaks at 890 and 700 nm which can be bleached by light, and also reversible bleached chemically with the midpoint potentials indicated in parentheses.[1]

In the case of the bacteria, the available free energy appears to be adequately explained by the difference in redox potentials between the well-characterized c-type cytochromes and P_{890}, and bacterial ferredoxin. In System I of plants, shown as the solid vertical arrow of Figure 4-4, the available energy significantly exceeds the potential difference between spinach ferredoxin, and cytochrome f and P_{700}. On the basis of the reduction of viologen dyes by illuminated chloroplasts, Kok[32] has recently proposed the existence of a System I chemical having a reduction potential in the vicinity of -0.7 eV. The thermodynamic calculations would tend to support this hypothesis.

Less is known about System II, which oxidizes water to molecular oxygen in order to generate a reductant. There are experiments which

indicate that the upper-end of System II terminates near plastoquinone. This is reasonable if one assumes that a powerful oxidant with a potential of greater than +1.0 eV is generated, and some losses are incurred in the oxidation of water. It is possible, however, for System II to move electrons from the potential of water to the potential of ferredoxin with just one photon per electron. These alternate possibilities are shown as the dashed and dotted verticals to the right in Figure 4-4.

Chapter 5

IRREVERSIBLE THERMODYNAMICS OF THE BIOCHEMICAL PATHWAYS

With the exception of the discussion of trapping rates in Section 2C, we have thus far neglected the effect of the biochemical pathways on the amount of free energy stored in photosynthesis, and on such parameters as the amount of luminescence. The chemical reactions and other processes which make up these pathways proceed at a finite rate. As a result, there is a drop in potential across the biochemical pathways which decreases the amount of free energy available for storage, and tends to increase the amount of luminescence.

For diffusive processes, such as electrical conduction, heat conduction, and molecular diffusion, there is a linear relationship between the thermodynamic potential across the diffusive step and the net flux through it; Ohm's law is the most familiar example of this linear relationship. I hope to show that, as a first approximation, this linear relationship is also true for the biochemical pathways of photosynthesis, and possibly for many biochemical pathways.

First we will attempt to make this relationship plausible by a theoretical treatment of the design of biochemical pathways, and then we will consider possible experimental tests.

a. Optimal Design for a Biochemical Pathway

In this theoretical discussion, we will again rely on the assumption that, particularly in fundamental biochemical processes, an organism is under great evolutionary pressure to maximize the storage of free energy and to minimize unnecessary expenditure of it.

Suppose that the chemical reaction $A \rightarrow B$ is one of a chain of reactions in some biochemical pathway. Our direct concern is the energy transformation reactions of photosynthesis, but the argument should have general application.

Suppositions: (1) The needs of the organism requires that the net rate of transformation of A into B be K per second. (In the energy storage pathways of photosynthesis, this rate would be set by the incident light intensity.) (2) This reaction is catalyzed by an enzyme which turns over at a rate of t per second; i.e., the total number of transformations A to B, and B to A, is t per second. (3) The cost to the organism of the enzyme (in free energy) is proportional to the number of enzyme molecules, and is d per enzyme molecule per second. This cost will include amortization of capital expenses (i.e., enzyme synthesis), housing costs (more enzyme, more volume occupied), and any other costs incurred due to the presence of more of this enzyme.

Object: Minimize the total expenditure of free energy when transforming A into B at the required rate. This expense is the sum of the free energy drop, ΔF, driving the reaction, and the cost for the enzyme.

The ratio of the rates for forward and reverse (i.e., B to A) catalysis is

$$\text{rate forward/rate back} = \exp(\Delta F/kT) \qquad (5\text{-}1)$$

By using this relation, together with the assumption that the gross rate of transformations is t per enzyme molecule per second, one easily finds that the net rate of forward reaction per enzyme molecule is

$$t \tanh(\Delta F/2kT), \tag{5-2}$$

Now we desire to find the number of enzyme molecules, n, for minimal total cost. From (5-2) we have the rate equality

$$K = n\, t \tanh(\Delta F/2kT), \tag{5-3}$$

The cost per second is

$$n\, d + K\Delta F, \tag{5-4}$$

and by substituting (5-3) into (5-4), this becomes

$$K \{ \Delta F + f \coth(\Delta F/2kT) \}, \tag{5-5}$$

where $f = d/t$, the enzyme cost per turnover.

By setting its differential with respect to ΔF equal to zero, we find that the cost (5-5) is minimal when

$$\sinh^2(\Delta F/2kT) = f/2kT. \tag{5-6}$$

Here we have a relationship between the optimal free energy drop across an enzyme catalyzed reaction, and the cost of building and maintaining the enzyme. This relationship is plotted in Figure 5-1.

We note that unless one enzyme in a chain of enzymes is much more expensive--say, 100-fold--than the others, no one enzyme should be "limiting" in the sense that its kinetics dominates the behavior of the chain.

It is instructive to consider a rough calculation of f: A typical enzyme turnover rate is 10^5 per minute; a typical cell doubling time is 100 minutes, so that enzymes must be replenished at roughly

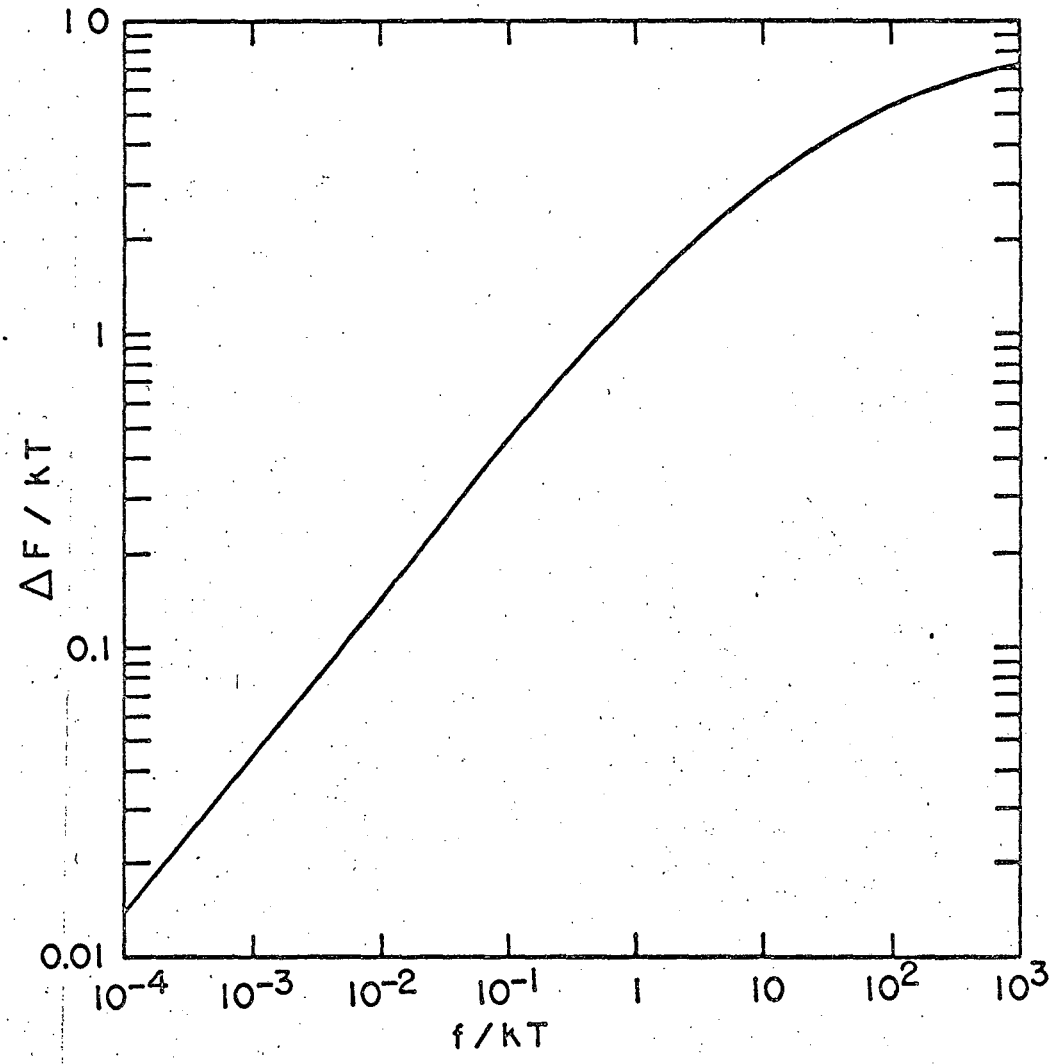

MUB-11264

Figure 5-1. Optimal free energy drop, ΔF, across an enzymatic reaction as a function of the cost of the enzyme per turnover, f.

that rate;[33] this means that we can spread our enzyme costs over about 10^7 turnovers. The molecular weight of an enzyme is about 10^5;[34] if we make the crude guess that the cost of the enzyme is 100 Kcal/mole per 100 molecular weight, then the cost is 10^5 Kcal/mole, or 2×10^5 kT per molecule. This makes f equal to 0.02 kT.

When f is 0.02 kT, the optimal free energy drop is 0.2 kT. However, f may vary by an order of magnitude or more from our estimate; this would mean that the optimal ΔF might be as high as kT for some enzymatic reactions. The relation between the net rate of an enzymatic reaction and ΔF, which is given by (5-2), deviates from linearity by less than 10% for ΔF less than kT. If it is true that most enzymatic reactions have a ΔF of kT or less, and that any other processes which occur in the energy storage process are linear in behavior, then we can anticipate a linear relationship between flux along the energy storage pathways, and the potential drop across the pathways.

If this linearity should hold, then the effect of the finite rates of chemical reactions is formally equivalent to that of an electrical resistance. Then we may consider the simplified model of photosynthesis expressed in Figure 5-2. Light incident on an absorber generates a photovoltage V_a which equals μ/q. The current i generated by the light travels through a resistance R to charge a storage cell with a potential of V_s (which may or may not be adjustable). The power stored is iV_s, and $iR = V_s - V_a$.

The optimization of power storage in the presence of such a resistance is considered in Part B, Section IV.

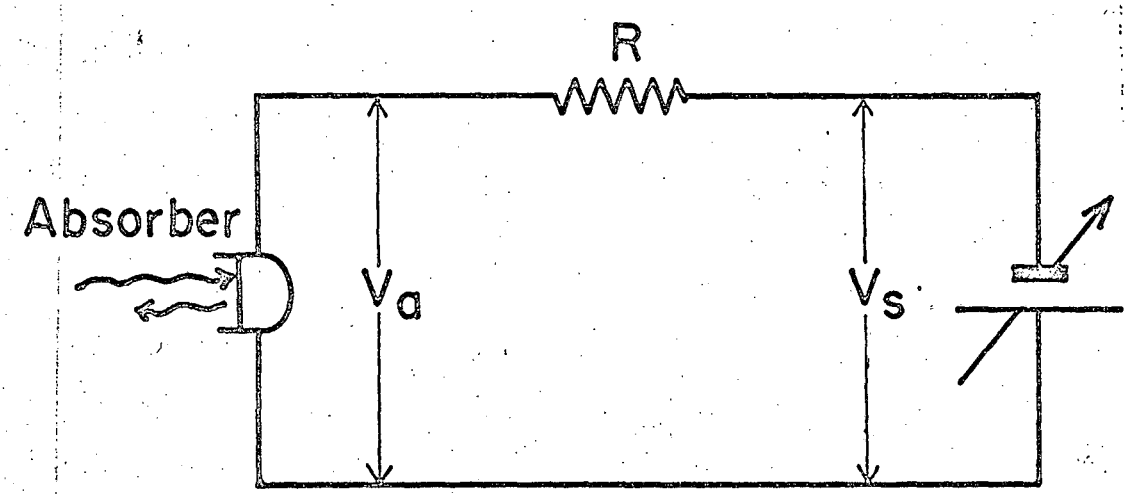

MUB-11258

Figure 5-2. Proposed electrical analogue of steady-state photosynthesis.

b. Experimental Tests of Diffusive Behavior

Light saturation curves

As the light intensity and consequent rate of excitations in an absorber increase, losses due to the resistance become more and more significant. At sufficiently high light intensities, these resistive losses increase to the point that further increases in the light intensity can produce little increase in the amount of free energy stored, and one describes the system as being saturated.

The dependence of power stored on incident light intensity depends on two variables: (1) the functional dependence of free energy drop on net flow along the storage pathway, and (2) the manner in which the free energy of storage is controlled. When the free energy drop is directly proportional to the net flow, as in the current situation, this light saturation surve depends very little on whether an optimal potential V_s is set at each light intensity, or whether a single potential is chosen which gives a good efficiency over a range of intensities.

The light saturation curves resulting from either of these procedures coincide closely with the empirical formulas which Smith[35,36] obtained from measurements of oxygen evolution in green plants. The fit using the linear, or diffusive, model is markedly better than the fit obtained when one assumes that one or two chemical reactions are limiting.

Comparison with Smith's data may not be an unambiguous check on the validity of the assumption of linearity between flux and potential drop. This same type of curve might also result (I haven't worked it out) from different light intensities present at different photosyn-

thetic units, due to the partial absorption of light by pigments in the light path preceeding a given photosynthetic unit. One way to avoid this is to investigate light saturation with monochromatic light of a wavelength which is only weakly absorbed. Recently Pickett and Myers[37] have investigated monochromatic-light saturation curves for another purpose. Preliminary analysis of their curves indicates that saturation curves obtained with weakly absorbed light also fits the diffusive model.

Luminescence yield curves

There is another experimental check on our "resistor" model. The presence of an impedance in the radiant energy conversion system causes an additional increase in the optimal potential at the absorber with increasing light intensity; in turn, this causes an increase in the yield of luminescence. The shape of the curve of luminescence vs. light intensity depends both on the form of the impedance and the manner in which the storage potential is set. Some data on luminescence intensity vs. light intensity are available, and they need to be compared with the theory.

c. Dynamic Response

The linear model which we have been discussing can easily be expanded to include passive transient response to a change in some potential, such as that which would be caused by a change in the incident light intensity. In the linear approximation, chemical pool size is formally equivalent to an electrical capacitance, and one may describe the energy storage pathway with the model in Figure 5-3.

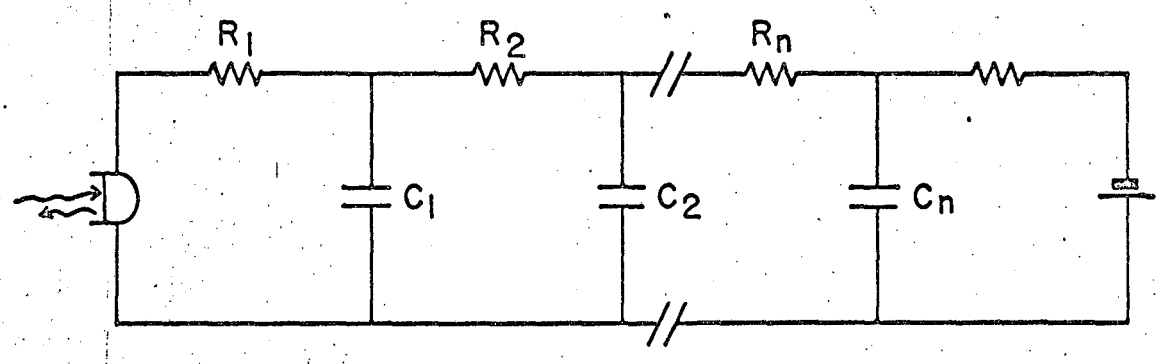

MUB-11259

Figure 5-3. Proposed electrical analogue of photosynthesis, designed to include passive transient changes.

This model does not provide for active control (e.g., the opening of new energy storage pathways at high light intensity), and one purpose of this line of investigation can be to see whether the energy conversion process is a passive system.

"Light on" luminescence transients

Immediately following the onset of illumination, the absorption of light by a photochemical system is almost completely irreversible. The concentrations of chemical intermediates are at a low level, and take some time to reach the steady state levels at which there is an appreciable back reaction. In terms of our model, this means that it takes a while for the capacitors to charge up, and until they do, the potential at the absorber remains low.

As a result of this, any luminescence from the photosynthetic pigments immediately after the light is turned on must be fluorescence due to the finite rate of transfer of excitations from the pigments to the energy storage pathway. This fluorescence yield should be independent of incident light intensity, and this has been found experimentally by Vredenberg and Duysens[38] in purple bacteria. The absolute value of this fluorescence yield would provide the ratio of K_{tran} to αK_{rad}.

The additional luminescence obtained under steady state conditions is due to the partial reversibility of the energy storage pathway. The quantum yield of this luminescence as a function of light intensity is the curve needed as a check on the "resistor" model. The transient kinetics can give information on the suitability of the "capacitor" model.

Delayed light emission

The photosynthetic apparatus of green plants luminesces with an intensity which decays roughly according to 1/time over the time interval of 10^{-3} to 10^{3} seconds after illumination is turned off.[39] This decay has been attributed to solid state phenomena, but our linear impedance model is adequate to explain this time course of decay: a capacitor discharging into a photochemical absorber will produce a luminescence whose intensity will decay as 1/t. The resistances shown in Figure 5-3 probably fail to dominate the time decay behavior because of the small fluxes involved.

REFERENCES

1. (a) R. K. Clayton, Molecular Physics in Photosynthesis (Blaisdell Publishing Company, New York, 1965); (b) R. K. Clayton, Science 149, 1346 (1965).

2. G. W. Robinson, Ann. Rev. Phys. Chem. 15, 311 (1964).

3. L. N. M. Duysens, Prog. in Biophysics 14, 3 (1964).

4. M. D. Kamen, Primary Processes in Photosynthesis (Academic Press, New York, 1963).

5. J. A. Bassham, Adv. Enzymol. 25, 39 (1963).

6. E. I. Rabinowitch, Photosynthesis (Wiley and Sons, New York, 1945, 1951, 1956).

7. W. Ruhland, ed., Handbuch der Pflanzenphysiologie, Vol. 5 (Springer-Verlag, Berlin, 1960).

8. L. N. M. Duysens, in Photochemical Apparatus (Brookhaven National Laboratory, Upton, New York, 1958), Brookhaven Symposium in Biology No. 11, p. 18.

9. R. G. Mortimer and R. M. Mazo, J. Chem. Phys. 35, 1013 (1961).

10. L. N. Bell, Zh. Eksperim. i Teor. Fiz. 46, 1117 (1964) [English transl.: Soviet Phys.--JETP 19, 756 (1964)].

11. W. Shockley and H. J. Queisser, J. Appl. Phys. 32, 510 (1961).

12. R. T. Ross, J. Chem. Phys. (in press); Part I.B.

13. E. H. Kennard, Phys. Rev. 11, 29 (1918).

14. B. I. Stepanov, Doklady Akad. Nauk S.S.S.R. 112, 839 (1957) [English transl.: Soviet Phys.--Doklady 2, 81 (1957)].

15. V. V. Gruzinskii and N. A. Borisevich, Opt. i Spektroskopiya 15, 457 (1963) [English transl.: Opt. Spectry. 15, 246 (1963)], and references cited therein.

16. Yu. T. Mazurenko and B. S. Neporent, Opt. i Spektroskopiya 12, 571 (1962) [English transl.: Opt. Spectry. 12, 317 (1962)].

17. At least I do not know of any published work. I am indebted to Martin Gouterman (University of Washington) for pointing out the existence of the Russian work.

18. W. van Roosbroeck and W. Shockley, Phys. Rev. 94, 1558 (1954).

19. T. S. Moss, Optical Properties of Semiconductors (Academic Press, New York, 1959).

20. J. M. Olson and E. K. Stanton, in The Chlorophylls, L. P. Vernon and G. R. Seely, eds. (Academic Press, New York, 1966).

21. R. K. Clayton, J. Gen. Physiol. 48, 633 (1965).

22. K. Sauer and J. Biggins, Biochim. Biophys. Acta 102, 55 (1965).

23. K. Sauer (this laboratory), private communication.

24. C. Weiss, Jr., Biophys. J. 6, 261 (1966).

25. K. Sauer and R. B. Park, Biochemistry 4, 2791 (1965).

26. J. Kelly and K. Sauer, Biochemistry 4, 2798 (1965).

27. N. Murata, M. Nishimura, and A. Takamiya, Biochim. Biophys. Acta 112, 213 (1966).

28. Ref. 6, Chapter 28.

29. R. B. Park (this laboratory), private communication.

30. P. Latimer, T. T. Bannister, and E. Rabinowitch, Science 124, 585 (1956).

31. E. Katz, E. C. Wassink, and R. Dorrestein, Enzymologia 10, 269 (1942).

32. B. Kok, H. J. Rurainski, and O. V. H. Owens, Biochim. Biophys. Acta 109, 347 (1965).

33. E. Baldwin, Dynamic Aspects of Biochemistry (Cambridge University Press, 1947), p. 142.

34. M. Dixon and E. C. Webb, Enzymes (Academic Press, New York, 1964), 2nd ed., p. 453.

35. E. L. Smith, J. Gen. Physiol. 20, 807 (1937).

36. E. L. Smith, J. Gen. Physiol. 22, 21 (1938).

37. J. M. Pickett and J. Myers, Plant Physiol. 41, 90 (1966).

38. W. J. Vredenberg and L. N. M. Duysens, Nature 197, 355 (1963).

39. W. Arnold and J. B. Davidson, in Photosynthetic Mechanisms in Green Plants, ed. B. Kok and A. T. Jagendorf (National Academy of Sciences Pub. 1145, Washington, 1963), p. 698.

PART I.B.

Scheduled for publication in the Journal of Chemical Physics, Vol. 45, No.1, July 1966.

Thermodynamic Limitations on the Conversion of Radiant Energy into Work*

ROBERT T. ROSS

Department of Chemistry and Lawrence Radiation Laboratory, University of California, Berkeley, California

(Received 20 December 1965)

The fraction of radiant energy incident on an absorber which may appear as work is limited by the radiation entropy, and entropy gained in irreversible transfer from the radiation field to an absorber. Irreversibility may result from directionality of the radiation field, and some irreversibility is necessary to cause a net flow of energy from a radiation absorber into work or free-energy storage. Impedance in the conversion apparatus may further limit the efficiency. Maximization of power storage under these constraints is discussed, and the general arguments are then applied to photoelectrical and photochemical systems; in these systems nonresonant decay of the excited state represents a major source of inefficiency, which may be minimized by appropriate choices fro the Boltzmann temperature and optical density of the absorber. The relationships are developed for narrow-band absorption, and application to broad-band systems is discussed only briefly.

I. INTRODUCTION

IN the past few years interest has intensified in biological photosynthesis, and in photochemical and photoelectrical devices for the conversion of solar energy into work. This interest has stimulated several theoretical considerations[1–3] of the fraction of monochromatic radiation energy which may appear as work, or the thermodynamic work equivalent, which is the Helmholtz free energy, $A=E-TS$.

Related derivations have considered the conversion of free energy into light,[4,5] the conversion of heat into light,[6] and thermodynamic limitations on the performance of a polarizer.[7]

The limits derived in this previous work have been based on the assumption of a reversible interaction between the radiation field and the absorber. In this paper we shall be primarily concerned with limits on the efficiency defined as

$$\eta = \text{work performed/energy incident.}$$

This definition of efficiency based on incident energy introduces several limitations beyond those present when one considers efficiency only on the basis of net absorbed energy. In theory developed specifically for p–n junction photovoltaic cells, Shockley and Queissar[8] have considered a number of the additional efficiency limitations treated more generally in this paper.

As shown in Fig. 1, the apparatus for converting light energy into work may be divided into two parts: an *absorber* and an *engine*. We define an absorber to be a set of degrees of freedom which interact directly with a radiation field, and which are characterized by a common temperature regardless of the nature of the radiation field. Thus, an absorber may constitute the whole of an absorbing material, or it may constitute as little as a single degree of freedom.

Some of the energy absorbed must be reradiated, some may be leaked to the environment, and some—hopefully most—of the absorbed energy is passed to an engine which converts it into work.

The *engine* might be of the conventional piston variety, or it might be present more abstractly, as, e.g., a pair of thermocouple junctions with wires connecting them to a locus of electrical work, or even a sequence of chemical reactions leading to a stable, energetic product.

The fraction of net absorbed energy which may appear as work is restricted by the Carnot limitation of classical thermodynamics: $1-T_L/T_H$, where T_H is the temperature of the absorber, and T_L is the ambient temperature. The Carnot efficiency is frequently described as a restriction on the engine; this is a convenient and meaningful terminology for conventional engines, but it has at times given the false impression that the Carnot factor may be circumvented by using apparatus which does not employ macroscopic heat reservoirs. Actually, the term $(1-T_L/T_H)$ represents the fraction of free energy in an energy increment at T_H, relative to a standard state at T_L:

$$\Delta A_L = \Delta E - T_L \Delta S,$$

$$\Delta S = \Delta E / T_H,$$

$$\Delta A_L = h\nu(1-T_L/T_H).$$

The Carnot engine formalism is simply a convenient manner of representing the entropy associated with net absorbed energy.

The next section of this paper shows how the interaction of the radiation field with the absorber limits the maximum possible T_H. Section III considers the

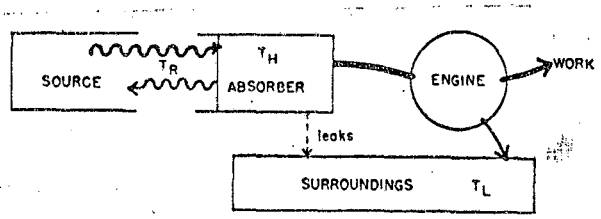

FIG. 1. Schematic diagram for the conversion of radiant energy into work.

irreversibility necessary for net absorption of energy, and shows how power storage may be maximized by an appropriate choice of T_H. The steady-state effect of impedance is treated briefly in Sect. IV.

In Sect. V we consider some additional features present in photochemical and photoelectrical systems, and consider the effect of absorber optical density on maximum efficiency.

Section VI outlines extension of the narrow-band treatment to the situation of broad-band absorption.

II. ABSORBER TEMPERATURE

Material located in the cavity of a blackbody will equilibrate at the temperature of this blackbody. Similarly, an absorber illuminated by a blackbody will, if not cooled by interactions with other surroundings, reach the temperature of the blackbody.

The radiation flux emitted by a blackbody of temperature T is[9]

$$I_\nu = (2\nu^2/c^2)[\exp(h\nu/kT)-1]^{-1} \tag{1}$$

photons per unit solid angle, per uint bandwidth, per unit area, per unit time. Convenient units for this *specific intensity* are photons per [steradian·(second^{-1})·square centimeter·second].

This equation may be rearranged to describe the temperature of a blackbody in terms of the specific intensity of the radiation which it emits:

$$T^{-1} = (k/h\nu)\ \ln(1+2\nu^2/c^2 I_\nu). \tag{2}$$

Equation (2) will also define the temperature of an absorber illuminated solely by a blackbody, and not coupled to any other system.

Now suppose that a very narrow bandpass filter is placed between the blackbody source and the absorber, so that the frequency and specific intensity are effectively constant across the pass band. If the absorber is sensitive (i.e., has nonzero absorptance) only for radiation within the band passed by the filter, then it will be unaffected by the elimination of other frequencies, and its temperature will continue to be defined by (2).

Such a narrow-band, essentially monochromatic, absorber will be unable to distinguish between radiation produced by a blackbody and radiation produced by any unpolarized source which has the same specific intensity at the absorption frequency of the absorber. Consequently, Eq. (2) defines the temperature of radiation from any source as a function of frequency.

A monochromatic absorber will be raised to the temperature specified by (2) only if the absorber is sensitive exclusively to radiation in the direction of the source. As seen from the absorber, most high-temperature sources are highly directional, so that the absorber must be quite directional if it is to attain the temperature of the source.

An absorber may be intrinsically directional, perhaps because it consists of an ordered array, or it may be made effectively directional through optical magnification of the source, as with the parabolic mirrors used in solar furnaces. But most absorbers are not highly directional.

An absorber will average the incident intensities over all the directions in which it is sensitive to radiation, and the temperature of the absorber will be determined from (2) with an average specific intensity. If an absorber is spherically symmetric with respect to its interaction with a radiation field, then the effective intensity is reduced to $I_\nu(\text{eff}) = \int I_\nu d\Omega/4\pi$.

For lower absorption symmetries, one must consider in detail the steady-state relationship between an absorber and a radiation field of intensity distribution $I(\nu,\Omega)$. Assume that the absorber has a probability of emitting or absorbing light which is dependent on angle $P(\Omega)$, and define the *effective raeiation temperature* T_R as the temperature of an absorber which interacts exclusively with the radiation field.

By requiring equality between the intensity emitted and the intensity absorbed, T_R is defined in the integral equation

$$\frac{2\nu^2}{c^2}\left[\exp\left(\frac{h\nu}{kT_R}\right)-1\right]^{-1}\int P(\Omega)\,d\Omega = \int I(\nu,\Omega)\,P(\Omega)\,d\Omega. \tag{3}$$

If the radiation as seen by the absorber falls in a range of solid angle in which the variation of $P(\Omega)$ from $P(\Omega_0)$ is small, then the right-hand side of (3) simplifies to

$$P(\Omega_0)\int I(\nu,\Omega)\,d\Omega. \tag{4}$$

As most radiation sources subtend a small solid angle, and most absorbers are not sharply directional, (4) will hold in most cases; it holds exactly for unidirectional light and for nondirectional absorbers.

We may relate the effective intensity of radiation (relative to a given absorber) to the effective radiation temperature by a modification of (2):

$$T_R^{-1} = (k/h\nu)\ \ln[1+2\nu^2/c^2 I_\nu(\text{eff})]. \tag{2'}$$

By solving (3) with (4) for T_R, we find the effective radiation intensity to be

$$I_\nu(\text{eff}) = P(\Omega_0)\int I(\nu,\Omega)\,d\Omega \Big/ \int P(\Omega)\,d\Omega. \tag{5}$$

The temperature varies as the logarithm of intensity, so only sharply directional absorbers can have an effective radiation temperature which is significantly greater than that for nondirectional absorbers.

The radiation temperature is a steeper function of intensity at lower frequencies. Consequently, reduction of the effective intensity, such as by dilution over solid angle, causes the most variation in radiation temperature at lower frequencies. Consider an absorber which is sensitive over a range of directions which is D times the solid angle subtended by a blackbody source of temperature T_S, i.e., $D = I_\nu(T_S)/I_\nu(\text{eff})$. By substitution of (1) into (2′) we find that

$$T_R^{-1} = (k/h\nu)\ \ln\{D[\exp(h\nu/kT_S)-1]+1\}. \tag{6}$$

For $h\nu/kT_S$ greater than 3, this simplifies to

$$T_R^{-1} \approx (k/h\nu)\ \ln D + T_S^{-1}. \tag{7}$$

Figure 2 shows T_R as a function of frequency for a source temperature of 6000°K and a reduction of intensity by 10^5; this corresponds to the effective radiation temperature of the sun as seen by a nondirectional absorber on Earth,[10] uncorrected for atmospheric absorption.

The appearance of net absorbed energy as work is limited by the Carnot factor, $1-T_L/T_R$, where T_L is the ambient temperature. Figure 3 plots this efficiency as a function of wavelength for $T_L=300$°K conversion of energy from a narrow-band absorber illuminated by a 6000° blackbody source. Curves are shown for an absorber which sees the full blackbody intensity, the 10^5 reduction of intensity characteristic of unfocused solar radiation on Earth, and a 10^{10} reduction.

III. RERADIATION LOSSES

Until now we have ignored a major consequence of the fact that an absorber at T_R emits (as resonant fluorescence) a photon flux equal to the flux absorbed: Energy may be withdrawn for doing work (or free-energy storage) at only an infinitesimal rate if the absorber is to remain at T_R.

If energy reradiated by the absorber is not considered, and if there are no other energy leaks, then the Carnot limit of $1-T_L/T_R$ can apply.

When there are losses from the absorber, however, then total efficiency is limited by the product of a Carnot efficiency, and the fraction of the absorbed quanta which are used for work or free-energy storage:

$$\eta=(1-T_L/T_H)(1-I_{\text{out}}/I_{\text{in}}), \tag{8}$$

where I_{in} is the input intensity, I_{out} is the loss intensity, and T_H is the absorber temperature.

When losses are present, the conditions for optimal efficiency may be found by determining the dependence of I_{out} on T_H, and setting the differential of (8) to zero.

The efficiency of most practical interest is the ratio of power storage to incident-energy flux; in this case I_{in} is the incident intensity, and I_{out} includes losses from reflection, transmission, absorber emission, and any energy leaks from the absorber. We will not consider reflection; transmission is considered for photochemical systems in Sec. V.

If the absorber is a leak-free ideal (narrow-band) blackbody, so that the only loss is the reradiation, then

$$I_{\text{out}}/I_{\text{in}}=(e^R-1)/(e^H-1), \tag{9}$$

where $R=h\nu/kT_R$ and $H=h\nu/kT_H$.

For wavelengths $\lesssim 1\mu$, the ones in (9) may be neglected except under conditions of extraordinarily high light intensity; we neglect them from now on, so that the efficiency becomes

$$\eta=(1-H/L)(1-e^{R-H}), \tag{10}$$

where $L=h\nu/kT_L$.

The condition on the absorber temperature for optimal power storage is that

$$H_{\text{opt}}=R+\ln X, \tag{11}$$

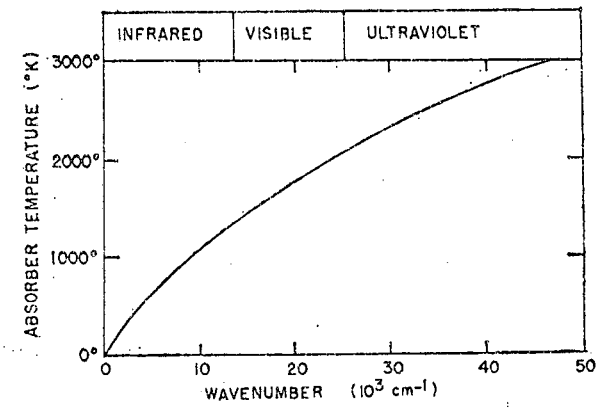

FIG. 2. Maximum temperature for a nondirectional narrow-band absorber on Earth illuminated by a 6000°K blackbody sun.

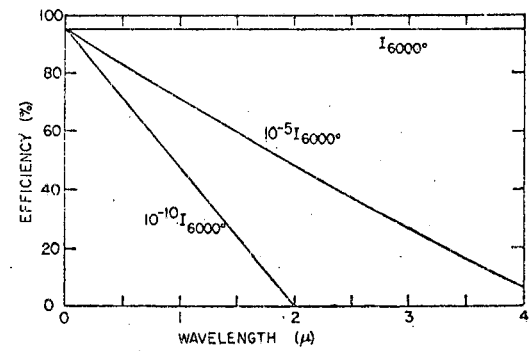

FIG. 3. Maximum efficiency from a narrow-band absorber illuminated by a 6000° blackbody source, with efficiency calculated on the basis of net absorbed light intensity. Curves from top for full blackbody intensity; intensity reduced by 10^5 (solar equivalent); reduction by 10^{10}.

where

$$X=1+L-H_{\text{opt}} \tag{12a}$$

$$=1+L-R-\ln[1+L-R-\ln(1+L-R-\cdots)], \tag{12b}$$

which converges quite rapidly.

The resulting optimum efficiency is

$$\eta=[1-(R+\ln X)/L](1-1/X). \tag{13}$$

The expression within the brackets is the Carnot term, and $1/X$ represents the fraction of quanta reradiated under optimum conditions.

As was true of decreased efficiency due to reduced incident intensity, the losses due to the presence of reradiation are largest at the long-wavelength end of the spectrum. Figure 4 demonstrates the effect of reradiation as a function of wavelength for a narrow band absorber illuminated by a 6000° blackbody sun (i.e., blackbody intensity reduced by 10^5). The difference between the highest and middle curves represents the decrease in Carnot efficiency necessary for maximum power storage; the gap between the middle and lowest curves shows the loss due to actual reradiation.

If T_H is not maintained at or near the optimal value, then the efficiency may be markedly lower than the maximum set by (13) (see, e.g., Fig. 5).

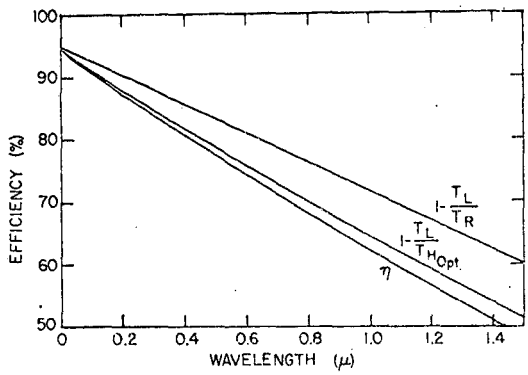

FIG. 4. Effect of reradiation on the efficiency from a narrow-band absorber on Earth illuminated by a 6000° blackbody sun. $1-T_L/T_R$: maximum Carnot efficiency; $1-T_L/T_H$: Carnot efficiency for maximum power storage; η: maximum efficiency calculated on the basis of incident light intensity.

IV. INTERNAL IMPEDANCE LOSSES

Any real transfer of energy from one place to another encounters some resistance, or impedance, to the transfer. Similarly, an apparatus, or *engine*, which transfers absorber energy to a locus of free-energy storage must have some impedance. Work must be expanded to cause a flow through this impedance, and the work used reduces the amount of work available for storage.

We can write the power stored as

$$P=\Delta A I_{\text{eng}},$$

where ΔA is the thermodynamic potential at the locus of free-energy storage and I_{eng} is the flux through the engine into storage: $I_{\text{eng}}=I_{\text{in}}-I_{\text{out}}$, assuming no leakage of flux other than that which can be attributed to the absorber.

The potential of storage is equal to the potential at the absorber, less the potential drop through the engine:

$$\Delta A=h\nu(1-T_L/T_H)-W, \tag{14}$$

where W represents the average work required to move the energetic products of one photon through the engine.

By combining these equations we find that as a result of this potential drop, the efficiency for the conversion of radiation energy into work becomes

$$\eta=\left(1-\frac{I_{\text{out}}}{I_{\text{in}}}\right)\left(1-\frac{T_L}{T_H}-\frac{W}{h\nu}\right). \tag{15}$$

W will be a function of the energy flow from the absorber into the engine. The form of this function will depend on the system which it describes, but it cannot be negative. If the function has continuous derivatives, then it may be expanded in a Maclaurin series:

$$W=w_0+w_1I_{\text{eng}}+w_2(I_{\text{eng}})^2+\cdots. \tag{16}$$

If w_0 is zero, then W equals w_1I_{eng} in the limit of small flux. This linear relationship between flux and thermodynamic potential difference holds with good accuracy for many transfer processes which operate at the molecular level; a familiar example is Ohm's law for electrical conduction. Diffusion and heat conduction are also typically linear.[11]

The notable exception to linearity occurs in chemical reactions, which are sure to be linear only for $W\ll kT$. If a chemical reaction may be considered as a sum of several elementary reactions, then the condition for linearity is relaxed to require only that the fre-energy change across each of the partial reactions be small with respect to thermal energies[12]; this may be the case in biological systems.

In linear systems Eq. (15) becomes

$$\eta=(1-H/L)(1-e^{R-H})-f(1-e^{R-H})^2, \tag{17}$$

where $f=I_{\text{in}}w_1/h\nu$. H may be adjusted for maximum power storage.

The dependence of power stored on light intensity under optimal conditions is shown in Fig. 6. The curve with impedance is for $f=10$ at intensity I_0. At intensities where f is very small, the effect of the resistance is negligible. For large f (e.g., high light intensities) the impedance places a ceiling on the power stored of

$$P=(h\nu/4w_1)(1-T_L/T_R)^2,$$

which is shown as a dotted line on the figure.

The parameters used for this figure are equivalent to 300°K conversion of 1μ radiation which at I_0 has the effective intensity of an unfocused 6000° blackbody Sun on Earth. The assumption of a relatively long wavelength serves to accentuate the slopes of the asymptotic curves, but the shape of the power curve is not strongly dependent on the parameters used.

V. PHOTOCHEMICAL SYSTEMS

We define an energy-conversion system to be photochemical if the absorber consists of a restricted number of degrees of freedom within the spatial bounds of the absorbing material. Any radiation conversion system which does not employ heat reservoirs in the usual macroscopic sense fits this definition, so that photoelectrical devices, as well as conventional photochemicals, are considered to be photochemical.

The temperature of the absorber T_H is represented by the relative populations of the ground and excited states resonant with the radiation.

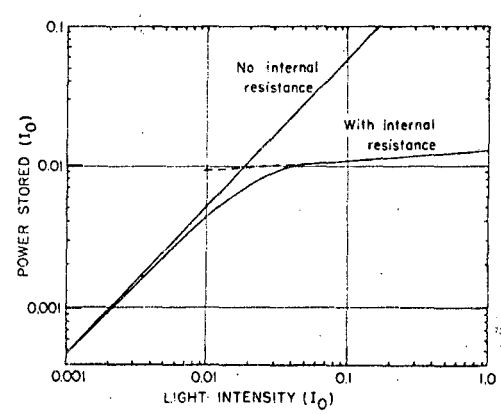

FIG. 6. Maximum stored power as a function of incident-light intensity. Upper curve: no impedance; lower curve: $f=10$ at I_0. Parameters are discussed in Sect. IV.

A characteristic feature of photochemical systems is the transfer of energy from the degree(s) of freedom resonant with the radiation to a degree of freedom which does not interact significantly with radiation and otherwise equilibrates with the surroundings only slowly. This transfer may be partially or wholly by processes such as ionization, molecular rearrangement, chemical reaction, intersystem crossing to another spin state, or migration of the excitation to a physically distinct "trap" species.

The total transfer process may frequently be described as involving several such steps, each of which has a progressively slower interaction with the surroundings: e.g., vibrational relaxation, intersystem crossing to a triplet state, then chemical reaction.

The final locus of free-energy storage is usually in reactable chemicals: Energy stored from a photovoltaic cell is likely to be in a battery of electrochemical cells; photosynthesis leads indirectly to firewood. This storage may be viewed as a metastable excitation of the degree of freedom represented by a chemical reaction coordinate.

By definition, energy transfer to nonuseful degrees of freedom (e.g., vibrational) represents a heat leak which is unique to photochemical systems. This transfer may be completely nonradiative, or it may involve a combination of radiative and nonradiative processes. The rate of these losses is usually directly proportional to the excited-state population, and thus a constant proportion of the radiative loss at the absorption frequency (the resonant fluorescence). The total rate of nonresonant loss may thus be represented as an absorber relaxation coefficient ξ times the rate of resonant fluorescence.

If I_{out} in (8) is multiplied by $(\xi+1)$, this is mathematically equivalent to reduction of the input intensity by the same factor. Consequently, the effect of absorber relaxation on optimal T_H and efficiency is precisely that of an external reduction in the effective radiation intensity. Equations (6) and (7) hold with $(\xi+1)$ multiplying D, and Fig. 3 demonstrates the effect of absorber relaxation on efficiency as a function of wavelength. The efficiency continues to be specified by (10) and (13), providing that

$$R_\xi = R + \ln(\xi+1) \tag{18}$$

is substituted for R in (10) through (13). The fraction $1/X$, representing loss from the absorber now includes losses from nonresonant decay.

This nonresonant absorber relaxation is caused by a coupling between the absorbing degrees of freedom and their surroundings. If a constant temperature is maintained throughout the absorber—which is required by our definition of a single absorber—then the rate of absorber heat leak due to nonresonant relaxation increases when more absorbing sites (degrees of freedom) are added to an absorber.

This introduces a question as to the optimum number of absorbing sites for maximum power storage. If the number of sites is quite large, then virtually all incident radiation may be absorbed, but the nonresonant losses will be relatively high. If the number of sites is small, then nonresonant losses are small, but a significant fraction of the incident radiation will pass through the absorber. When the number of absorbing sites, or—equivalently—the optical density, is controllable, then (8) may be optimized with respect to this variable also.

Consider unidirectional irradiation normal to a planar absorber which is made up of an ensemble of absorption sites, each of which has a site relaxation coefficient defined analogously to ξ. If different sites have different relaxation coefficients, then the accuracy of our treatment requires that the mean site relaxation coefficient α be essentially constant when averaged over the mean free path of a photon having the absorption frequency.

The fraction of light passing completely through the absorber is e^{-S}, where S is the thickness of the absorber in units of the photon mean-free path.

The fraction of incident intensity I_{in} lost due to resonant radiative decay is $\frac{1}{2}(1-t)\exp(R-H)$, where R is defined for a spherical absorber, and $\ln\frac{1}{2}$ corrects this to the flat-plate value. The mean transparency averaged over solid angle t is the order of e^{-S}/S for large S; this correction is so small that we neglect it.

Assuming that any directionality in the absorption of individual sites is eliminated by averaging, the fraction of I_{in} lost by nonresonant absorber relaxation is $\alpha S\exp(R-H)$.

Substituting these expressions into (8), we find that

$$\eta = (1-H/L)[1-e^{-S}-(\alpha S+\tfrac{1}{2})\exp(R-H)]. \tag{19}$$

Differentiating with respect to S, we find that for maximum efficiency

$$S_{\text{opt}} = H - R - \ln\alpha. \tag{20}$$

Substituting this into (19), the efficiency becomes

$$\eta = (1-H/L)[1-(\alpha S_{\text{opt}}+\alpha+\tfrac{1}{2})\exp(R-H)]. \tag{21}$$

By comparison with (10) and (18), we note that this expression is that of an absorber with

$$\xi+1 = \alpha S_{\text{opt}}+\alpha+\tfrac{1}{2}. \tag{22}$$

Accordingly, from (11), (18), and (22) we have that

$$H_{\text{opt}} = R + \ln(\alpha S_{\text{opt}}+\alpha+\tfrac{1}{2}) + \ln X. \tag{23}$$

By combining (20) and (23), and recalling (12a), one obtains a convenient set of coupled equations for maximum power storage:

$$H = R + S + \ln\alpha, \tag{24a}$$

$$X = 1 + L - H, \tag{24b}$$

$$S = \ln X + \ln[1 + S + (1/2\alpha)]. \tag{24c}$$

If α, R, and L are known, then H, X, and S for maximum efficiency may be determined accurately by a few cyclic iterations of (24).

Maintaining T_H at the optimum in photochemical systems corresponds to keeping the relative population of the excited state(s) at a proper value. Raising the population above this level results in increased losses from absorber relaxation. If the population of the excited state is below the optimum value, then the

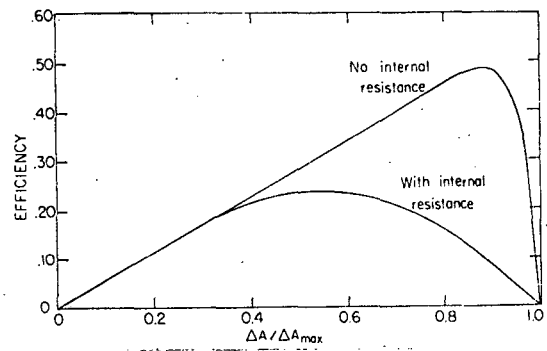

FIG. 5. Dependence of efficiency on the thermodynamic potential at the locus of free-energy storage. Upper curve: no impedance; lower curve: $f=0.3$. Parameters are discussed in Sect. V.

free-energy gain in the energy-storage process is less than optimal.

As we see in (14), T_H is controlled by the sum of the thermodynamic potential at the locus of free-energy storage and the potential drop across any impedance. The storage potential is usually the independent variable; Fig. 5 plots the efficiency as a function of this ΔA for no impedance and also for a linear impedance with $f=0.3$. The curves shown are for parameters equivalent to 300°K conversion of 1-μ radiation from a 6000° source with dilution by 10^8. For radiation of higher intensity and/or shorter wavelength, the impedance free curve would peak even more closely to the right edge.

For photovoltaic devices Fig. 5 represents power delivered as a function of load voltage, without and with an internal resistance.

During the course of a typical photochemical reaction, the thermodynamic activities of the reactants will vary, altering the free energy of reaction. Usually the reaction starts at equilibrium and progresses to a photostationary state by depleting the supply of reactants and increasing the concentration of products. This is equivalent to moving along Fig. 5 from the left to the right edge. The mapping of time onto the horizontal axis of the figure will depend on the reaction considered. A significant free energy of reaction builds up rather readily, so that motion away from the left edge will be relatively rapid. The rate of approach to the right-hand edge will be slow, and asymptotic to aero, as the quantum yield goes to zero.

The inefficiencies we have discussed do not include any effects due to a finite rate of transfer from an excited state, from which losses occur, to more stable species further along the storage pathway. Attainment of good efficiency requires that the gross forward rate of any transfer step be very much faster than the rate of energy leakage from the state preceding the step. The intrinsic quantum yield for a transfer is $k_t/(k_t+k_l)$, where k_t is the forward transfer rate, and k_l is the loss rate. This effect is independent of the thermodynamic losses discussed, and is quite significant in many photochemical and photoelectrical systems.[13]

VI. BROAD-BAND ABSORPTION

Few radiant-energy sources are anywhere near being monochromatic, making it necessary for practical energy converters to utilize radiation in a broad-band of frequencies.

The monochromatic efficiency limitations may be applied to a broad-band of frequencies by averaging $\eta(\nu)$, weighted by the frequency distribution of incident energy. To attain this efficiency for an arbitrary distribution of intensity over frequency, it appears that a conversion system would have to be composed of a large number of subsystems, each of which was designed to optimize the conversion of a narrow band of frequencies. This is technically difficult, and any real conversion apparatus has no more than a few such subsystems. Understanding this substructure of a broad-band absorber may permit the setting of a limit on the efficiency which is significantly below the band-averaged monochromatic limit.

If the absorber for all frequencies is a conventional heat bath, in which all degrees of freedom are in thermal equilibrium, then the knowledge that T_H is independent of frequency permits a straightforward evaluation of the efficiency attainable with a specified radiation field and absorber. Such calculations have been used extensively in determining the thermal utilization of solar energy.[14]

If the absorber is not a heat bath, so that—by our definition—the system is photochemical, then the thermodynamic potential of the absorber is usually independent of frequency; knowledge of this permits easy evaluation of efficiencies for broad-band photochemical systems.[13]

VII. CONCLUSIONS

There are several sources of inefficiency in the transformation of light into work which may be considered in thermodynamic terms: (1) directional radiation incident on a nondirectional absorber; (2) irreversibility necessary to get a directional flow of energy into work or free-energy storage; (3) internal resistance losses; and (4) energy leaks from the absorber.

Efficiency, as defined by the amount of power stored, is most significantly affected by control of the thermodynamic potential at the locus of free-energy storage; indirectly, this means control of the absorber temperature. The latitude in this control for good efficiency in a photochemical system is indicated in Fig. 5.

As shown in Fig. 3, absorber directionality and absorber relaxation rate must change by at least an order of magnitude to significantly affect the thermodynamically limited maximum efficiency. The loss due to absorber relaxation in a given chemical system may be minimized by an appropriate choice of optical density for the absorber.

Internal resistance losses may be reduced by removing some of the resistance, but the significance of such a reduction depends on the degree of saturation (see Fig. 6).

An understanding of these sources of inefficiency may be useful in the design of radiation converters, such as in efforts to devise a simple photochemical system for the effective capture of solar energy.

The process may also be reversed: Information can be obtained about a radiation conversion system by studying its efficiency, or parameters such as chemical potential or fluorescence yield, as a function of the variables considered in this paper. Biological photosynthesis is the system which originally motivated this work, and we hope that an understanding of the thermodynamics of radiation conversion may be particularly useful in this area.

ACKNOWLEDGMENTS

The development and expression of these ideas has benefited greatly from spirited discussions with D. R. Gentner, E. A. Dratz, and other colleagues in the Chemical Biodynamics Laboratory, and from critiques by David Phillips and Professor Walter Knight in the Physics Department. I particularly thank I. D. Kuntz, Jr., for his encouragement and extensive advice, and Professor Melvin Calvin for his guidance and interest.

* This work was supported, in part, by the U.S. Atomic Energy Commission.

[1] L. N. M. Duyesns, *Photochemical Apparatus* (Brookhaven National Laboratory, Upton, N.Y., 1958), Brookhaven Symposium in Biology No. 11, p. 18.

[2] R. G. Mortimer and R. M. Mazo, J. Chem. Phys. **35,** 1013 (1961).

[3] L. N. Bell, Zh. Eksperim. i Teor. Fiz. **46,** 1117 (1964) [English transl.: Soviet Phys.—*JETP* **19,** 756 (1964)].

[4] J. E. Mayer, *The Luminescence of Biological Systems*, F. H. Johnson, Ed. (American Association for the Advancement of Science, Washington, 1954), p. 248.

[5] Yu. T. Mazurenko, Opt. i Spektroskopiya **18,** 49 (1965) [English transl.: Opt. Spectry. **18,** 24 (1965)] and references cited therein.

[6] M. A. Weinstein, J. Opt. Soc. Am. **50,** 597 (1960).

[7] R. C. Jones, J. Opt. Soc. Am. **52,** 747 (1962).

[8] W. Shockley and H. J. Queisser, J. Appl. Phys. **32,** 510 (1961).

[9] M. Planck, *Theory of Heat Radiation*, transl. by M. Masius (Dover Publications, Inc., New York, 1959).

[10] The sun subtends 0.54×10^{-5} of the celestial sphere as seen from Earth.

[11] I. Prigogine, *Introduction to Thermodynamics of Irreversible Processes* (Interscience Publishers, Inc., New York, 1961), 2nd ed.

[12] See Ref. 11, pp. 57–60.

[13] R. T. Ross (unpublished work).

[14] Numerous calculations have been published in the journal *Solar Energy* (Association for Applied Solar Energy, Phoenix, Ariz.), and similar articles appearing elsewhere are abstracted in this journal.

PART II

PARAMAGNETIC RESONANCE OF TRANSITION METAL COMPLEXES HAVING BIOLOGICAL INTEREST

A. Applications of EPR in the Investigation of Biological Metals

Chapter 1

INTRODUCTION

The purpose of this part of the thesis is to consider the uses to which electron paramagnetic resonance (EPR) spectroscopy can be put in elucidating the structure and function of biologically occurring transition metal complexes. Such use might be the direct investigation of a biological material, or the technique might be used to investigate model complexes.

There are several obvious requirements for the magnetic resonance of a metal complex to have biological interest:

1. First, the metal ion must be of biological interest. In other words, it must occur in biological processes, or the study of a given metal ion must give information about a metal ion which does occur in biological processes.

2. The ligands bound to the metal ion must be of biological interest. They must occur in biological systems, or they must be sufficiently analogous to biologically occurring ligands that study of the resulting complex can give useful information about a biologically occurring complex.

3. We must have a reasonable expectation that the oxidation state studied occurs in biological systems.

4. The complex must be observable with EPR.

5. Physical information should be obtainable from the spectroscopy, and, hopefully, some biological information will be obtainable from the physical information.

Now let us consider these requirements in somewhat greater detail:

Metal ions of biological interest[1-3]

The first row transition elements, vanadium, manganese, iron, cobalt, copper and zinc, and the second row element, molybdenum, are of direct interest because they are known to be required for biochemical reactions in living systems. Nickel is known to catalyze certain biochemical reactions *in vitro*, and it seems reasonable that a biological role for it, and for chromium, may be found in the future.

Manganese(II) and cobalt(II) are of additional interest because they can substitute for other metal ions in a number of metal ion-activated enzymatic reactions. For instance, a study of the cobalt(II) complex of carbonic anhydrase has yielded significant information about the role of zinc in the reaction catalyzed by this enzyme.

Ligands of biological interest[4-7]

One needs to have a liberal point of view about this, because we do not know the full range of biologically occurring ligands. We can expect biologically occurring ligand bonds with water; with the inorganic anions which are stable in water, such as chloride, sulfate, and phosphate; and with practically any organic functional group which contains a sterically accessible oxygen, nitrogen, or sulfur atom. Bonds are particularly common with sulfhydryl, carboxylate, enolate, ammine, and ring nitrogen groups.

Biological metal ions also bond to other types of groups. The iron of hemoglobin binds to molecular oxygen (and to carbon monoxide,

unfortunately), and the cobalt of vitamin B_{12} has a direct bond to a carbon atom.

Stable oxidation states[8]

Much of biology takes place in an aqueous environment, where the possible oxidation of water to oxygen and the possible reduction of hydronium ions to hydrogen place the upper and lower limits on the oxidizing strength of the ions present. Of the transition elements known to be required by a biological system, the following oxidation states are stable in water: V(III), V(IV), V(V), Mn(II), Fe(II), Fe(III), Co(II), Cu(I), Cu(II), Zn(II) and Mo(III) through (VI). In addition to those, a number of complexes of Mn(III) and Co(III) are stable in aqueous solution. Cobalt(III) occurs biologically in the vitamin B_{12} compounds, and manganese is also thought to occur biologically in the trivalent state.

In addition to the oxidation states just mentioned, it is possible that others occur biologically which are stabilized by covalent coordination, or that are stable in some non-aqueous region. One possibility is Mn(IV). One should keep in mind, however, that the assignment of an oxidation state to the metal ion requires a decision as to where the electron orbital is; for instance, should one call a complex $Co^{2+}L_2$ or $Co^{4+}(L^-)_2$?

Observability by magnetic resonance

I assume that the reader has a reasonable familiarity with EPR. For the uninitiated chemist or biochemist, the recent book by Bersohn and Baird, An Introduction to Electron Paramagnetic Resonance,[9] provides

a readable introduction with a minimum of specialized jargon. At a somewhat more advanced level are a monograph by Pake[10] and a review article by Jarrett.[11] Before tackling these, the chemist with only a little background in quantum mechanics should work through the superbly written book by Schlicter.[12] Much of the discussion below is contained in the reviews by Bleaney and Stevens[13] and Low.[14]

The fundamental requirement for EPR is the presence of electrons whose paramagnetic moment can reorient with the absorption of electromagnetic radiation. This requires, first of all, that the metal ion be paramagnetic and, secondly, that it have at least one pair of energy levels which are no further apart than the energy of the microwave quanta used in the EPR spectrometer.

The requirement of paramagnetism prohibits the observation of ions with a full d shell, such as Cu(I) and Zn(II), and ions with an empty d shell, such as V(V) and Mo(VI). It also prevents observation of the low spin (spin paired) form of those ions which have an even number of electrons; for instance, Co(III) and Mo(IV) are usually diamagnetic and hence not observable. Most transition metals form polynuclear complexes, in which the metal-metal interactions may cause the complex to be diamagnetic.

What of the requirement of a pair of closely spaced energy levels? A fundamental theorem due to Kramers states that any system with an odd number of electrons will always have at least one pair of energy levels which remain degenerate in any arbitrary electrostatic field; this de-

generacy results from the time-reversal symmetry properties of these systems. A laboratory magnetic field may be used to split these energy levels and EPR may be performed between the halves of this Kramers doublet. Thus, we can anticipate that paramagnetic resonance observations will usually be possible on transition metal ions which have an odd number of d electrons.

A contrasting theorem proved by Jahn and Teller states that any system in a static environment which possesses a degeneracy not required by group theoretic reasons (i.e., a Kramers degeneracy) will achieve a lower energy if it distorts, removing the degeneracy. This means that transition metal ions with an even number of d electrons may not have any energy levels between which conventional EPR may be performed. The theorem does not predict the magnitude of the splittings, and the splittings between the energy levels may range from an unobservably small value upwards to several hundred wavenumbers. If the energy splittings developed by the distortion are all greater than one wavenumber, then EPR cannot be performed with the usual commercial spectrometers, which use microwave radiation of wavelengths 3 cm and 8 mm.[15]

In addition to the question of whether or not an appropriate pair of energy levels exists, these even electron systems are much more susceptible to electron relaxation processes, which may also render observation of a signal difficult or impossible, particularly at room temperature. We discuss this more fully in the next chapter.

Information available from magnetic resonance

The uses of magnetic resonance are essentially the same as those of any other kind of spectroscopy. One of the primary advantages of spectroscopy as a research tool, particularly in biology, is the relatively small disturbance it creates in the system investigated. Ideally, this is particularly true of EPR, with its low energy quanta and potentially high sensitivity.

The biological uses are as follows:

1. One may study a biological system, or an extract therefrom, in order to determine the presence, or kinetics, of a complex (or family of complexes) which has a known pattern of spectroscopic parameters. This is the easiest direct application of spectroscopy, and the most often used so far in the EPR of biological systems.

2. One can study a structurally characterized biologically occurring compound in order to understand its architecture and biochemical function in terms of its electronic structure. On occasion it may be easier to study simpler analogs of the biologically occurring compound.

3. One may study a structurally uncharacterized, biologically occurring compound to help determine its architecture.

4. As a prerequisite to effective application of the technique to biological systems, one must study relatively simple model compounds in order to improve one's understanding of the relationships between the spectroscopic parameters and electronic structure and molecular architecture.

The relationships between the electronic structure and EPR spectroscopic parameters were first derived by Abragam and Pryce,[16] and have been reviewed in a number of articles and books.[10-13,17,18]

Chapter 2

LIMITS ON THE OBSERVATION OF METAL ION EPR

a. Spin Lattice Relaxation[9,10,13,14,19]

Line width is frequently a problem in the use of EPR to investigate transition metal ions. Rapid thermal equilibration between the electron spin energy levels and the bulk environment, called spin-lattice relaxation, causes the absorption peak to be broadened according to the Heisenberg uncertainty relation. As the relaxation rate approaches the frequency of observation (10^{10} cps), the absorption becomes unobservable.

Even with slower relaxation times, the broadening of individual lines may cause adjacent lines to overlap, smearing the spectrum and resulting in a decreased availability of information and less sensitivity.

Considering only an individual line, the height of an absorption peak is decreased in proportion to the width of the absorption line, and hence in proportion to the rate of relaxation. As EPR spectrometers detect the derivative of the absorption spectrum, sensitivity drops as the square of the relaxation rate (at constant modulation intensity).

There are a number of ways in which relaxation can occur between two paramagnetic energy levels, but they are all variants on the same theme: The energy spacing between the levels is a function of some parameter, x. If x is then varied with a frequency near the frequency

corresponding to the energy gap between the levels, then this will induce transitions between the states in the same manner as an external microwave field of the same frequency.

The energy spacing depends on the spectroscopic parameters g, A and D -- respectively, the spectroscopic splitting factor in a magnetic field, the energy of the electron-nuclear coupling, and the energy level splitting in the absence of a magnetic field. These parameters may depend upon the orientation of the complex with respect to the laboratory magnet, and on parameters of the electronic structure such as the degree of electron delocalization, and the electrostatic field at the metal atom due to the ligands.

Thermal fluctuations of things such as metal atom-ligand distance, or orientation of the complex, cause fluctuations of the spectroscopic parameters which, in turn, cause a variation in the energy gap. The Fourier component of these fluctuations in the vicinity of the resonant frequency causes transitions between the states.

The extent to which these thermal fluctuations induce transitions depends on the degree to which the spectroscopic parameters depend upon the physical parameters which are fluctuating thermally. For instance, if the g value is very strongly dependent on the orientation of the complex, then rotation of the complex due to Brownian motion will be an effective relaxation mechanism. If, on the other hand, the g value is isotropic, this would not be an effective relaxation mechanism.

Another important relaxation mechanism is due to fluctuations in g value caused, in the crystal field approximation, by fluctuations in the ligand-induced electrostatic field at the metal ion. Changes in

this field cause changes in the electronic energy levels of the metal atom. The g value observed depends on spin-orbit coupling between the ground electronic state and the excited electronic states, so that changes in the energy gaps between the states, particularly when it is small, can significantly affect the g value and effectively relax the spin.

The splittings in spin energy levels in the absence of a magnetic field, the zero field splittings, depend on the spin-orbit coupling between states in a similar fashion, except that here the spectroscopic parameter is very dependent on the symmetry of the ligand field. This has two effects: The first is that the presence of a strong static asymmetry may split the energy levels so far apart that EPR microwave quanta cannot bridge the gap between them. (As we observed earlier, odd electron systems must have at least one pair of spin levels which are not split by a crystal field.) The second implicaton is that thermal fluctuations which lower the symmetry of the ligand field, or appreciably increase any asymmetric components, will provide an effective relaxation mechanism which at room temperature will almost always result in these transitions not being observable by EPR.

b. Effects of Sample Condition

Cooling the sample

The operation of biology in solution, and at what solid state physicists consider high temperature, accentuates these relaxation problems. Because the relaxation mechanisms depend on thermal fluctuations, the rate of relaxation will decrease with lowered temperature. Lower-

ing the temperature also results in an increased population difference between spin levels, increasing signal strength.

As a result, the observability of EPR signals of transition metals is usually significantly enhanced by cooling the sample. This is as true of metal ions in biological systems as elsewhere, so that more and more biological metal ion EPR is being done at liquid nitrogen temperatures, or even at liquid helium temperatures.

In addition to reducing relaxation rates, and thus sharpening individual absorption lines, the cooling of a sample has a number of other advantages. Of course, there are a number of disadvantages also.

One advantage, which has been exploited for the investigation of enzyme kinetics, is the possibility of stopping a chemical reaction at any desired time by suddenly cooling the reaction mixture to much lower temperatures.[20-22] The concentration of paramagnetic species present may then be determined at leisure by taking an EPR spectrum of the frozen reaction mixture.

There are a couple of disadvantages to this method, however. One is that a fresh sample may be required for each point in time that a spectrum is taken, and the whole procedure is rather tedius.

More important than this is the possibility that cooling the sample alters the physical-chemical situation in such a way that one's interpretation of the low temperature spectrum does not accurately predict the situation at room temperature.

We found one such change during our research:[23] When an aqueous solution is frozen, microcrystals of pure ice form, concentrating the solute species in an "solution" phase. If the solution contains

paramagnetic ions, then this concentration process forces the ions closer together. If they become so close together that their dipole moments interact significantly, then the resulting EPR spectrum will be broadened with a loss in sensitivity and information.

To prevent dipolar broadening due to concentration of the paramagnetic species, the "solution" phase containing these ions must be large enough that the volume concentration of the metal ions is no more than 1 part per thousand. As the amount of water in the phase will be little more than that required to hydrate the ions and hydrogen-bonding species present, the total solute concentration must be at least 200 to 500 times the paramagnetic concentration. These amounts of diamagnetic solutes are usually present in biological systems, but serious errors have been made in model systems by ignoring the tendency of water to freeze pure. One is frequently fooled by a "glassy" appearance, and no observable dependence of the EPR spectrum on the rate of cooling.

Our observations on this subject are presented in Part II.B. of this thesis.

Glass spectra[24-26]

If one is looking at a small ion in a solution, and this solution is then frozen, there is one other important feature which is different between the ion in solution and the ion held in a frozen matrix. Recall that the EPR spectrum of an ion may depend upon the orientation of the ion with respect to the laboratory magnet. Small ions in solution will tumble so rapidly that this anisotropy is averaged out, and one sees a homogeneous spectrum in which the angular dependence has been removed.

If the solution containing these ions is then frozen, the ions cannot tumble rapidly, and cannot change their orientation with respect

to the magnet; different individual ions will be oriented differently with respect to the magnetic field. We now have an inhomogeneous system in which the ions oriented in one particular way will have one absorption spectrum, and the ions oriented some other way will have a different spectrum. The spectrum which one will observe is the average of the spectra for all orientations. This averaging results in a somewhat smeary spectrum, and at first it was felt that these "glass" spectra would not contain the amount of information available from spectra taken of solutions. Quite the opposite has proven true; fixing the orientation of the complexes by cooling has made it possible to find the dependence of the spectroscopic parameters on angle, instead of just the average value. The use of digital computers has made it possible to compute what a glass spectrum with given parameters looks like,[27] and this theoretical spectrum can then be compared with the experimental spectrum. The parameters used in calculating the computer spectrum can then be varied until the calculated spectrum fits the observed spectrum. This method has been so successful that Nieman and Kivelson[25] were moved to observe that the glass spectra compared favorably in the amount of information obtainable with spectra taken of single crystals.

Single crystals[13,14]

Spectroscopy on a single crystal is the ideal situation; one can place the crystal in different orientations with respect to the laboratory magnetic field and determine the angular dependence of spectroscopic parameters with good accuracy. If the crystal structure is known, then this variation with angle can be related to specific metal-ligand bonds.

The chief drawback of the single crystal method is the need for a single crystal; getting a single crystal is difficult, if not impossible, for most materials of biological interest.

In addition, the paramagnetic ions within the crystal must be sufficiently far apart that dipolar interactions will not smear out the EPR spectrum. In the chemically simple systems which the solid state physicists investigate, this is usually done by diluting the paramagnetic complexes in a crystal of a diamagnetic host. For the larger complexes of biological interest, this is not as easy to do, as it is rarer to find paramagnetic and diamagnetic complexes of shape and chemistry such that one may substitute in the crystal lattice of the other.

Besides this difficulty, there may be more than one paramagnetic ion per unit cell of the crystal. If this is true, which it usually is, then--although the crystal has but one orientation with respect to the magnetic field--the paramagnetic complexes may have several orientations. Particularly if the crystal structure is unknown, it may be relatively difficult to sort out the spectra due to the different orientations.

Chapter 3

SURVEY OF THE EPR OF BIOLOGICAL METAL COMPLEXES

With the foregoing as background, we can review the metals which occur biologically to see that is known about the EPR of these metals, what EPR of biological interest has been done, and what the limitations are on the observability of EPR signals in these metals.

Beinart and Palmer[30] have recently reviewed much this same topic, but with the point of view of enzymologists instead of that of a physical chemist. In addition, their review emphasized certain metals, notably copper and molybdenum, while this review emphasizes others, especially manganese. Thus, this review should be complementary to theirs in two respects.

Much of my discussion of the EPR of metal ions in general leans heavily on the classic paper by Abragam and Pryce,[16] on the early review by Bleaney and Stevens,[13] and on the more recent books by Griffith[17] and Ballhausen.[18] There are also several recent compilations of EPR data in inorganic systems.[14,28,29]

Vanadium

Not too much is known about the biological role of vanadium. The nutritional requirement for this metal in algae is well established, and it has been shown to have a beneficial effect on higher plants, but little seems to be known about what it does.[31-33] The higher oxidation states of vanadium have a chemistry which is similar to the higher oxidation states of molybdenum, and some nutritional studies indicate that vanadium may be able to replace molybdenum in some biological situations.[31,33] As molybdenum is known to function with flavoproteins

(see below), it is possible that vanadium may do this also.

Most animals do not seem to require vanadium, but the most famous of the biological uses of this metal occurs in the tunicates, a primitive marine subphylum of the vertebrates. The vanadium occurs in corpuscles in the blood in a complex called hemovanadin, which is thought to be a tetrapyrolle connected to a protein.[31,34]

The stable oxidation states of vanadium are V(III), V(IV), and V(V). Vanadium(V) has no d electrons and is thus diamagnetic. Vanadium(III) has a $3d^2$ electron configuration; because it has an even number of electrons, it should be difficult to see with EPR, and we are not aware of it having been seen. Susceptibility measurements of the ammonium alum indicate a zero-field splitting of 5 cm^{-1},[13] which is much more than the energy available from EPR spectrometers.

Vanadium(IV) has one electron in the 3d shell. Those familiar with crystal field theory will recall that, in an octahedral field, three of the five d orbitals are degenerate and lie lowest in an octahedral field. Slight deviations from octahedral symmetry split these energy levels somewhat, and the lone d electron of V(IV) will occupy the lowest of these levels. Because these states are nearly degenerate, their interaction via spin-orbit coupling is very large, so that very slight thermal fluctuations in the crystal field lead to rapid relaxation among the spin states of an octahedral d^1 complex. As a result, the paramagnetic resonance of octahedral V(IV) complexes can be observed only at very low temperatures.

Fortunately for our purposes, V(IV) reacts with water to form the vanadyl ion, VO^{2+}, and it is this species which dominates the chemistry of V(IV) complexes. The covalently bound oxygen splits the degeneracy

of the octahedral ground state widely, leaving an orbital singlet lowest. This results in slow relaxation and in an isotropic g value close to 2. A recent review of the chemistry of VO^{2+} includes a listing of the EPR work which has been done.[35]

The vanadyl ion is easily seen by EPR in aqueous solution, and can be readily identified by the 8-line hyperfine pattern due to the 7/2 nuclear spin of V^{51} (Fig. 1). Observe the uneven widths of the hyperfine lines in Figure 1. The vanadyl ion provides the classic example of relaxation due to thermal reorientation of the complex with respect to the applied magnetic field. This theory was first developed by McConnell,[36] and was applied to vanadyl by Rogers and Pake.[37]

Paramagnetic resonance does not seem to have been used very extensively in investigating the biological role of vanadium. Beinart and Palmer[30] display without analysis a vanadium EPR spectrum obtained by Musso from a mushroom extract, and this is the only biological vanadium EPR spectrum of which we are aware.

Due to the ease of seeing vanadyl EPR, it would seem that EPR is well suited for investigating the biological role of vanadium, and we are somewhat surprised that more does not seem to have been done with it.

Manganese

In a recent review, Cotzias[38] commented that "the biology of manganese suffers from the lack of unifying principles," but we can note that a fair amount of information is beginning to accumulate. Manganese is known to be required in animals,[38] and for photosynthesis in plants.[39,40] Manganese(II) is known to activate a large number of enzymatic reactions *in vitro*, many of which are also activated by

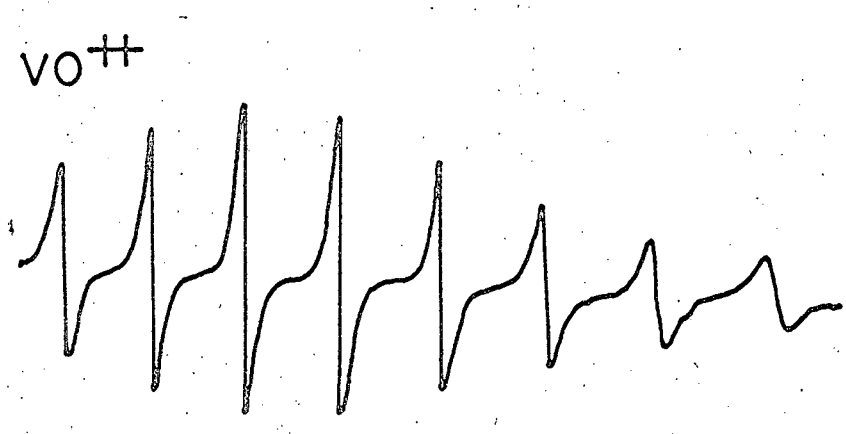

MUB-11253

Figure 1. EPR spectrum of the VO^{2+} ion in aqueous solution (X-band). The spacing between lines is about 120 oe.

magnesium.[33] The requirement of some organisms for manganese is decreased by the availability of magnesium,[41] suggesting that the lack of metal ion specificity *in vitro* carries over into the living organisms for at least some enzymatic reactions. In addition to this non-specific role for Mn(II), it is known to be a specific activator for the enzyme prolidase, and to be the metal ion which activates the enzyme arginase *in vivo*.[33]

One of the very features which makes the manganous ion so useful as an enzyme activator, its lability, also makes it difficult to study these complexes. Manganese(II), with its half filled d shell, forms relatively weak complexes, making it very difficult to isolate a manganese activated biochemical with the metal atom still bound to its original site.

An additional difficulty, also due to the d^5 configuration, is that the optical d-d transitions of Mn(II) are spin forbidden, and hence very weak; this eliminates optical spectroscopy as a convenient tool for investigating these ions.

Although Mn(III) is unstable in water,

$$Mn^{2+} = Mn^{3+} + e^- \qquad E^\circ = -1.51\ V\ ,$$

the addition of complexing agents significantly enhances the stability of this oxidation state and a number of Mn(III) complexes are known. It seems almost certain that Mn(III) occurs in biological systems and that manganese is used in this oxidation state for some biological purposes. There is some evidence for this in animals,[38] and the role of manganese in the oxygen evolution process of photosynthesis makes it likely that an elevated oxidation state occurs here also.[40]

It may even be that Mn(IV) occurs in biological systems. Complexes stable in aqueous solution with this oxidation state are known, or postulated, with biguanides,[42-44] with bypyridyl,[45] and with phthalocyanines and porphyrins.[40,46] It is known or suspected that most of these complexes are binuclear.

As Mn(III) has an even number of electrons, the observation of EPR of this oxidation state requires enough luck to have two spin energy levels less than 1 cm^{-1} apart; we can expect this only with a ligand field of high symmetry. The EPR of Mn(III) has been observed in TiO_2 at 77°K and below,[47] but we can have little hope of observing this oxidation state in complexes having the lower symmetry characteristic of biological compounds.

On the other hand, Mn(IV), with a $3d^3$ configuration, must have a Kramers degeneracy. The ground term is an orbital singlet, so that the g value should be close to 2, and not vary significantly with the orientation of the ion. This has been observed in several different crystals,[48] and the EPR spectra of Mn(IV) in pyrosulfuric acid solution, both at room temperature and at liquid nitrogen temperatures,[49] are in agreement with this picture.

We made the Mn(IV) biguanide complex, and checked it for EPR signals in aqueous solution, and as a polycrystalline sample at room temperature and at liquid nitrogen temperature. We observed no signal, probably due to the metal-metal interactions hypothesized for this compound. In retrospect, our failure to observe a signal in a solid sample might have been due to our naiveté in ignoring the possibility of intermolecular interactions, but it would seem that mononuclear Mn(IV) complexes should be observable in solution. Because of

the seeming ubiquity of metal-metal interactions in these compounds, temperature susceptibility measurements may be preferable to EPR in investigating the chemistry of these complexes.

Manganese(II) is perhaps the most easily observed metal ion in solution, and it is easily identified by its 6-line hyperfine pattern due to the 100% abundant Mn^{55} spin 5/2 nucleus (Fig. 2). Because of its half filled 3d shell, Mn(II) has a spherically symmetric, non-degenerate ground state, which to first order is not connected by spin-orbit coupling to any other electronic state. This means that Mn(II) has an isotropic g value of 2.00, and its relaxation should be slow.

Early in the history of EPR it was observed that the addition of complexing agents to a solution of manganous ion results in the disappearance of the characteristic 6-line spectrum, with nothing, or at most, a broad weak spectrum in its place.[50] Practically anything added to a Mn(II) solution will broaden the EPR lines. Alcohol, sugar, chloride ion, and nitrate ion will all do the trick. More "strongly" bonding ligands, such as EDTA or bipyridyl, virtually obliterate the signal in solution, so that a solution 0.1 F in Mn(II) is barely observable.

Morgan and his students have worked extensively on the relaxation mechanisms of Mn(II) in solution, and have concluded that the relaxation of $Mn(H_2O)_6^{++}$ is due to a fluctuating zero-field splitting caused by random fluctuations in the positions of water molecules in the vicinity of the ion.[51]

Hayes and Myers[52] considered the effect of chloride and sulfate on EPR linewidth, and concluded that the additional width due to these ions

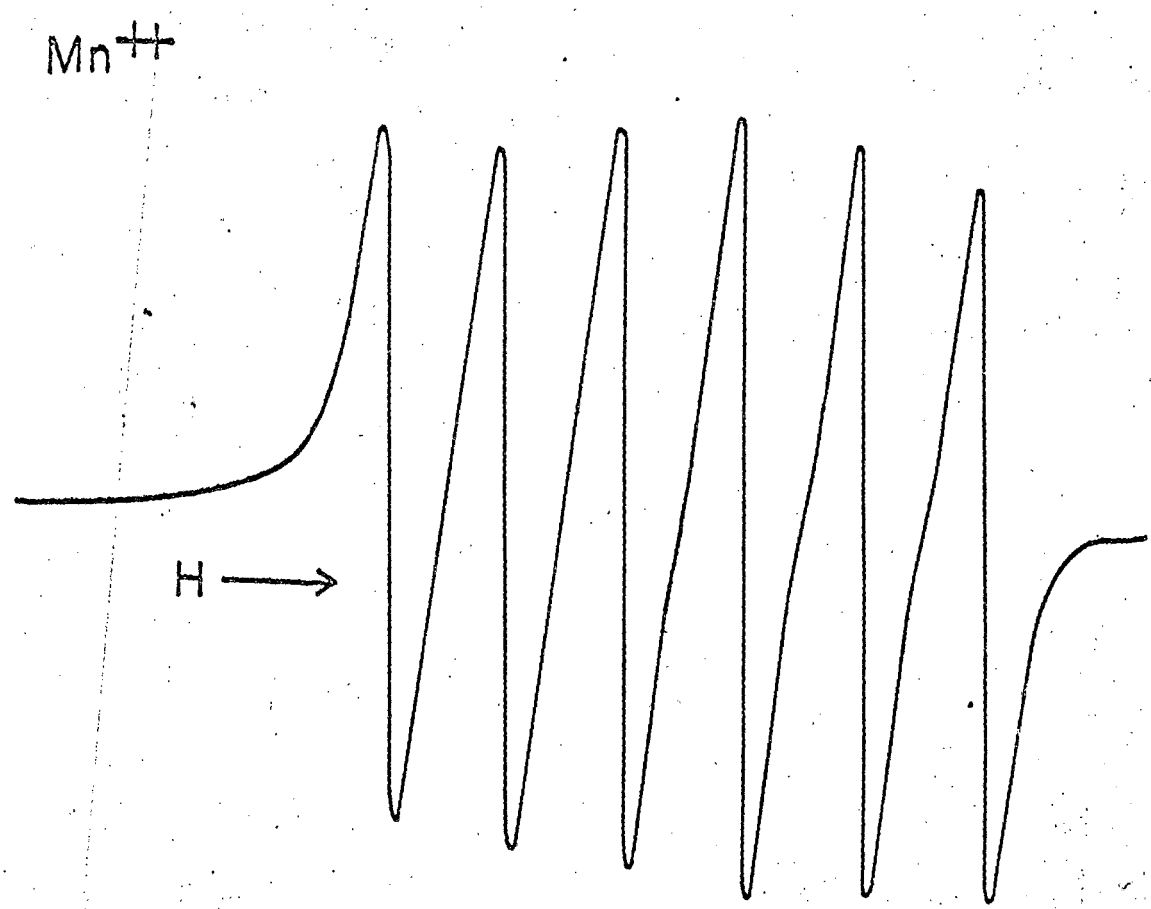

MUB-11255

Figure 2. EPR spectrum of the Mn^{2+} ion in aqueous solution (X-band). The spacing between lines is about 95 oe.

was caused by chemical exchange in the first and second coordination spheres.

The relaxation mechanism for Mn with polydentate ligands has not been established, but it seems likely that this is either due to reorientation of the complex with respect to the laboratory magnet, or due to fluctuations in the ligand field strength.

Practically any whole cell biological specimen placed in an EPR spectrometer at room temperature will give the spectrum characteristic of uncomplexed manganous ion, and this is a convenient method of assaying for uncomplexed Mn(II).

When a solution of $Mn(H_2O)_6^{++}$ is frozen, and the solute concentrations are such that dipolar broadening does not occur, then a characteristic EPR spectrum results (Fig. 3). Note the additional pairs of lines between each of the six main peaks; these are due--formally--to simultaneous nuclear spin flips. This same sharp spectrum has been reported for a number of biological samples (e.g., Refs. 30, 53, 54), both at room and at reduced temperatures. These signals may be due to hexaquo Mn(II), or it is possible that other octahedrally coordinated Mn(II)--particularly to oxygen ligands--gives essentially the same spectrum.

In contrast, the manganese EDTA complex has a significantly different spectrum (Fig. 4) in a glass at liquid nitrogen temperatures. Apparently, the crystal field caused by this chelating agent is sufficiently strong that it can cause a significant zero field splitting due to second order spin-orbit interactions.

It would be difficult, if not impossible, to extract spectroscopic parameters from this X-band spectrum, and the use of a spectrometer which uses higher energy microwave quanta is indicated. Even with a

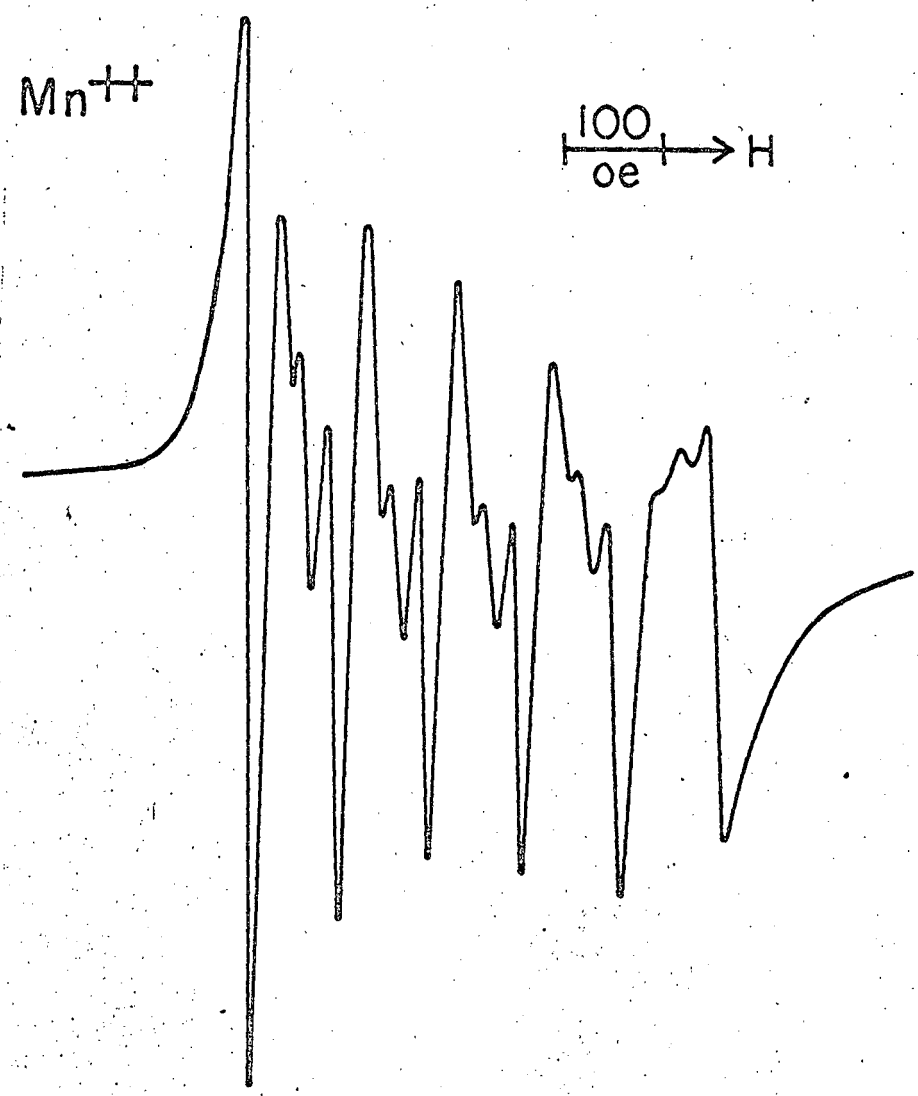

MUB-11254

Figure 3. EPR spectrum of Mn^{2+} in frozen aqueous solution (X-band, 100°K). Methanol, 25 vol %, added to prevent dipolar broadening.

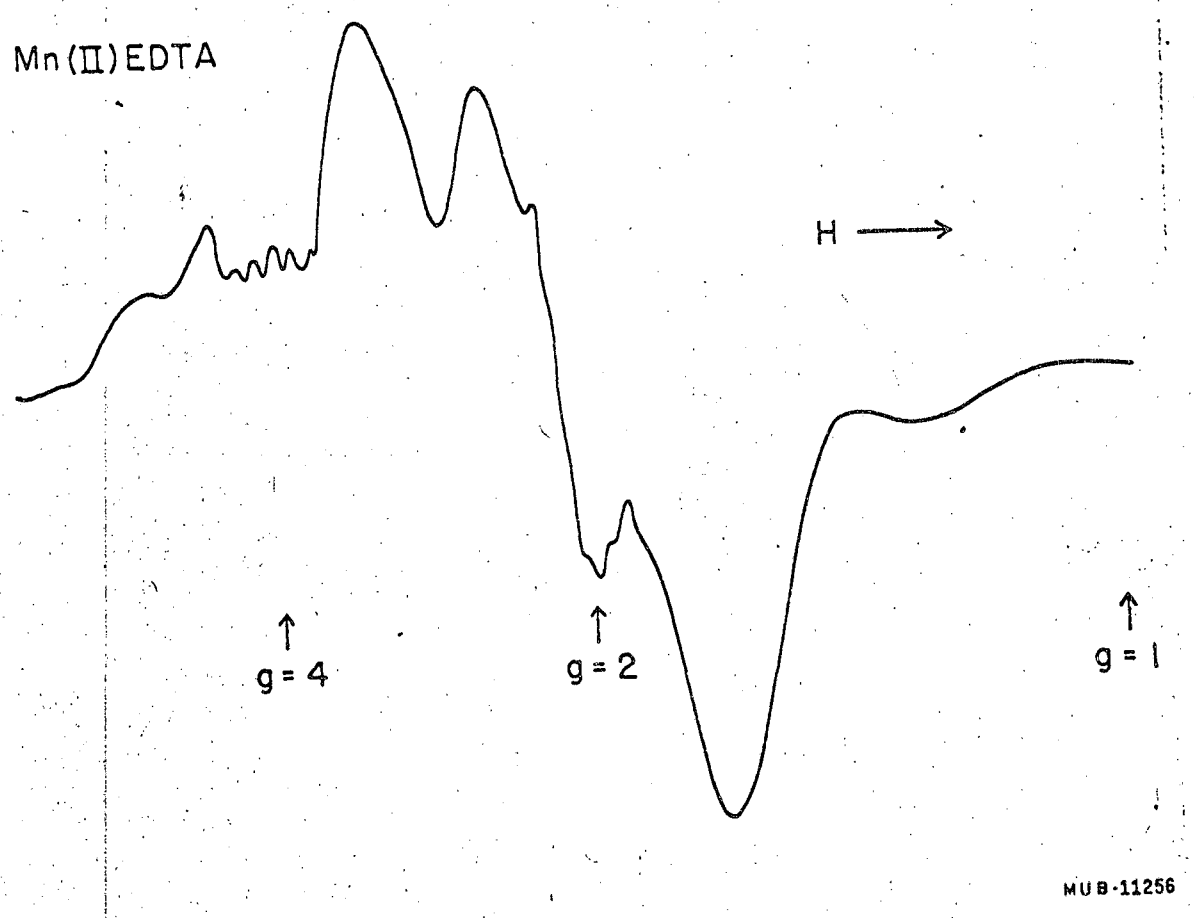

Figure 4. EPR spectrum of manganous EDTA in frozen aqueous solution (X-band, -100°C, pH 10 before freezing). Glycerol, 25 vol %, added to reduce dipolar broadening.

single crystal to work with, Seed[55] found it necessary to use a Q-band spectrometer to analyze the EPR spectrum of Mn^{2+} in the ternary system of NH_4Cl-$MnCl_2$-H_2O, which has a zero-field splitting of 0.15 cm^{-1}.

We suspect that zero-field splittings of 0.1 to 0.2 cm^{-1} are common in Mn(II) complexes of biological interest, so that it would be generally advisable to study these complexes with a Q-band spectrometer. Even then, the combined difficulty of extracting spin parameters from a 5-spin spectrum, and then interpreting the spin parameters in terms of second order spin-orbit interactions in a 5 electron configuration, makes it unlikely that the EPR of Mn(II) complexes will be used as other than a "fingerprint" technique by other than physicists.

Iron

Iron is by far the most important of the transition metals in biology, occurring in a variety of compounds serving a number of different functions.[56] In many of these compounds, among them the heme moiety of hemoglobin, the iron is bound in a planar porphyrin ring. Because of their biological importance, and the ease with which they can be observed with optical spectroscopy, these heme iron compounds have been the objects of considerable study for a number of years. It is only recently that other biological iron compounds, frequently lumped together as "non-heme iron", have come under intensive investigation.[57]

The iron in biological compounds occurs in both the ferrous and ferric states, and it appears that one of the most useful attributes of iron, as with several of the other transition metals, is its ability to readily change its oxidation state.

Ferrous iron has a $3d^6$ electron configuration, with all of the difficulties of EPR observation true for any even electron system. For several years, however, a free radical-like (i.e., narrow) EPR signal at

g = 1.94 has been observed in biological systems, and associated with reduced iron.[30,58] Recently, this mystery has been cleared up by Blumberg,[59,60] who explained that the signal is due to a free radical whose g value is altered by electron exchange with a coordinated spin-paired ferrous ion.

Ferric iron has a $3d^5$ electron configuration, isoelectronic with Mn(II). However, because of its greater nuclear charge, iron(III) binds to ligands more strongly so that second order spin-orbit coupling to excited electronic states is significant for virtually all of its complexes. The true g value of the ground state remains very close to an isotropic 2.00, but the relatively strong crystal field creates a zero-field splitting of several wavenumbers.

This splitting is so large that one defines the spin quantum number in terms of the crystal field axes, instead of the usual procedure of defining them with respect to the magnetic field. The application of a magnetic field is then considered as a small perturbation on the states so defined. One may then classify the spin levels according to the projection of this spin along the crystal field axis, and consider the levels with $M_s = \pm 1/2$, $\pm 3/2$, and $\pm 5/2$ as three independent doublets. Each of these doublets, considered individually, can then be assigned an effective g value which reflects the size of the energy splitting of the doublet in a magnetic field. These g values will depend on the symmetry of the zero field splitting.

In an axial field (one with a three or more fold axis of symmetry), the $\pm 1/2$ doublet has an effective g value ranging from 2 to 6, depending on orientation. In a glassy sample, this gives rise to an EPR spectrum with a large peak at g = 6, and a smaller one at g = 2. As

the symmetry becomes less than axial, a broad resonance at $g = 4.3$ develops. The $g = 4.3$ signal was first explained by Castner, Newell, Holton, and Slichter,[61] and the general treatment of the effective g values is given by Wickman, Klein, and Shirley.[62]

Apparently because the effective g values are sensitive to the relative crystal field strengths in different directions, Wickman *et al.*, in their work on ferrichrome-A, found it necessary to go down to a temperature of 1°K in order to detect some of the resonances.

In view of this recent development in the theory of Fe(III) magnetic resonance, and the value of observation at very low temperatures, most of the biological Fe(III) EPR work performed to date is more or less outmoded. The notable exception to this is the work which has been done on different heme compounds.[63]

Cobalt

Cobalt is needed by many, if not all, animals, and by some microorganisms, for vitamin B_{12} (cyanocobalamin),[64] the chemistry of which has been recently reviewed by Bonnett.[65] It has not been proven that cobalt is required by higher plants, but beneficial effects have been observed upon its addition.[66]

Cobalt(II) activates a number of enzymatic reactions *in vitro*, and it is particularly noted for its ability to activate enzymes which utilize zinc *in vivo*. As zinc has a full 3d shell, its complexes cannot be studied by EPR, susceptibility measurements, or d-d electronic transitions; consequently, the study of its substitution by another metal is of particular importance.

In its ordinary aqueous chemistry, cobalt has two important oxidation states, II and III. In aqueous solutions containing no

complexing agents, the oxidation to Co(III) is very unfavorable:

$$Co^{2+} = Co^{3+} = e^- \qquad E^\circ = -1.84\ V\ .$$

However, in the presence of complexing ligands, the stability of the trivalent state is greatly enhanced:

$$[Co(NH_3)_6]^{2+} = [Co(NH_3)_6]^{3+} + e^- \qquad E^\circ = -0.1\ V\ .$$

One therefore expects both of these oxidation states in biological systems.

Cobalt(III) has a d^6 electron configuration, isoelectronic with ferrous iron. The free ion has four unpaired electrons, but a quite weak crystal field suffices to cause spin pairing. With the exception of $(CoF_6)^{3-}$, which has S = 2, all of the ionic cobalt(III) complexes known have diamagnetic ground states. All of the Co(III) porphyrin and other tetrapyrolle complexes related to vitamin B_{12} are diamagnetic.

Cobalt(II) is d^7, and may have a ground state having either 1 or 3 unpaired electrons. A tetrahedral ligand field cannot produce the low spin state, but a number of octahedral and tetragonal complexes of cobalt(II) have spin 1/2; square planar complexes, such as the tetrapyrolles, are particularly likely to have this configuration.

High spin cobalt(II) has a ground state which is triply degenerate orbitally in an octahedral field. As in the case of octahedral vanadium(IV), this orbital degeneracy makes the spin levels very susceptible to relaxation, so that the EPR of high spin cobalt(II) may be seen only at very low temperatures.

Low spin Co(II) is also susceptible to relaxation due to spin-orbit interaction between the ground state and low lying excited levels. Depending on the distance between the ground and first excited state, a given complex may be quite easily observable at liquid nitrogen temperatures, or not observable except at considerably lower temperatures.[67]

The native vitamin B_{12} compounds have been characterized with reasonable certainty as containing diamagnetic Co(III), which cannot be studied by EPR. The chemistry of the reduction of vitamin B_{12} is possibly of some biological importance, and is still poorly defined. Even if the reduced compounds do not occur in living systems, an increased understanding of them may contribute to knowledge about the biological species. For this reason, the Co(II) complexes of corrin-like compounds are of some interest.

Hogenkamp, Barker, and Mason[68] have taken EPR spectra at liquid nitrogen temperatures of photolyzed coenzyme B_{12} and of reduced vitamin B_{12}. With the resolution obtained, the two spectra were identical, and closely matched the g values known for Co(II) phthalocyanine.[69,70] More recently, Assour[71] has studied the spin resonance of cobalt phthalocyanine quite extensively, and has succeeded in observing hyperfine splittings due to nitrogen nuclei in heterocyclic compounds bound in the axial positions of the complex. In view of this, it might be profitable to reinvestigate some of the B_{12} compounds to see if nitrogen hyperfine, or even C^{13} hyperfine, splittings might be observed.

Copper

Cuprous copper, Cu(I), has a full 3d shell and is thus diamagnetic. Cupric copper, Cu(II), has a $3d^9$ configuration, which may be considered as a full d shell plus one positive hole.

More biological EPR, and a greater variety of it, has been done on copper than on any other metal. This is for a number of reasons: Copper is important biologically; its tendency to bond covalently makes its biological compounds more easily isolable intact; and the brilliant color of the cupric compounds makes them relatively easy to identify and isolate. Its EPR is attractive because biological oxidations and reductions can be followed by appearance and disappearance of the EPR signal; the EPR signal is easily observable, particularly at liquid nitrogen temperatures;[25,26] and the fact that it is a one electron problem makes the theoretical analysis of the spectra relatively more easy.[18]

The metabolism of copper has been reviewed by Adelstein and Vallee,[72] the copper proteins have been reviewed by Malmstrom and Neilands,[7] and the extensive applications of EPR to biological copper have been covered in two recent reviews.[30,73]

Molybdenum

A major biological use, if not the sole use, of molybdenum is in connection with flavoproteins, and work with both model compounds[74] and enzyme systems[75] seems to indicate that oxidation and reduction occur between Mo(V) and Mo(VI), and the flavin. Paramagnetic resonance observations of the Mo(V) EPR signal, and the EPR of other paramagnetic species present, has played a major role in the elucidation of the mechanism of these enzyme reactions. Much of this work has

been done in the group headed by Beinart at Madison, and it has been recently reviewed by them.[30,75]

From the aqueous chemistry,[67] the oxidation states III through VI are possible. Molybdenum(VI) has no 4d electrons, which eliminates it as a possibility for magnetic resonance, and the +4 state is usually diamagnetic also. The EPR of both Mo(III) and Mo(V) is easily seen.

REFERENCES

1. C. A. Lamb, O. G. Bentley, and J. M. Beattie, eds., Trace Elements (Academic Press, New York, 1958).
2. C. L. Comar and F. Bronner, eds., Mineral Metabolism, Vol. 2B (Academic Press, New York, 1962).
3. F. C. Steward, Plant Physiology, Vol. 3, "Inorganic Nutrition of Plants" (Academic Press, New York, 1963).
4. L. A. Johnson and M. J. Seven, eds., Biological Aspects of Metal Binding, Fed. Proc. 20, Supp. 10 (1961).
5. A. E. Martell and M. Calvin, Chemistry of the Metal Chelate Compounds (Prentice-Hall, New York, 1964).
6. F. P. Dwyer and D. P. Mellor, eds., Chelating Agents and Metal Chelates (Academic Press, New York, 1964).
7. B. G. Malmstrom and J. B. Neilands, Ann. Rev. Biochem. 33, 331 (1964).
8. F. A. Cotton and G. Wilkinson, Advanced Inorganic Chemistry (Interscience Publishers, U.S.A., 1962).
9. M. Bersohn and J. Baird, An Introduction to Electron Paramagnetic Resonance (W. A. Benjamin, New York, 1966).
10. G. E. Pake, Paramagnetic Resonance (W. A. Benjamin, New York, 1962).
11. H. S. Jarrett, Solid State Phys. 14, 215 (1963).
12. C. P. Slichter, Principles of Magnetic Resonance (Harper and Row, New York, 1963).
13. B. Bleaney and K. W. H. Stevens, Repts. Progr. Phys. 16, 108 (1953).

14. W. Low, Paramagnetic Resonance in Solids, Supp. 2 to Solid State Physics (Academic Press, New York, 1960).

15. Varian Associates, Palo Alto, California.

16. A. Abragam and M. H. L. Pryce, Proc. Roy. Soc. (London) 205A, 135 (1951).

17. J. S. Griffith, The Theory of Transition-Metal Ions (Cambridge Univ. Press, Cambridge, England, 1961).

18. C. J. Ballhausen, Introduction to Ligand Field Theory (McGraw-Hill Book Co., New York, 1962).

19. A. Carrington and G. R. Luckhurst, Mol. Phys. 8, 125 (1964).

20. R. C. Bray, Biochem. J. 81, 189 (1961).

21. G. Palmer, R. C. Bray, and H. Beinert, J. Biol. Chem. 239, 2657 (1964).

22. (a) R. C. Bray, in Rapid Mixing and Sampling Techniques in Biochemistry, B. Chance, R. H. Eisenhardt, Q. H. Gibson, and K. K. Lonberg-Holm, eds (Academic Press, New York, 1964), p. 195; (b) G. Palmer and H. Beinert, ibid., p. 205.

23. R. T. Ross, J. Chem. Phys. 42, 3919 (1965).

24. R. H. Sands, Phys. Rev. 99, 1222 (1955).

25. R. Neiman and D. Kivelson, J. Chem. Phys. 35, 156 (1961).

26. H. R. Gersmann and J. D. Swalen, J. Chem. Phys. 36, 3221 (1962).

27. J. D. Swalen and H. M. Gladney, I.B.M. J. Research Develop. 8, 515 (1964).

28. K. D. Bowers and J. Owen, Repts. Progr. Phys. 18, 304 (1955).

29. J. W. Orton, Repts. Progr. Phys. 22, 204 (1959).

30. H. Beinert and G. Palmer, Adv. Enzymol. 27, 105 (1965).

31. A. Nason, in Ref. 1, p. 269.

32. E. J. Hewitt, in Ref. 3, p. 97.

33. A. Nason and W. D. McElroy, in Ref. 3, p. 451.

34. D. A. Webb, Pubbl. staz. zool. (Naples) 28, 273 (1956).

35. J. Selbin, Chem. Revs. 65, 153 (1965).

36. H. McConnell, J. Chem. Phys. 25, 709 (1956).

37. R. N. Rogers and G. E. Pake, J. Chem. Phys. 33, 1107 (1960).

38. G. C. Cotzias, in Ref. 2, p. 403.

39. A. Pirson, in Ref. 1, p. 81.

40. M. Calvin, Rev. Pure and Appl. Chem. 15, 1 (1965).

41. D. J. D. Nicholas, Ref. 3, Chapt. 3.

42. M. M. Ray and P. Ray, J. Ind. Chem. Soc. 35, 601 (1958).

43. P. Ray, Chem. Rev. 61, 313 (1961).

44. R. S. Banerju and S. Basu, J. Inorg. Nucl. Chem. 27, 359 (1965).

45. R. S. Nyholm and A. Turco, Chem. and Ind. 1960, 74 (1960).

46. L. K. Phillips, Ph.D. Thesis, University of California, Berkeley, 1966 (in preparation).

47. H. J. Gerritsen and E. S. Sabisky, Phys. Rev. 132, 1507 (1963).

48. S. Geschwind, P. Kisliuk, M. P. Klein, J. P. Remeika, and D. L. Wood, Phys. Rev. 126, 1684 (1962), and references cited therein.

49. H. C. Mishra and M. C. R. Symons, J. Chem. Soc. 1963, 4490 (1963).

50. M. Cohn and J. Townsend, Nature 173, 1090 (1954).

51. B. B. Garrett and L. O. Morgan, J. Chem. Phys. 44, 890 (1966).

52. R. G. Hayes and R. J. Myers, J. Chem. Phys. 40, 877 (1964).

53. J. E. Maling, L. T. Taskovitch, and M. S. Blois, Jr., Biophys. J. 3, 79 (1963).

54. D. W. Nebert and B. T. Allen, Biophys. J. 6, 189 (1966), and references cited therein.

55. T. J. Seed, J. Chem. Phys. 41, 1486 (1964).

56. C. V. Moore and R. Dubach, in Ref. 2, p. 287.

57. A. San Pietro, ed., Non-Heme Iron Proteins (Antioch Press, Yellow Springs, Ohio, 1965).

58. H. Beinert, in Ref. 57, p. 23.

59. W. E. Blumberg and J. Peisach, in Ref. 57, p. 101.

60. W. E. Blumberg (Bell Telephone Laboratories), private communication.

61. T. Castner, G. Newell, W. Holton, and C. P. Slichter, J. Chem. Phys. 32, 668 (1960).

62. H. H. Wickman, M. P. Klein, and D. A. Shirley, J. Chem. Phys. 42, 2113 (1965).

63. Reviewed by J. S. Griffith, Biopolymers, Symposium No. 1, p. 35 (1964).

64. E. L. Smith, in Ref. 2, p. 349.

65. R. Bonnett, Chem. Revs. 63, 573 (1963).

66. E. J. Hewitt, in Ref. 3, Chapt. 2.

67. The chemistry of cobalt and molybdenum complexes, and their EPR, is reviewed by R. J. P. Williams in Advances in the Chemistry of the Coordination Compounds, S. Kirschner, ed. (Macmillan, New York, 1961), p. 65.

68. H. P. C. Hogenkamp, H. A. Barker, and H. S. Mason, Arch. Biochem. Biophys. 100, 353 (1963).

69. J. F. Gibson, D. J. E. Ingram, and D. Schonland, Disc. Faraday Soc., No. 26, 72 (1963).

70. J. S. Griffith, Disc. Faraday Soc., No. 26, 81 (1958).

71. J. M. Assour, J. Am. Chem. Soc. 87, 4701 (1965).

72. S. J. Adelstein and B. L. Vallee, in Ref. 2, p. 371.

73. A. S. Brill, R. B. Martin, and R. J. P. Williams, in Electronic Aspects of Biochemistry, B. Pullman, ed. (Academic Press, New York, 1964), p. 519.

74. P. C. H. Mitchell and R. J. P. Williams, Biochim. Biophys. Acta 86, 39 (1964).

75. R. C. Bray, G. Palmer, and H. Beinert, in Oxidases and Related Redox Systems, T. E. King, H. S. Mason, and M. Morrison, eds. (John Wiley and Sons, New York, 1965), Vol. 1, p. 359.

Reprinted from THE JOURNAL OF CHEMICAL PHYSICS, Vol. 42, No. 11, 3919–3922, 1 June 1965
Printed in U. S. A.

Dipolar Broadening of EPR Spectra Due to Solute Segregation in Frozen Aqueous Solutions*

ROBERT T. ROSS

Department of Chemistry and Lawrence Radiation Laboratory, University of California, Berkeley, California

(Received 16 December 1964)

EPR spectra of Mn^{2+} and Gd^{3+} in a number of frozen aqueous solutions show that ice crystallization causes extensive segregation of solutes. The concentration of paramagnetic ions thus induced results in dipolar broadening of EPR spectra, and published spectra of frozen aqueous Mn^{2+} are reinterpreted accordingly. This segregation effect may be reduced by the addition of quantities of experimentally inert solute.

INTRODUCTION

SOLUTIONS cooled to low temperatures are frequent subjects for a variety of spectroscopic investigations. This cooling may cause high local concentrations of a solute molecule under study, and the interactions thus induced may significantly affect some measurements. In electron paramagnetic resonance (EPR) spectroscopy, high local concentrations of paramagnetic species can result in electron spin dipole broadening of the lines in the EPR spectrum.

Most studies of frozen solutions by EPR have used an organic matrix,[1–3] but recently some use has been made of frozen aqueous solutions,[4–6] in which segregation induced by freezing may be a problem. The art of preparing organic glasses is highly developed,[7] but the difficulty of making an aqueous glass seems to have induced a disregard for the consequences of ice-crystal formation. Aggregation or crystallization of a solute in a homogeneous solvent is familiar, but the solvent itself also may separate as a crystalline phase. Particularly in aqueous solutions, where strong hydrogen bonding makes the ice structure very reluctant to include a foreign ion, crystallization of solvent as a virtually pure phase will greatly concentrate solute species in the interstices of solvent crystallites.

In this paper, we discuss what effect the use of different aqueous mixtures has on paramagnetic ion–ion distances as detected by EPR. The results confirm that segregation is extensive in frozen aqueous solutions, and some published EPR observations are reinterpreted accordingly.

* Supported in part by a National Science Foundation Predoctoral Fellowship, and in part by the U.S. Atomic Energy Commission.

[1] H. R. Gershmann and J. D. Swalen, J. Chem. Phys. **36**, 3221 (1962).
[2] R. Neiman and D. Kivelson, J. Chem. Phys. **35**, 156 (1961).
[3] D. Kivelson and S. K. Lee, J. Chem. Phys. **41**, 1896 (1964).
[4] F. E. Wakim and A. V. Nolle, J. Chem. Phys. **37**, 3000 (1962).
[5] B. T. Allen and D. W. Nebert, J. Chem. Phys. **41**, 1983 (1964).
[6] G. Palmer, R. C. Bray, and H. Beinert, J. Biol. Chem. **239**, 2657 (1964).
[7] F. J. Smith, J. K. Smith, and S. P. McGlynn, Rev. Sci. Instr. **33**, 1370 (1962).

THEORY

The dipolar interaction between two paramagnetic species is given by the classical relation

$$E_d = \mu r^{-3}(1-3\cos^2\phi).$$

Van Vleck[8] considered the effect of this interaction on the shape of an EPR line; for a sample with randomly oriented ions, its contribution to the width of the line between points of maximum slope is given by the relationship

$$\Delta H = 2g\beta[\tfrac{3}{5}S(S+1)]^{\frac{1}{2}}\langle(\sum_{i\neq j} r_{ij}^{-6})^{\frac{1}{2}}\rangle,$$

where $\langle\ \rangle$ signifies an average over j.

The value of this average over all ions depends markedly on the distribution of ion–ion distances. For a completely random distribution, it is approximately equal to $5C$, where C is the volume concentration of paramagnetic ions. If the sample is not homogeneous, the EPR linewidth due to this interaction is a measure of a rather local concentration.

For a spin $N/2$ system with $g=2$, the linewidth contribution is approximately $50N$ Oe per molar concentration. Exchange narrowing has not been considered, so this model is not accurate for high concentrations. The effect of paramagnetic species other than the one being observed is reduced by a factor of $\frac{2}{3}$.[8]

EXPERIMENTAL PROCEDURES

The EPR spectra were obtained with an X-band spectrometer operating at 9.1 Gc/sec. A derivative presentation of the spectrum resulted from phase-sensitive detection of the absorption with 100-kc/sec field modulation of 3-Oe amplitude. A rectangular TE_{102} cavity (Varian V4531) was used with a quartz-jacketed gas-flow cooling system (Varian V4547). Liquid samples at room temperature were placed in 3-mm-bore quartz sample tubes and cooled by immersion in liquid nitrogen before placement in the cavity. Sample temperature in the cavity was about 90°K and was not a critical parameter.

[8] J. H. Van Vleck, Phys. Rev. **74**, 1168 (1948).

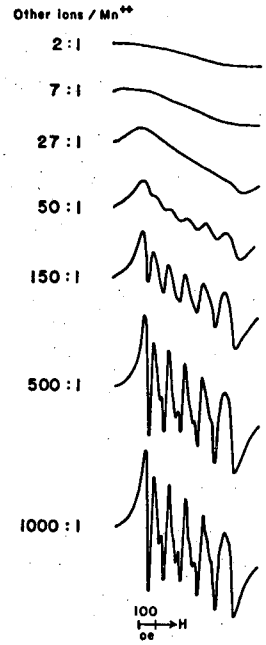

FIG. 1. Effect of added sodium perchlorate on the derivative EPR spectrum of 0.005*M* Mn^{++} in frozen aqueous solution. "Other ions" refers to total concentration of anions and cations not Mn^{++}.

All solutions used were saturated with air. The paramagnetism of O_2 had no observable effect on EPR linewidths in frozen aqueous solution.

Identical Mn^{++} spectra were obtained from commercial CP manganous nitrate and from manganese perchlorate made from $MnCO_3$ and perchloric acid.

Gadolinium perchlorate was made by the addition of 3*M* perchloric acid to Gd_2O_3, and dilution to the desired strength. The stock solution used was 0.0040*M* in $Gd(ClO_4)_3$, and was 0.040*M* in $HClO_4$ to hinder hydrolysis.

EXPERIMENTAL RESULTS

Addition of increasing amounts of sodium perchlorate to aqueous 0.005*M* manganous nitrate results in a progressively sharper and more intense EPR spectrum of the frozen solution (see Fig. 1). The dependence of the spectrum on concentration of additive was also investigated in detail with methanol, perchloric acid, and nitric acid used as additives, with results similar to those shown for sodium perchlorate.

Spectra for 0.005*M* manganese in 25 and 75 vol% aqueous methanol were equivalent and were as distinct as any spectra obtained. If the intensity (absolute maximum minus absolute minimum slope of the absorption) of the derivative EPR spectrum of the 25% methanol sample is assigned the value 100, various frozen aqueous solutions yielded the intensities listed in Table I. A convenient measure of the clarity of detail in a Mn^{++} spectrum is the ratio of the difference between the first minimum and second maximum to the difference between the first maximum and last minimum. The 25% methanol spectrum has a clarity index of 106 (in percent). Values for other frozen solutions are given in Table I.

Frozen aqueous solutions of Gd^{3+} were also found to have an EPR signal which progressively narrows and increases in intensity upon the addition of diamagnetic solutes before freezing. Our hopes of using Gd^{3+} to obtain a clear-cut dipolar broadening effect on a single EPR line were frustrated by a broad background absorption, probably due to the presence of more than one chemical species. Typical spectra are illustrated in Fig. 2.

To further check the assumption that dipolar broadening is responsible for the phenomena observed, the effect of added Ni^{++} on the Mn^{++} spectrum was compared with the effect of increased Mn^{++} concentration. The effect of added Ni^{++} on the clarity and specific intensity is about the same as 5% as much added Mn^{++}.

DISCUSSION

Regardless of the additive used in the manganese experiments, the same characteristic spectrum prevails. The only species common to all the systems tried are Mn^{++} and H_2O, implying that hydrated manganous ion is responsible for the spectrum.

The manganous ion has consistently been found to have a coordination number of 6.[9] Single-crystal EPR studies of the $Mn(H_2O)_6^{++}$ ion have been made in several diamagnetic hosts.[10] Values found for the axial splitting parameter D are in the range 0.014 to 0.027 cm^{-1}. Comparison of the powder spectrum of $Mn(H_2O)_6^{++}$ in a Tutton salt, $(NH_4)_2Zn(SO_4)_2 \cdot 6H_2O$, at room temperature ($D = +0.024$ cm^{-1}), with that of Mn^{++} in a frozen solution shows that the frozen solute has a mean distortion from cubic symmetry equal to or

TABLE I. Intensity and clarity of detail of the derivative EPR spectrum of 0.005*M* Mn^{++} in different frozen aqueous solutions. Scales are arbitrary and are defined in the text.

Solution	Intensity	Clarity
25% Methanol	100	106
2*M* Methanol	67	83
2*M* K acetate	45	85
2*M* H_2SO_4	45	82
25% Glycerol	44	84
25% Pyridine	42	74
2*M* HNO_3	39	73
2*M* $NaClO_4$	32	75
2*M* $HClO_4$	17	36
25% Dioxane	16	5
2*M* HCl	9	69
2*M* KNO_3	8	5

[9] An isolated and understandable exception is the seven-coordinate $Mn(H \cdot EDTA)(H_2O)^-$ complex [J. L. Hoard, B. Pederson, S. Richards, and J. V. Silverton, J. Am. Chem. Soc. 83, 3533 (1961)].

[10] K. D. Bowers and J. Owen, Rept. Progr. Phys. 18, 304 (1955).

slightly smaller than that for $Mn(H_2O)_6^{++}$ in the Tutton salt. We conclude from this and the chemical evidence which has been presented that the spectrum in the frozen aqueous solution is due to $Mn(H_2O)_6^{++}$.

Manganese complexes involving nonwater ligands contribute at most a broad background signal. Only the $M=+\frac{1}{2}\leftrightarrow M=-\frac{1}{2}$ transitions are observable in the hexahydrate spectrum. A first coordination sphere which is not composed of all identical ligands will create a much greater crystal-field splitting, broadening even these transitions into oblivion.[11]

We propose that the broad structureless line observed by Wakim and Nolle[4] and by Allen and Nebert[6] for frozen solutions of manganous salt alone in water is caused by manganese–manganese dipolar broadening. The resolution of hyperfine structure obtained by Allen and Nebert on the addition of chloride is due to a decrease in dipolar interactions rather than a change in crystal-field parameters. Allen and Nebert obtained a Mn^{++} spectrum in methanol identical to the unbroadened frozen aqueous spectra; as the solution used was made by the addition of hydrated salt to undried alcohol, we suggest that this spectrum is also due to $Mn(H_2O)_6^{++}$.

The broad background absorption found in the gadolinium experiments is probably due to the presence of more than one chemical species. The unpaired electrons of an ^8S rare-earth ion are sufficiently insulated from the ligands that complexes, such as $Gd(H_2O)_5Cl^{2+}$ or $Gd(H_2O)_9^{3+}$, will have little greater crystal-field splitting than $Gd(H_2O)_6^{3+}$.

Considering the difference in magnetic moments and the statistical factor of $\frac{2}{3}$, Ni^{++} should be 36% as effective in broadening Mn^{++} as is manganese itself, but the experiments tried gave only a 5% effect. The remaining factor of 7 may be due to a tendency for the two kinds of ions to go into different phases on freezing; an alternate possibility is that rapid electronic relaxation of the Ni^{++} renders it less effective in inducing Mn^{++} relaxation.

A given additive may have two distinct effects on the EPR spectrum of frozen Mn^{++}: A decrease in dipolar interactions will both improve the clarity and increase the intensity of the spectrum. Complex formation with the additive will decrease the amount of $Mn(H_2O)_6^{++}$ present, reducing signal intensity.

By comparing the intensity and clarity figures for the different additives, we estimate that 75% to 85% of the Mn^{++} in the $2M$ HCl solution is a chloride complex. In all the other solutions, at least 40% of the manganese seems to remain as the hydrate which produces the characteristic spectrum. This is true even for $2M$ pyridine and sulfate, which complex Mn^{++} moderately strongly in aqueous solution.[12,13]

Subsequent to the concentration induced by ice crystallization, a solute may aggregate or crystallize, or else rapid cooling may trap individual molecules in a disordered phase. A disordered phase may be crystals of the solvent (ice) or of other solute with the solute of interest occurring as defects, or the phase may be noncrystalline.

Noncrystalline ("glass") regions will result on cooling a liquid only if diffusion is halted by increasing viscosity before chemical equilibrium can be attained. Glass formation will be favored if the diffusion rate is slow at the freezing point, if crystal nucleation is difficult, or if the rate of crystal growth is slow.[14,15]

The use of a mixture introduces a number of possibilities for favoring glass formation: Freezing points can be lowered. Eutectic mixtures may be stable crystalline phases, causing crystal growth to be slower because of the more complex crystal structure. All rates of crystal growth will be reduced by the presence of foreign molecules, which must diffuse away from a growing crystal plane before a new layer can be added. The amount of intermolecular bonding not corresponding to a stable structure may be increased.

By examining the available physicochemical data[16] with the above points in mind, one may explain reasonably well the relative effectiveness of different additives in decreasing dipolar broadening in frozen aqueous solution.

The alcohols have eutectics below $-100°$, and also have been found to have the greatest retarding effect on the growth of ice crystals from aqueous solution.[17] Accordingly, the usefulness of methanol in reducing segregation is understandable.

Glycerol, which is extraordinarily difficult to crystallize, might also be expected to be quite effective. This compound is routinely used to protect biological cells on freezing, and it has been proposed that its primary mode

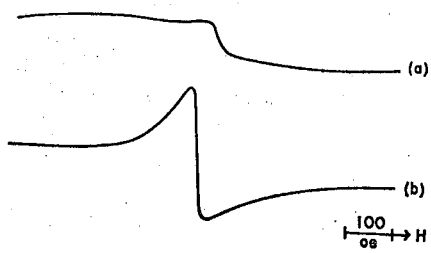

FIG. 2. EPR derivative spectrum of Gd^{3+} in frozen aqueous solution. (a) $0.002M$ $Gd(ClO_4)_3$, $0.02M$ $HClO_4$; (b) a+$1.0M$ $NaClO_4$. Spectrum is centered on $g=2$.

[11] A detailed discussion of linewidth as a function of D is given by B. Bleaney and R. S. Rubins, Proc. Phys. Soc. **77**, 103 (1961).

[12] G. Atkinson and J. E. Bauman, Jr., Inorg. Chem. **2**, 64 (1963).

[13] T. Bjerrum, G. Schwarzenbach, and L. G. Sillen, *Stability Constants* (The Chemical Society, London, 1958), Part II.

[14] The kinetics of crystal growth are reviewed by G. H. Nancollas and N. Purdie in Quart. Rev. **18**, 1 (1964).

[15] Glass formation is discussed by R. W. Douglas in *Non-Crystalline Solids*, edited by V. V. Frechette (John Wiley & Sons, Inc., New York, 1958), p. 374.

[16] J. Timmermans, *Physico-Chemical Constants of Binary Systems in Concentrated Solutions* (Interscience Publishers, Inc., New York, 1960).

[17] C. V. Lusena, Arch. Biochem. Biophys. **57**, 277 (1955).

of action is prevention of cell damage due to greatly increased ionic concentrations which result on freezing.[18] Glycerol is fairly effecting in sharpening EPR spectra, but methanol and potassium acetate seem to surpass it easily.

Solutions of potassium acetate are relatively viscous, and extrapolation of the available freezing-point data[16] places the eutectic in the vicinity of $-70°C$, so the clarity produced by this additive is not unexpected. Sulfuric acid has five eutectics with water and seems to confuse the water molecules successfully.

Dioxane and common mineral salts such as KNO_3 have eutectics only a few degrees below zero and are expected to be ineffective.

More rapid freezing of the sample may help to reduce segregation effects. The conventional plunging of a sample tube into liquid nitrogen is convenient, but it requires several seconds to freeze a sample. Rapid freezing techniques developed for the EPR study of enzyme kinetics[6,19] can freeze an aqueous solution in about 10 msec. However, one should note that at $-10°C$ ice crystallizes at a rate of 70 μ/msec[20,21]; this is sufficient to allow considerable ice crystallite formation.

[18] J. E. Lovelock, Biochim. Biophys. Acta **10**, 414 (1953).

ACKNOWLEDGMENTS

The author gratefully acknowledges helpful advice and criticism from many members of the diversely talented staff of the Laboratory of Chemical Biodynamics. I particularly thank Professor Melvin Calvin and Dr. M. P. Klein for their advice and encouragement.

[19] R. C. Bray, Biochem. J. **81**, 189 (1961).

[20] C. S. Lindenmeyer, G. T. Orrok, K. A. Jackson, and B. Chalmers, J. Chem. Phys. **27**, 822 (1957).

[21] W. B. Hillig in *Growth and Perfection of Crystals*, edited by R. H. Doremus, B. W. Roberts, and D. Turnbull (John Wiley & Sons, Inc., New York, 1958), p. 350.

This report was prepared as an account of Government sponsored work. Neither the United States, nor the Commission, nor any person acting on behalf of the Commission:

A. Makes any warranty or representation, expressed or implied, with respect to the accuracy, completeness, or usefulness of the information contained in this report, or that the use of any information, apparatus, method, or process disclosed in this report may not infringe privately owned rights; or

B. Assumes any liabilities with respect to the use of, or for damages resulting from the use of any information, apparatus, method, or process disclosed in this report.

As used in the above, "person acting on behalf of the Commission" includes any employee or contractor of the Commission, or employee of such contractor, to the extent that such employee or contractor of the Commission, or employee of such contractor prepares, disseminates, or provides access to, any information pursuant to his employment or contract with the Commission, or his employment with such contractor.